2011

Phase 2 Final Report
System Disinfection Contact Basin Project

This document contains the Phase 1 literature review, the Phase 2 research performed through experimental studies and computational models, and the Phase 3 disinfection analysis of the pre-engineered system.

Jordan Wilson, Qing Xu, and Dr. Karan Venayagamoorthy
Department of Civil and Environmental Engineering, Colorado State University
6/17/2011

Table of Contents

1. Introduction

Under the recently promulgated Ground Water Rule, groundwater systems will have stricter regulatory oversight. Those systems that can demonstrate 4-log inactivation of viruses are exempt from the triggered source water monitoring. Further, systems with susceptible groundwater sources and new systems will be required to demonstrate 4-log inactivation of viruses or they will have to install a system upgrade with an approved design.

Currently, the Water Quality Control Division determines the disinfection log inactivation using the protocol described in the US Environmental Protection Agency (USEPA), 2003, *Long Term 1 Enhanced Surface Water Treatment Rule (LT1ESWTR) Disinfection Profiling and Benchmarking Technical Guidance Manual*. The USEPA document has a general baffling factor description chart (see Table 1.1 below) and some example baffling configurations.

Table 1.1 Baffling Factors from LT1ESWTR Disinfection Profiling and Benchmarking Technical Guidance Manual

Baffling Condition	Baffling Factor	Baffling Description
Unbaffled (mixed flow)	0.1	None, agitated basin, very low length to width ratio, high inlet and outlet flow velocities.
Poor	0.3	Single or multiple unbaffled inlets and outlets, no intra-basin baffles.
Average	0.5	Baffled inlet or outlet with some intra-basin baffles.
Superior	0.7	Perforated inlet baffle, serpentine or perforated intra basin baffles, outlet weir or perforated launders.
Perfect (plug flow)	1.0	Very high length to width ratio (pipeline flow), perforated inlet, outlet, and intra-basin baffles.

The contact basin baffling factor is a potentially imprecise factor in the log inactivation calculation. Furthermore, the USEPA baffling conditions have limited applicability for the contact tanks configurations utilized by many small public water systems in Colorado. For example, the USEPA baffling factors do not address multiple small tanks in series, the impact of inlet/outlet piping configurations, and short pipeline segments.

1.1. Objective

The purpose of this document is to identify potential "pre-engineered" configurations appropriate for small groundwater systems as described in chapter 5. Chapter 2 contains the Phase 1 literature review. Chapter 3 contains the computational fluid dynamic (CFD) results for the investigated prototype small public drinking water disinfection systems. Chapter 4 describes the performed tracer studies and provides a comparison to CFD model results on the prototype systems. Chapter 5 also contains sample disinfection calculations for the suggested pre-engineered system.

Appendix A provides a standard operating procedure (SOP) for conservative tracer analysis of small systems. Appendix B provides an SOP for conductivity analysis of small systems. Appendix C contains additional results comparing experimental and numerical model results. Appendix D contains a sample application form for transient non-community system for use with

sodium hypochlorite. Appendix E contains the Masters thesis work of Qing Xu entitled *Internal hydraulics of baffled disinfection contact tanks using computational fluid dynamics*. Appendix F contains the work of Qing Xu and Dr. Venayagamoorthy entitled *Hydraulic efficiency of baffled disinfection contact tanks* as presented at the 6th International Symposium on Environmental Hydraulics. Appendix G contains the Masters thesis work of Jordan Wilson entitled *Evaluation of flow and scalar transport characteristics of small public drinking water disinfection systems using computational fluid dynamics*. Appendix H contains the peer-reviewed journal article of Jordan Wilson and Dr. Venayagamoorthy entitled *Evaluation of hydraulic efficiency of disinfection systems based on residence time distribution curves* as found in Environmental Science and Technology. Finally, Appendix I also contains the work of Jordan Wilson and Dr. Venayagamoorthy entitled *Hydraulics and mixing efficiency of small public water disinfection systems* presented at the 2011 ASCE World Environmental and Water Resources Congress.

2. Literature Review

2.1. Summary

2.1.1 Small Water Systems

The following points outline major considerations about small water systems and measuring system efficiency. A detailed description of these points can be found later in the document.

- 94% of the 156,000 public water systems in the United States serve fewer than 3,300 people (USEPA 2010)
- 94% of Safe Water Drinking Water Act (SWDA) annual violations are attributed to small systems
  - Approximately 77% of these small systems violations are for Maximum Contaminant Level (MCL) of microbiological contaminants (USEPA 2000)
- Chlorine is the disinfectant of choice due to its effectiveness, low cost, and reliability
- CT method of baffling efficiency $BF=t_{10}/TDT$
  - TDT – theoretical detention time (*volume / flow rate*)
  - t_{10} represents the time at which 10% of the maximum concentration is observed in the effluent
- As BF approaches a value of 1, the system efficiency increases (see Table 1.1)

2.1.2 Tracer Studies

The following points outline major considerations about tracer studies. A detailed description of these points can be found later in the document.

- System should be evaluated for two to four flow rates (USEPA 2003)
- Evaluate system volume (for determination of *TDT*)
- Determine methodology best suited for system
  - Step-dose – constant feed of tracer
  - Slug-dose – single slug/volume of tracer input
- Select appropriate tracer
  - Should be conservative (i.e. lithium and fluoride)
  - Effluent concentration not to exceed Secondary Maximum Contaminant Level (SMCL)
- Develop sampling protocol and sample the effluent in a sufficient quantity for analysis
- Analyze the samples for tracer concentration using appropriate means
  - Inductively coupled plasma mass spectroscopy (ICP-MS), atomic absorption spectroscopy,
- Develop RTD curve for the tracer study and determine BF

2.1.3 Computational Fluid Dynamic (CFD) Modeling

The following points outline major considerations about CFD modeling. A detailed description of these points can be found later in the document.

- Level of sophistication
  - Two-dimensional models
    - Take advantage of symmetry or depth averaged flow characteristics in the system

- Reduce computational time without sacrificing accuracy
  - Three-dimensional models
  - Analyze the complete flow dynamics
  - More cost effective than physical tracer studies
    - Accepted in some states (i.e. Texas) in place of physical tracer studies
- Validation
  - Comparison of computational models and experimental results

2.2. Introduction and Objectives

The goal of this initial phase was to perform a literature review on contact tank baffling factors. This literature review discusses water treatment research, contact time and tank characteristics, tracer studies, modeling methods, and software.

2.3. Water Treatment Research

2.3.1. Small Water Treatment Facilities

The United States Environmental Protection Agency (USEPA) defines a small system as one that serves fewer than 3,300 people. Definitions may differ even between federal agency involves. For example, the USGS defines a small system as one that serves fewer than 10,000 people. In effect, the issues under discussion relate more to the availability of resources and operating characteristics than to the actual size of the system. Therefore, a small system may be defined as one that has pressing limitation in terms of resource and technology available to produce and monitor for "safe" water. In Colorado, small public water systems constitute approximately 75 percent of the state's total water systems. While all public water systems are required to meet the same quality requirements, these small systems face technical, managerial, and financial difficulties oftentimes not present in much larger government-supported municipal facilities (USEPA 2010). Figure 2.1 shows some of the considerations in the planning process for these small systems.
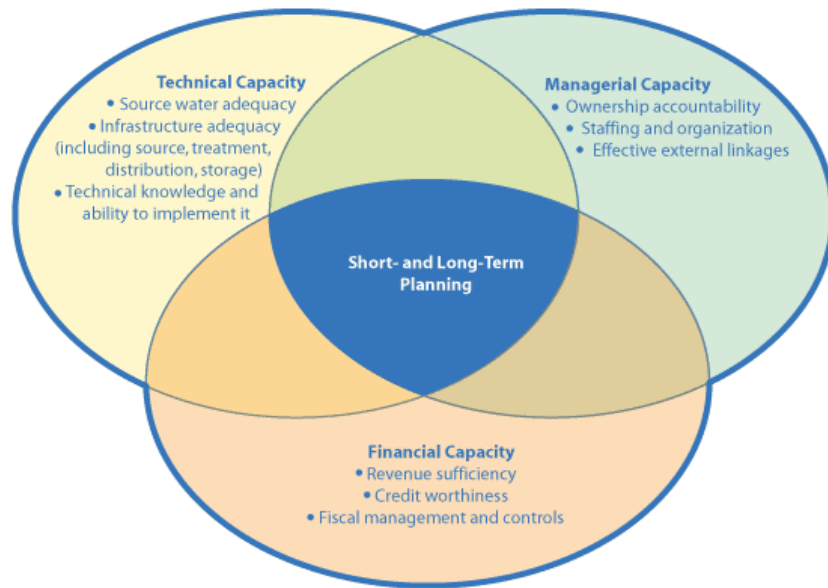
Figure 2.1. Short-and Long-Term Planning Considerations for Small Public Water Systems (USEPA 2010).

Background. There are approximately 160,000 small community and non-community drinking water treatment systems in the United States. Approximately 50,000 small community systems and 110,000 non-community systems provide drinking water for more than 68 million people. However, countless small systems are having difficulty complying with the ever-increasing number of regulations and regulated contaminants.

Currently, 94 percent of Safe Drinking Water Act (SDWA) annual violations are attributed to small systems. Nearly 77 percent of these are for Maximum Contaminant Level (MCL) violations, often directly related to microbiological violations. The EPA conducts in-house technology development and evaluation to support small communities in addressing the cause of these violations. The EPA makes this information to the small system operators, consultants, and utilities. Disinfection technology for small water treatment system is the most important element in addressing quality concerns. Figure 2.2 shows a schematic for an example small water treatment system.

Figure 2.2. Schematic for an example small public water system

Disinfection. Historically chlorine has been the world's most widely used disinfectant. Shortly after the chemical was first used as a germicide in the 19th century, drinking water chlorination became a worldwide practice. However, with the discovery of health hazardous chlorination by-products (CBP) in the 1970's, other technologies have been developed and applied for disinfection purposes, such as ozonation, ultraviolet radiation, and ultrasonics. These technologies have not replaced chlorine's near universal use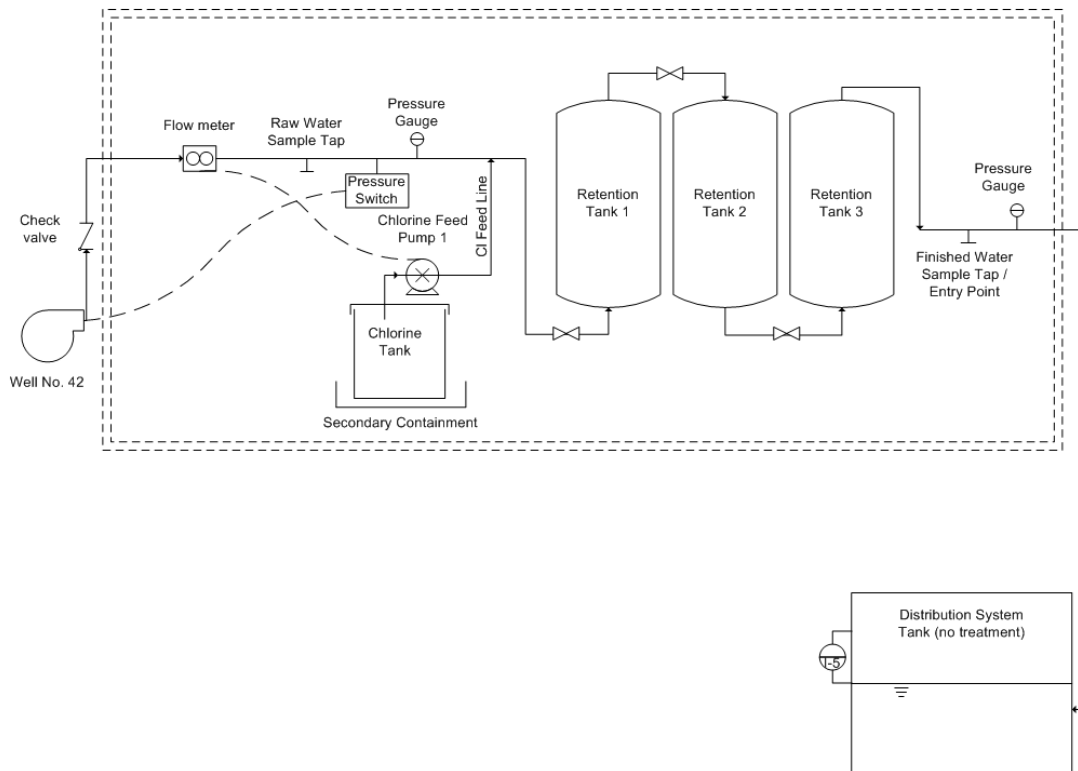, either as the sole disinfectant in a water treatment plant or in conjunction with other technologies. Regardless of the disinfection technology, all water systems must maintain a detectable chlorine residual throughout the distribution system at all times. Chlorine remains the primary disinfectant in small treatment systems due to its wide availability, relative ease of use, and effectiveness.

2.4. Contact Time and Hydraulic Efficiency

The USEPA determines the effectiveness of contact tanks and pipes for disinfection by the *CT* method (described in further detail in chapter 5). *C* is the concentration of disinfectant at the outlet of the tank and *T* is usually taken as the T_{10} value. The T_{10} value is the time required for 10% of the fluid to leave the tank, or the time at which 90% of the fluid is retained in the tank and subjected to at least a disinfectant level of *C*. A high T_{10} value will allow the treatment plant to achieve a high level of disinfection credit for a given concentration of disinfectant. The ratio of T_{10} and *TDT* determines the contactor hydraulic efficiency, or baffling factor ($BF=T_{10}/TDT$). The number and character of the internal baffles, inlet and outlet locations, and the contact tank geometry can influence the T_{10}/TDT ratio or the baffle factor (Crozes et al. 1998).

However, it is useful to be able to predict not just the T_{10}/TDT (baffle) factor, but also the entire residence time distribution (RTD) curve. The entire RTD curve can then be used to predict the overall microbial inactivation level as well as the formation of disinfection by-product (DBPs) Bellamy *et al.* 1998, 2000; Ducoste *et al.* 2001). In a recent study, researchers have shown that the use of the entire RTD curve with more appropriate microbial inactivation/DBP models could lead to a reduction in the disinfectant dose, while still maintaining the same credit for Giardia inactivation specified by the USEPA CT tables (Ducoste *et al.* 2001).

RTD curves constructed from tracer study results are one of the main tools used to assess the hydraulic efficiency of disinfection systems. The shape of the curve provides insight to the nature of the flow in the system (Stamou 2002). For example, a steeper gradient represents conditions closer to plug flow dominated by advection and a flatter gradient represents conditions further from plug flow dominated by diffusive processes. While the curve reveals the nature of transport through the system resulting from the flow dynamics, hydraulic indices are used to more easily interpret the RTD curves. These indices are separated into short circuit and mixing indicators but often describe a multitude of physical phenomena (e.g., advection, diffusion, short-circuiting, mixing, recirculation, and dead zones). Short-circuiting describes the degree to which fluid leaves the system earlier than the *TDT* and mixing describes the "random" spreading of fluid throughout the system via turbulent diffusion and recirculation via flow separation (Teixeira & Siqueira 2008). While turbulence is often viewed as a random and chaotic process, in reality it is a somewhat orderly transference of energy between scales (Pope 2000). Short-circuiting is an important aspect of system operation but is not of significant importance to this research because it describes initial concentration front which is only one portion of the overall hydraulic mixing efficiency. Table 2.1 describes common mixing indices and literature references as described by Teixeira and Siqueira (2008).

Table 2.1. Common hydraulic mixing indices and references.

Index	Definition	References
σ^2	*Dispersion index* - Ratio between the temporal variance of the RTD function (σ_t^2) and (t_g^2)	Levenspiel (1972), Lyn and Rodi (1990), Marske and Boyle (1973), Stamou and Adams (1988), Stamou and Noutsopoulos (1994), Teixeira (1993), and Thirumurthi (1969)
MI	*Morril index* - Ratio between the times necessary for 10 and 90 percent of the mass of tracer that was injected at the inlet section to reach the outlet of the unit, $MI = t_{90}/t_{10}$	Hart (1979), Hart *et al.* (1975), Marske and Boyle (1973), Rebhun and Argaman (1965), Sawyer and King (1969), Stamou and Noutsopoulos (1994), Teixeira (1993), and Thirumurthi (1969)
t_{90}-t_{10}	Time elapsed between t_{10} and t_{90}	Stamou and Noutsopoulos (1994)
t_{75}-t_{25}	Time elapsed between t_{25} and t_{75}, where t_{25} and t_{75} are the respective times necessary for 25 and 75 percent of the tracer that was injected at the inlet section to reach the outlet of the unit	Lyn and Rodi (1990), Stamou and Noutsopoulos (1994), and Stamou and Rodi (1984)
d	*Dispersion number* - Indicator of system dispersion with 0 equal to perfect plug flow	Trussell and Chao (1977), Marske and Boyle (1973), Levenspiel (1972), Hart (1979), and Levenspiel and Smith (1957)
BF	*Baffle factor* - The ratio of t_{10} to *TDT*	USEPA (1986 and 2003)

The temporal variance of the RTD function is given by

$$\sigma_t^2 = \frac{T^2 \int_0^\infty \theta^2 E(\theta)\, d\theta}{\int_0^\infty E(\theta)\, d\theta}, \tag{2.1}$$

where T is the total residence time, θ is the non-dimensional time (T/TDT), and $E(\theta)$ is the value of the probability density function for a pulse input tracer study. The center of mass of the RTD curve, t_g, is given by

$$t_g = \frac{T \int_0^\infty \theta E(\theta)\, d\theta}{\int_0^\infty E(\theta)\, d\theta}, \tag{2.2}$$

where T is the time, θ is the non dimensional time, and $E(\theta)$ is the value of the probability density function for a slug-dose tracer study. This study addresses hydraulic efficiency from a quantitative perspective of flow processes rather than on the statistical nature of RTD curve development.

Teixeira and Siqueira (2008) commented that while each of the indices analyzed had advantages, none of the tested mixing indices were adequate measures of hydraulic efficiency. The dispersion index is mostly a statistical parameter relating the temporal variance of the RTD curve but is difficult to replicate. On the other hand, t_{90}-t_{10} and t_{75}-t_{25} were much easier to replicate but only provide a difference in arrival times which is difficult to interpret in terms of efficiency. The Morril Index (MI) evaluates the amount of diffusion in a system based on the ratio t_{90}/t_{10} which is also difficult to interpret because it has no upper limit to bound values between pure advection and pure diffusion (at least in theory) (USEPA 1986 and Teixeira & Siqueira 2008).

Marske and Boyle concluded that the dispersion number d was the most reproducible of the mixing indices (1973). This quantity can also be interpreted as a non-dimensional diffusivity. As d decreases, the contact system approaches plug flow in a similar manner as MI approaches 1. Using dye curves instead of conservative trace analysis, Levenspiel and Smith (1957) developed between the relationship between the dye curve and the dispersion number seen in equation 2.6

$$E_\theta = \frac{1}{\sqrt{4\pi\theta d}} exp\left[\frac{-(1-\theta)^2}{4\theta d}\right] \tag{2.3}$$

where E_θ is the probability density function of the fluid residence time, θ is the non-dimensional time, and d is the dispersion number. However, the dispersion number is not a global representation of hydraulic efficiency since the same dispersion number can be obtained from multiple curves with differing gradients and it is empirically derived.

The need for a design parameter for disinfection systems with the appropriate contact time, or t_{10}, prompted the USEPA's development of the *BF* classification system. *BF* is often assumed to be synonymous with mixing efficiency when in actuality it is only a partial measure of hydraulic efficiency with t_{10} resulting from the flow dynamics and scalar transport properties of the system and *TDT* resulting from the ideal plug flow assumption (Teefy 1996). The *BF* formulation fails to take into account the actual dynamics going on in any given disinfection system beyond t_{10}

and therefore, in all cases (at least for the all cases discussed in this research) tends to provide an overestimation of the hydraulic efficiency.

An extensive literature review has shown that all existing indicators of hydraulic efficiency have flaws in a global sense. The dispersion index σ^2 gives a good representation of a system's efficiency but is difficult to replicate. The dispersion number d, while easy to replicate, is not always indicative of the system at hand and can give the same result for hydraulically differing systems. The dispersion number also incorporates the inherent assumption of ideal plug flow through normalizing time to *TDT* which is not an actual parameter of the system. t_{90}-t_{10} and t_{75}-t_{25} are also easy to replicate but do not provide a good assessment of the system's efficiency. *BF*, while technically a system design parameter and not a mixing index, only provides a partial assessment of efficiency. The Morril Index is the best indicator of those found in literature but is often difficult to interpret leaving the door open to a better indicator of hydraulic efficiency.

2.5. Tank Designs

2.5.1. Impact of Design Characteristics

Clearwells or disinfection contactors serve a variety of roles at water treatment plants including storage, water pressure equalization, and disinfection. The significant design characteristics include length-to-width ratio, the degree of baffling within the basins, and the effect of inlet baffling and outlet weir configuration. These physical characteristics of the contact basins affect their hydraulic efficiencies in terms of dead space, plug flow, and mixed flow proportions. The dead space zone of a basin is the basin volume through which no flow occurs. The remaining volume where flow occurs is comprised of plug flow and mixed flow zones. The plug flow zone is the portion of the remaining volume in which no mixing occurs in the direction of flow. The mixed flow zone is characterized by complete mixing in the flow direction and is the complement to the plug flow zone. All of these zones were identified in studies for each contact basin.

Comparisons were then made between the basin configurations and the observed flow conditions and design characteristics. The ratio T_{10}/*TDT* was calculated from the data presented in the studies and compared to its associated hydraulic flow characteristics. Both studies resulted in *BF* values that ranged from 0.3 to 0.7. The results of the studies indicate how basin baffling conditions can influence *BF*, particularly baffling at the inlet and outlet to the basin. As the basin baffling conditions improved, higher *BF* values were observed, with the outlet conditions generally having a greater impact than the inlet conditions.

Marske and Boyle (1973) and Hudson (1975) showed that a *BF* value is more related to the geometry and baffling of the basin than the function of the basin. For this reason, *BF* values may be defined for five levels of baffling conditions rather than for particular types of contact basins. General guidelines were developed relating the *BF* values from these studies to the respective baffling characteristics. These guidelines can be used to determine the T_{10} values for specific basins.

2.5.2. Baffling Classifications

The purpose of baffling is to maximize utilization of basin volume, increase the plug flow zone in the basin, and minimize short-circuiting. Ideal baffling design reduces the inlet and outlet flow velocities, distributes the water as uniformly as practical over the cross section of the basin, minimizes mixing with the water already in the basin, and prevents entering water from short-circuiting to the basin outlet as the result of wind or density current effects. Some form of baffling at the inlet and outlet of the basins is used to evenly distribute flow across the basin. Additional baffling may be provided within the interior of the basin (intra-basin) in circumstances requiring a greater degree of flow distribution.

Five general classifications of baffling conditions - unbaffled, poor, average, superior, and perfect (plug flow) were developed to categorize the results of the tracer studies for use in determining T_{10} from the *TDT* of a specific basin. Table 1.1 contains these classifications. The *TDT* fractions associated with each degree of baffling are summarized in Table 1.1. However, in practice the theoretical *TDT* values of 1.0 for plug flow and 0.1 for mixed flow are seldom achieved because of the effect of dead space. Conversely, the *TDT* values shown for the intermediate baffling conditions already incorporate the effect of the dead space zone, as well as the plug flow zone, because they were derived empirically rather than from theory.

The three basic types of basin inlet baffling configurations are a target-baffled pipe inlet, an overflow weir entrance, and a baffled submerged orifice or port inlet. Typical intra-basin baffling structures include diffuser (perforated) walls; launders; cross, longitudinal, or maze baffling to cause horizontal and/or vertical serpentine flow; and longitudinal divider walls, which prevent mixing by increasing the length-to-width ratio of the basin(s). Commonly used baffled outlet structures include free-discharging weirs, such as sharp-crested and multiple V-notch, and submerged ports or weirs. Weirs that do not span the width of the contact basin, such as Cipolleti weirs, should not be considered for baffling as their use may substantially increase weir overflow rates and the dead space zone of the basin. Figures 2.3, 2.4, and 2.5 show poor, average, and superior baffling conditions rectangular and circular contact basins, respectively.

Plan View

Section View

(a)

Plan View

Section View

(b)

Figure 2.3. Poor Baffling Conditions for (a) rectangular and (b) circular contact basins (USEPA 2003).

Plan View

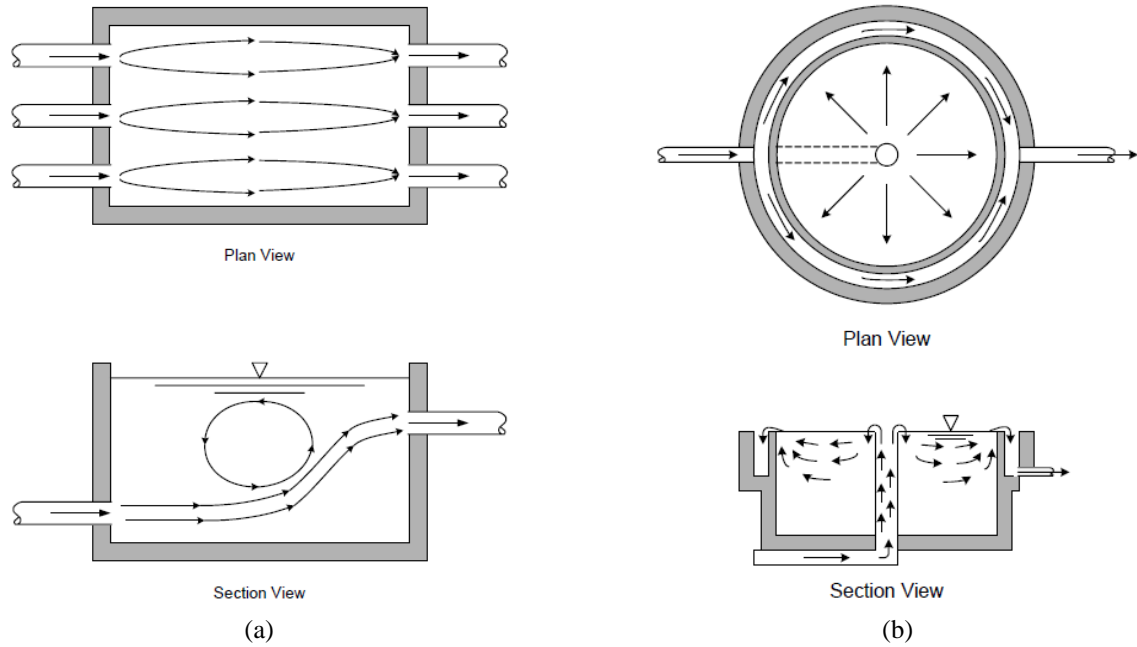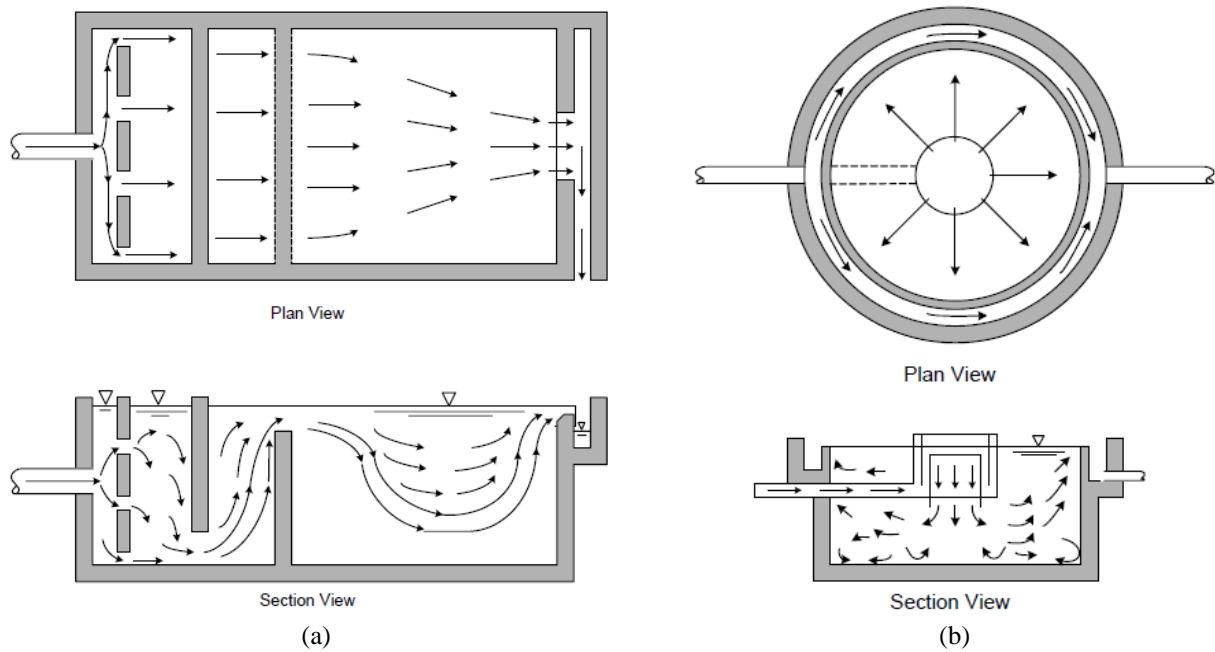Section View

(a)

Plan View

Section View

(b)

Figure 2.4. Average baffling conditions for (a) rectangular and (b) circular contact basins (USEPA 2003).
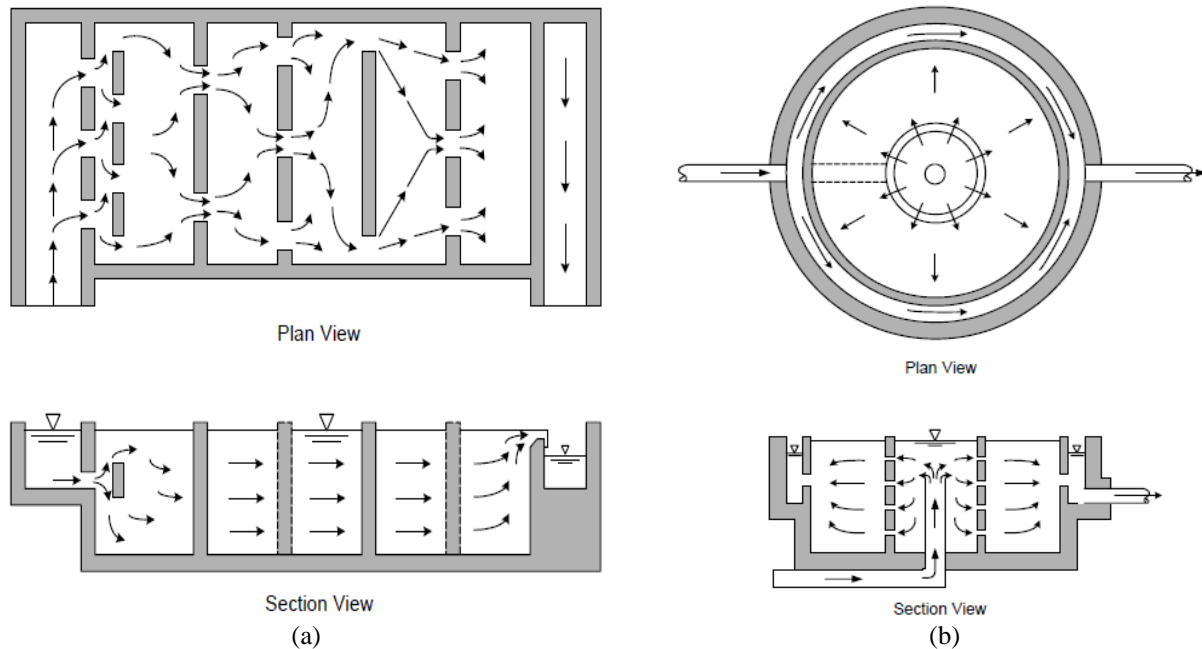
Figure 2.5. Superior baffling conditions for (a) rectangular and (b) circular contact basins (USEPA 2003).

The above figures show the influence of baffling on mixing efficiency within each of the respective tanks.

2.6. Tracer Study Considerations

2.6.1. Flow Evaluation

Ideally, tracer tests should be performed for at least four flow rates that span the entire range of flow for the segment being tested. The flow rates should be separated by approximately equal intervals to span the range of operation, with one near average flow, two greater than average, and one less than average flow. It may not be practical for all systems to conduct studies at four flow rates. The number of tracer tests that are practical to conduct is dependent on site-specific restrictions and resources available to the system.

The most accurate tracer test results are obtained when flow is constant through the segment during the course of the test. However, variability will always exist in flow rates due to numerous factors. Thus, the tracer study should be conducted at a relatively constant flow rate with minimal fluctuations.

For a treatment plant consisting of two or more equivalent process trains, a constant flow tracer test can be performed on a segment of the plant by holding the flow through one of the trains constant while operating the parallel train(s) to absorb any flow variations. Flow variations during tracer tests in systems without parallel trains or with single clearwells and storage reservoirs are more difficult to avoid. In these instances, T_{10} should be recorded at the average flow rate over the course of the test.

2.6.2. Volume Evaluation

In addition to flow conditions, detention times determined by tracer studies depend on the water level and subsequent volume in treatment units. This is particularly pertinent to storage tanks, reservoirs, and clearwells, which, in addition to being contact basins for disinfection are often used as equalization storage for distribution system demands and storage for backwashing. In such instances, the water levels in the reservoirs vary to meet the system demands. The actual detention time of these contact basins will also vary depending on whether they are emptying or filling.

For some process units, especially sedimentation basins that are operated at a near constant level (that is, flow in equals flow out), the detention time determined by tracer tests should be sufficient for calculating *CT* when the basin is operating at water levels greater than or equal to the level at which the test was performed. If the water level during testing is higher than the normal operating level, the resulting concentration profile will predict an erroneously high detention time. Conversely, extremely low water level during testing may lead to an overly conservative detention time. Therefore, when conducting a tracer study to determine the detention time, a water level at or slightly below, but not above, the normal minimum operating level is recommended. For many plants, the water level in a clearwell or storage tank varies between high and low levels in response to distribution system demands. In such instances, in order to obtain a conservative estimate of the contact time, the tracer study should be conducted during a period when the tank level is falling (flow out greater than flow in).

2.6.3. Disinfection Segments

For systems that apply disinfectants at more than one point, or choose to profile the residual from one point of application, tracer studies should be conducted to determine T_{10} for each segment containing a process unit. The T_{10} for a segment may or may not include a length of pipe and is used along with the residual disinfectant concentration prior to the next disinfectant application or monitoring point to determine the *CT* for that segment. The inactivation ratio for the section is then determined. The total log inactivation achieved in the system can then be determined by summing the inactivation ratios for all sections.

For systems that have two or more units of identical size and configuration, tracer studies could be conducted on one of the units but applied to both. The resulting graph of T_{10} versus flow can be used to determine T_{10} for all identical units. Systems with more than one segment in the treatment plant may determine T_{10} for each segment:

- By individual tracer studies through each segment; or,
- By one tracer study across the system.

If possible, tracer studies should be conducted on each segment to determine the T_{10} for each segment. In order to minimize the time needed to conduct studies on each segment, the tracer studies should be started at the last segment of the treatment train prior to the first customer and completed with the first segment of the system. Conducting the tracer studies in this order will prevent the interference of residual tracer material with subsequent studies.

For ozone contactors, flocculators or any basin containing mixing, tracer studies should be conducted for the range of mixing used in the process. In ozone contactors, air or oxygen should be added in lieu of ozone to prevent degradation of the tracer. The flow rate of air or oxygen used for the contactor should be applied during the study to simulate actual operation. Tracer studies should then be conducted at several air/oxygen to water ratios to provide data for the complete range of ratios used at the plant. For flocculators, tracer studies should be conducted for various mixing intensities to provide data for the complete range of operations. Lithium, fluoride, chloride, and sodium are commonly used conservative tracers. Lithium is the tracer of choice when analysis means (atomic spectroscopy) are available due to the extremely low background levels.

2.6.4. Other Considerations

Detention time may also be influenced by differences in water temperature within the system. For plants with potential for thermal stratification, additional tracer studies are suggested under the various seasonal conditions that are likely to occur. The quantity of studies should be sufficient to characterize any thermal stratification phenomena that occur within the system.

2.7. Tracer Study Methods

There are two common methods of tracer addition employed in water treatment evaluations: the step-dose method and the slug-dose method.

In general, the step-dose procedure offers the greatest simplicity. However, both methods are theoretically equivalent for determining T_{10}. While either method is acceptable for conducting drinking water tracer studies, each has distinct advantages and disadvantages with respect to tracer addition procedures and analysis of results. The choice of the method may be determined by site-specific constraints.

2.7.1. Slug-Dose Method

A pulse input tracer study involves placing a known mass of conservative tracer instantaneously upstream of the contact tank inlet where it must be completely mixed with the influent stream. Generally, the mixing time required should be less than 1 percent of the *TDT*. Sampling in pulse input tracer studies should occur early on to ensure the fast-moving rising limb is captured. The RTD curve produced from this testing method exhibits a rising limb as the concentration increases, a maximum, and a falling limb as the tracer leaves the system. Figure 2.7 shows a RTD curve for a pulse input tracer study performed on an arbitrary disinfection system with time normalized to the *TDT*.
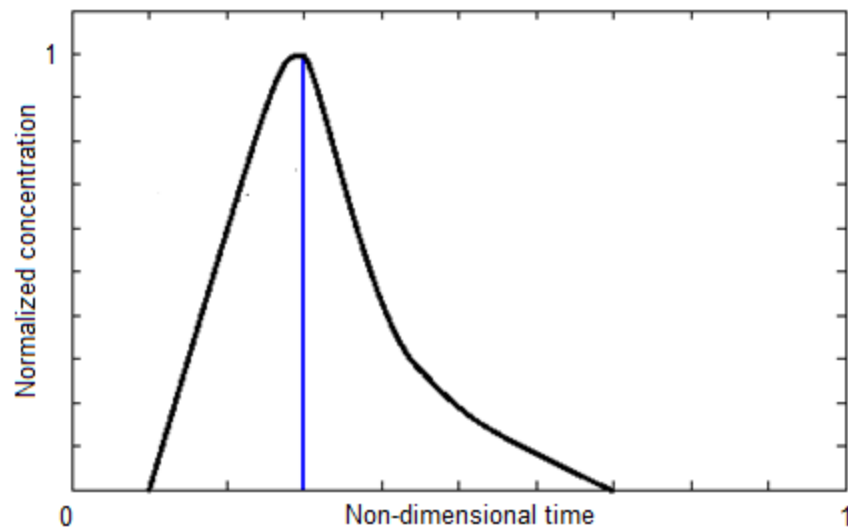
Figure 2.7. RTD curve for a pulse input tracer study for an arbitrary disinfection system as compared to a step impulse function.

Normalization of the tracer concentration and time allows for comparison of the behavior of different systems. While the pulse input method is easier to perform in most circumstances, the results require more extensive analysis for interpretation. Table 2.2 presents the advantages and disadvantages of pulse input tracer studies (Teefy 1996).

Table 2.2. Summary of advantages and disadvantages of pulse input tracer study.

Advantages	Disadvantages
Less chemical is needed for pulse input than for a step input	Danger of missing the peak if sampling frequency is not correct
Mean residence time, recovery rate, and variance can be determined more readily	More mathematical manipulation of results is needed to obtain t_{10}
Chemical addition can be simple in some situations	Cannot repeat the test easily (no receding curve available)
	Difficult to determine the amount of tracer that should be added for the test

2.7.2. Step-Dose Method

In comparison, a step input tracer study is performed by feeding a conservative tracer at a constant rate into the system until the concentration reaches a steady state in the effluent stream. An advantage of the step input method is the possibility to obtain results from the increasing mode as the tracer is constantly fed into the system and the receding mode after steady state is reached and the tracer input is discontinued. These studies can be performed using existing chemical feed equipment or by constructing a temporary input system as long as the feed rate is constant for the increasing mode and the system flow rate remains constant through both modes.

Sampling for step input tracer studies should occur at regular intervals and ensure that steady state is captured. Again, plotting the normalized concentration against the normalized time as seen in Figures 2.8(a) and (b) displays the nature of the system for both increasing and receding modes.
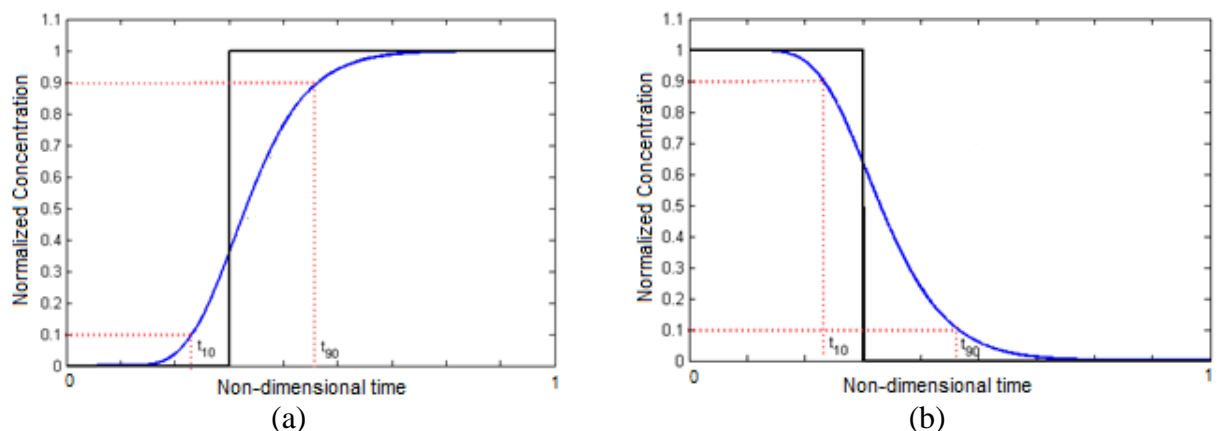

(a)   (b)

Figure 2.8. (a) rising RTD curve and (b) receding RTD curve for a step input tracer study for an arbitrary disinfection system as compared to a step impulse function.

While these plots for pulse and step input tracer studies display the same information about the systems, t_{10} can be more easily interpreted from a step input RTD curve (Teefy 1996). Table 2.3 presents the advantages and disadvantages of step input tracer studies (Teefy 1996).

Table 2.3. Summary of advantages and disadvantages of step input tracer study.

Advantages	Disadvantages
Sometimes can be done with existing plant chemical feed equipment	More tracer chemical is required than in a pulse input test
t_{10} can be determined graphically from curve	Cannot reliably calculate mass recovery or mean residence time to check validity
Results can be verified by monitoring the receding curve	May have to install chemical feed equipment if not already present

In cases where multiple tracer studies cannot be performed, the USEPA *Guidance Manual* (1986) recommends the following equation be used for prediction of contact time based on the same *BF*.

$$T_{10S} = T_{10T} \times Q_T/Q_D \, , \tag{2.3}$$

where T_{10S} is t_{10} at the system flow rate, T_{10T} is t_{10} at the tracer study flow rate, Q_T is the tracer study flow rate, and Q_D is the system flow rate.

2.8. Tracer Selection

An important step in any tracer study is the selection of a chemical to be used as the tracer. Ideally, the selected tracer chemical should be readily available, conservative (i.e. a chemical that is not reactive or removed during treatment), easily monitored, and acceptable for use in potable water supplies. Chlorides and fluorides are the most common tracer chemicals employed in drinking water plants since they are approved for potable water use.

Fluoride can be a convenient tracer chemical for step-dose tracer tests of clearwells because it is frequently applied for finished water treatment. However, when fluoride is used in tracer tests on clarifiers, allowances should be made for fluoride that is absorbed on floc and settles out of water (Hudson, 1975). Additional considerations when using fluoride in tracer studies include:

- It is difficult to detect at low levels,
- The federal secondary and primary drinking water standards (i.e. the MCLs) for fluoride are 2 and 4 mg/L, respectively.

For safety reasons, particularly for people on dialysis, fluoride is not recommended for use as a tracer in systems that normally do not fluoridate their water. The use of fluoride is only recommended in cases where the feed equipment is already in place. The system may wish to turn off the fluoride feed in the plant for 12 or more hours prior to beginning the fluoride feed for the tracer study. Flushing out fluoride residuals from the system prior to conducting the tracer study is recommended to reduce background levels and avoid spiked levels of fluoride that might exceed USEPA's MCL or SMCL for fluoride in drinking water. In instances where only one of two or more parallel units is tested, flow from the other units would dilute the tracer concentration prior to leaving the plant and entering the distribution system. Therefore, the impact of drinking water standards on the use of fluoride and other tracer chemicals can be alleviated in some cases.

Lithium is another suitable conservative tracer that can be used in tracer studies if very accurate results are required. However, onsite monitoring of concentration profiles is not possible since advanced laboratory analysis such as atomic absorption spectroscopy (AAS) or inductively coupled plasma atomic emission spectroscopy (ICP-AES) is required to detect concentration of the metal. However, Lithium is often a prime candidate since the only very small amount of a Lithium salt is required in a tracer studies since the background concentrations of Lithium in water is much less than 1μg/L.

2.9. Test Procedure

A standard operating procedure for conservative tracer analysis on small public drinking water disinfection systems can be found in appendix A. In preparation for beginning a tracer study, the raw water background concentration of the chosen tracer chemical should be established. The background concentration is important, not only to aid in the selection of the tracer dosage, but also to facilitate proper evaluation of the data.

The background tracer concentration should be determined by monitoring for the tracer chemical prior to beginning the test. The sampling point for the pre-tracer study monitoring should be the

same points as those used for residual monitoring to determine *CT* values. Systems should use the following monitoring procedure:

- Prior to the start of the test, regardless of whether the chosen tracer material is a treatment chemical, the tracer concentration in the water is monitored at the sampling point where the disinfectant residual will be measured for *CT* calculations.
- If a background tracer concentration is detected, monitor it until a constant concentration, at or below the raw water background level, is achieved. This measured concentration is the baseline tracer concentration.

Following the determination of the tracer dosage, feed and monitoring point(s), and a baseline tracer concentration, tracer testing can begin.

Equal sampling intervals, as could be obtained from automatic sampling, are not required for either tracer study method. However, using equal sample intervals for the slug-dose method can simplify the analysis of the data. During testing, the time and tracer residual of each measurement should also be recorded on a data sheet. In addition, the water level, flow, and temperature should be recorded during the test.

2.10. Computational Fluid Dynamics (CFD) Methods

2.10.1. Background

Computational fluid dynamics (CFD) studies are increasingly been used recently in simulate and understand contact tank hydraulics. However, most CFD studies on contact tanks have focused on understanding the hydrodynamics only without simulating the tracer transport (Gualtieri 2004). The flow inside a contact tank is usually modeled on the premise that the variations of all relevant quantities in the vertical direction, except in the thin boundary layer near channel bottom and possibly near the free surface, are substantially smaller that variations across the width or in streamwise direction. Thus, two-dimensional or depth-averaged models may be applied to describe hydrodynamics and mass-transfer processes for systems with a uniform flow velocity in the vertical direction. More complex flow situations require three-dimensional analysis. These CFD models are based on the mass conservation equation and the Navier-Stokes equations of motion. Since the flow in the tank is turbulent, these equations must be averaged over a small time increment applying Reynolds decomposition, which results in the Reynolds-averaged Navier-Stokes (RANS) equations. Once the flow velocity is computed, the residence time distribution (RTD) curves may be obtained by solving a tracer transport equation using the velocity field obtained from the solution of the Navier-Stokes equations.

2.10.2. Theory

A more complete view of the theory involved in the CFD modeling of the prescribed systems can be found in appendices E and G.

The theoretical basis of CFD modeling is the Navier-Stokes fluid dynamics equations, which are used to model fluid flow parameters such as velocity, temperature, and pressure. Velocity

contours can be used to trace the paths of particles that travel through the modeled unit process, which allows residence time distributions to be calculated.

The Navier–Stokes equations describe the motion of fluid parcels. These equations arise from applying Newton's second law to fluid motion, together with the assumption that the fluid stress is the sum of a diffusing viscous term (proportional to the gradient of velocity), plus a pressure term.

Equation 2.1 gives the general form of the Navier-Stokes equations (in tensor notation) with the Boussinesq approximation.

$$\frac{\partial u_i}{\partial t} + \frac{\partial}{\partial x_j}(u_i u_j) = -\frac{1}{\rho_o}\frac{\partial P}{\partial x_i} + \nu\frac{\partial^2 u_i}{\partial x_i \partial x_j} - \frac{g}{\rho_o}\rho\delta_{i3} \qquad (2.1)$$

where u_i is the velocity field, P is the pressure, ρ is the density of the fluid, and ν is the kinematic viscosity. The Boussinesq Approximation involves using an algebraic equation for the Reynolds stresses which include determining the turbulent viscosity, and depending on the level of sophistication of the model, solving transport equations for determining the turbulent kinetic energy and dissipation.

2.10.3. Turbulence and Turbulence Models

A more description of turbulence and turbulence models appendices E and G.

Turbulence is the time dependent chaotic behavior seen in many fluid flows. It is generally believed that it is due to the inertia of the fluid as a whole: the culmination of time dependent and convective acceleration; hence, flows where inertial effects are small tend to be laminar (the Reynolds number quantifies how much the flow is affected by inertia). It is believed, though not known with certainty, that the Navier–Stokes equations describe turbulence properly.

The numerical solution of the Navier–Stokes equations for turbulent flow is extremely difficult, and due to the significantly different mixing-length scales that are involved in turbulent flow, the stable solution of this set of equations requires a very fine mesh resolution resulting computational times that are prohibitively expensive. To counter this, time-averaged equations such as Reynolds-Averaged Navier-Stokes (RANS) equations, supplemented with turbulence models (such as the *k-ε* model), are used in practical CFD applications for modeling turbulent flows.

Another technique for solving numerically the Navier–Stokes equation is the Large-eddy simulation (LES). This approach is computationally more expensive than the RANS method (in time and computer memory), but produces better results since the larger turbulent scales are explicitly resolved. A brief summary of the three state-of-the-art approaches to solving turbulent flow problems are provided in Table 2.4.

Table 2.4. Summary of Turbulence Models

Turbulence Model	Summary	Pros	Cons
Direct Numerical Simulation (DNS)	Exact solution to the Navier-Stokes and scalar transport equations	Provides complete resolution of turbulence, flow and scalar transport	Requires massive computational power and time Only applicable to the simplest problems
Large Eddy Simulation (LES)	Direct solution to the largest eddies, averaged solution to the smallest eddies, or near wall regions (hybrid of DNS and RANS solutions)	Provides a high degree of resolution Broader spectrum of uses than DNS	Requires orders of magnitude more computational power than RANS
Reynolds-Averaged Navier-Stokes (RANS)	Solutions based on averaged flow equations Numerous RANS models are available for various applications (see Appendix D)	Comparatively low computation time Applicable to nearly all flows	Does not provide as fine a resolution as LES or DNS

2.11. CFD Software Packages

2.11.1. Ansys FLUENT

The theoretical basis of CFD modeling is the Navier-Stokes fluid dynamics equations, which are used to model fluid parameters such as velocity, temperature, and pressure. FLUENT is a commercially available CFD software used in both research and industry. The features of this program are largely driven by industry but also incorporate many state-of-the-art features. FLUENT has been successfully used in many previous studies of disinfection contact chambers. In a recent study (Stovin and Saul, 1998), the use of the particle tracking routine contained within the FLUENT software for the prediction of sediment deposition in storage chambers is described. The paper details the way in which the particle tracking routine was configured to produce realistic efficiency results for the comparison of storage chamber performance. Consideration was given to the physical characteristics of the sediment, the injection location, the boundary conditions, and a number of relevant simulation parameters. The sensitivity of efficiency prediction to the selection of these parameters is emphasized. The paper also demonstrates the potential application of particle tracking to the prediction of probable deposit locations. In this way, CFD modeling is analogous to conducting a virtual tracer test.

In another field CFD modeling study (Templeton, et al. 2006), two-dimensional CFD modeling was performed for clearwells using FLUENT and the associated Gambit preprocessor (for meshing). Two-dimensional models were used because of the large surface area to depth ratio of the clearwells (ratio >180 in all cases) and based on useful results obtained from previous application of two-dimensional modeling for cases with similar surface area to depth ratios (Hannoun et al.1998; Crozes et al. 1999). Two-dimensional models drastically reduce the computation time and the overall complexity of the modeling when compared to three-dimensional models. Modeled clearwell geometries were created based on the best available

engineering drawings supplied by plant personnel. Geometry creation and grid generation were performed in Gambit and then transferred to FLUENT for definition of the boundary conditions and solution of the governing fluid dynamics equations. The grids generated in Gambit had more than 100,000 grid points in each case. The standard k-ε turbulence model and no-slip boundary conditions were specified.

A particle tracking function in FLUENT was used whereby virtual particles (>1000) were released from the same modeled locations as where the actual tracer was injected. The CFD software tracked the residence time of each particle, from which T_{10} values and baffle factors were calculated. The CFD models also allow tracers to be considered as a chemical species, however in this case particle tracking was used so that the paths of discrete microorganisms through the clearwells could be modeled, since it is the residence time of pathogenic organisms that is of primary interest in disinfection. The particles were assumed to be spherical and of approximately the same density (i.e. neutrally buoyant) as the water. Figures 2.9 through 2.12 shows the velocity field and particles tracks from CFD simulations of three different clearwells in Ontario as described in Templeton et al. (2006).
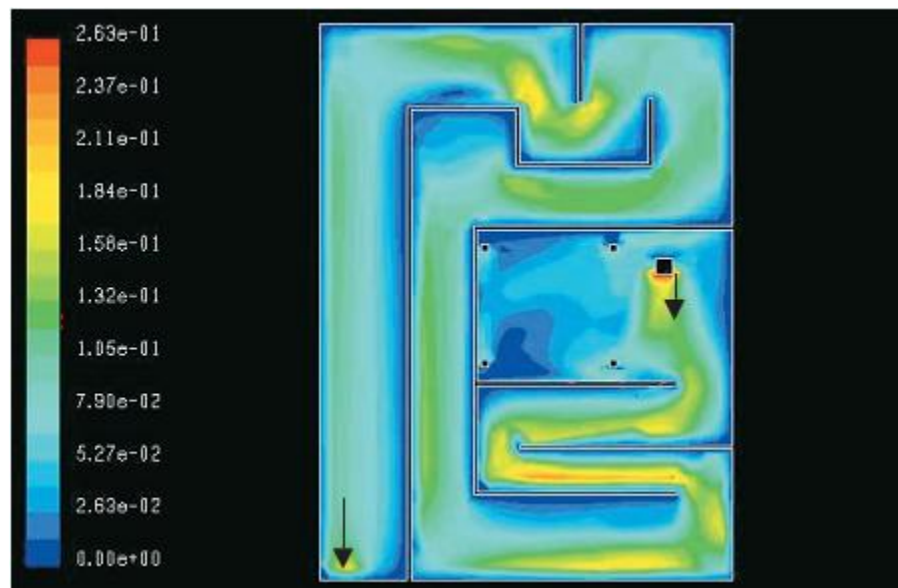

Figure 2.9. Velocity Contours through Britannia WPP (Ottawa, Ontario) Clearwell 2 @ 139.0 MLD Arrows show the direction of flow in and out.
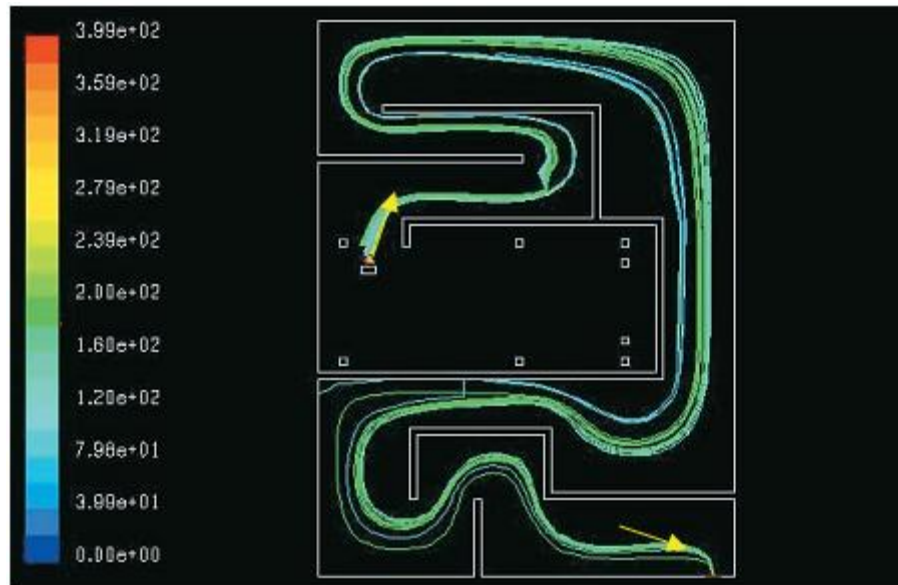
Figure 2.10. Example Particle Tracks through Britannia WPP (Ottawa, Ontario) Clearwell 1 @ 111.2 MLD
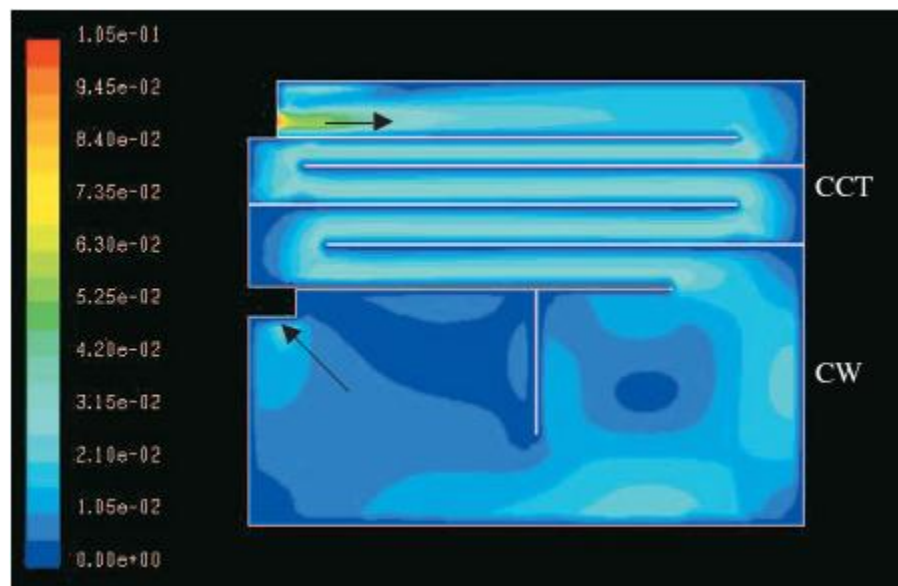

Figure 2.11. Velocity Contours through Lemieux Island WPP (Ottawa, Ontario) Combine North and South Clearwells (NCW, SCW) @ 153.6 MLD.
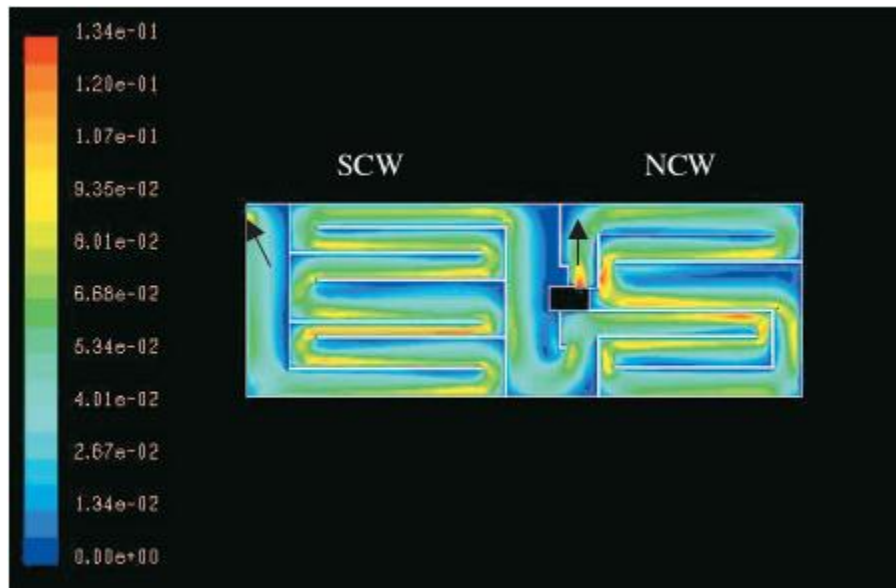
Figure 2.12. Velocity Contours through the Peterborough WTP (Peterborough, Ontario) Combined CCT and Clearwell @ 35.2 MLD

The results of this study suggest that CFD modeling can successfully predict clearwell residence times for different arrangements of baffle configurations and flow rates, based on comparisons with full-scale tracer test results. The two-dimensional models developed in this study provided baffle factor estimates that matched tracer results to within 17 percent in all cases, and were accurate to within 10 percent in most cases. Model prediction effectiveness was related to flow rate, clearwell volume, or clearwell baffle configuration for the examples that were evaluated.

2.11.2. COMSOL Multiphysics

Two-dimensional steady state and time-variable numerical simulations were performed in a contact tank geometry using COMSOL Multiphysics (Gualtieri 2004). COMSOL Multiphysics is a software package that is based on the finite-element method for the solution of fluid flow and transport equations. The work by Gualtieri (2004) presents preliminary results of a numerical study undertaken to investigate hydrodynamics and turbulent transportation and mixing inside a contact tank. Flow field and mass-transport processes are simulated using k-ε model and advection-diffusion equation.
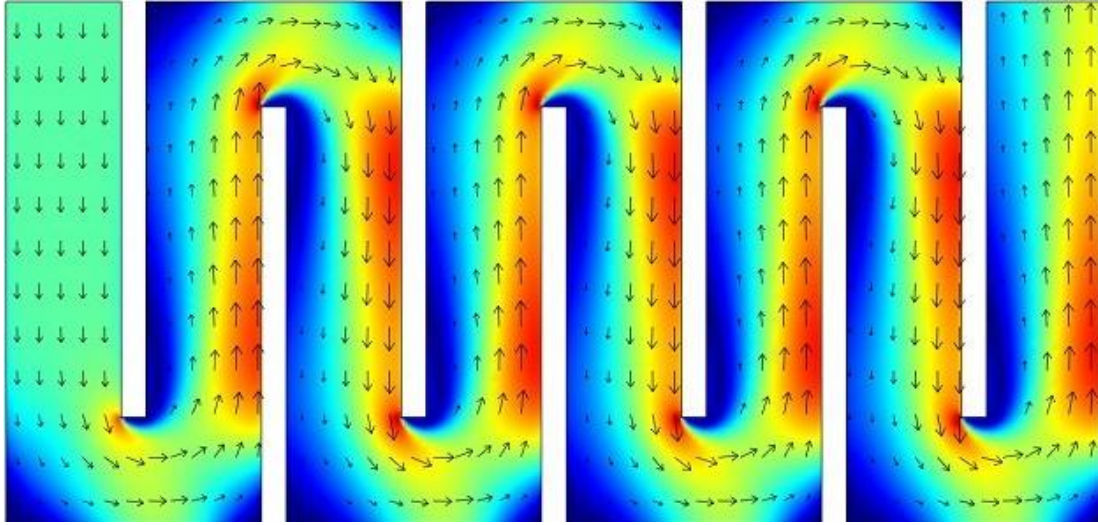
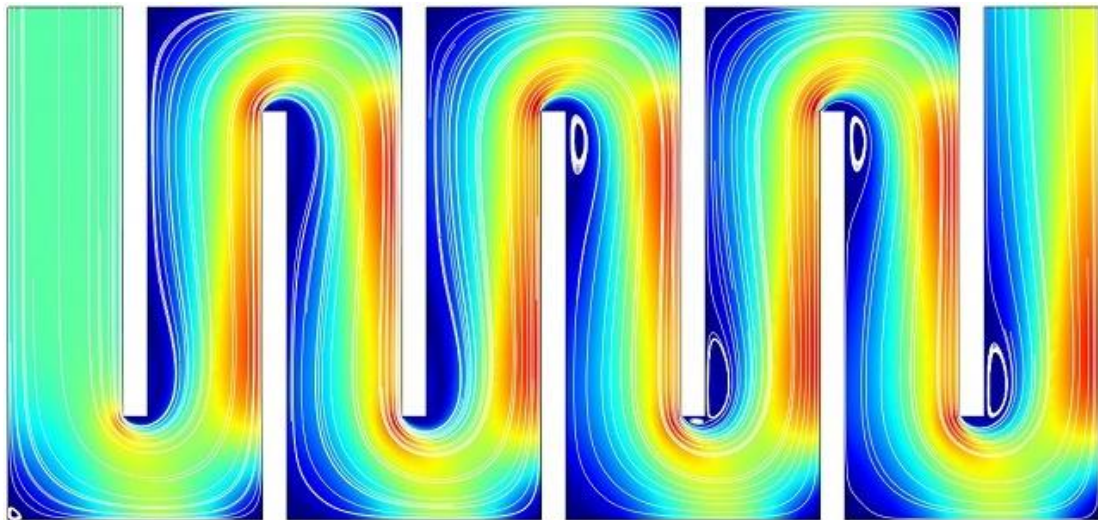**Figure 2.13. Simulated Flow Field and Velocity Vectors in Contact Tank**

Figure 2.14. Streamlines in Contact Tank

Numerical results were in good agreement with the observed data for both flow field and tracer transport and mixing. Particularly, CFD results reproduced the recirculation regions that were experimentally observed behind the baffles and in the corners at the junctions between the baffles and the tank walls. Since experimental works demonstrated that the flow could be considered as two-dimensional only in compartments 5 through 7, future studies should address this issue using a 3D CFD model of the tank.

2.12. Conclusions

Though the tracer study described in *LTIESWTR* is thorough, reliable and traditional, computational fluid dynamics modeling has several advantages over tracer studies. These include:

- Less time spent in modeling compared to full tracer testing
- Does not interrupt plant operations, whereas tracer tests require testing different flow rates and can be involved considerable interruptions to operation.
- A range of flow and temperature conditions can be simulated that may not feasible using physical tracer tests.
- Consideration of alternative baffling arrangements that do not physically exist is also possible with CFD modeling.
- Further, CFD modeling foregoes the handling of sometimes harmful tracer chemicals (e.g., hydrofluoricacid) and potentially time-consuming process of obtaining regulatory approval to inject tracer into a public water system.

CFD modeling can successfully predict clearwell residence times for different baffle configurations and flow rates, based on comparisons with full-scale tracer test results. However, it is important to note that before any reliable conclusions are drawn, it is of utmost importance to validate the CFD model that will be used for designing new contact tanks or modifying existing system. In what follows, a validation study of the FLUENT model is carried using a pipe loop pilot system where a complete tracer study was conducted. The is the first step in using CFD for designing efficient contact tanks for small scale drinking water systems.

3. CFD Model Studies

Most contact tanks exhibit uneven flow paths, representative of dead zones, or regions of recirculation or stagnation, flow separation, and turbulent effects (Wang & Falconer 1998). These dead zones rely on much slower and less effective processes (e.g., diffusion) to distribute the scalar (e.g., conservative tracer or chlorine-containing species). These flow phenomena result in some particles residing longer in the system than others that are simply advected. The degree to which particles reside longer in the system (e.g. the more recirculation, turbulence, and stagnation fluid particles encounter) than those advected describes the system's hydraulic efficiency which is discussed more in depth in chapter 4. Traditionally, measurement of disinfection system flow characteristics used existing contact tank systems or relied on scaled similarity models (e.g., see Shiono and Teixeira 2000) using laser or acoustic anemometry. Such methods are often costly and, on the full-scale, can only be performed using pre-existing infrastructure. Difficulty also arises in analyzing the flow through closed, pressurized systems such as pipe loops. As shown in literature, and in this study, CFD is a valid tool for analyzing the flow characteristics and scalar transport through contact tank systems. This chapter presents the flow and resulting scalar transport analysis of a pipe loop system, series of pressurized tank system, two open surface tank systems, and a baffled tank system and their respective scalar transport characteristics.

The following subsections describe the flow and scalar transport characteristics of the disinfection systems analyzed in this study, primarily a pipe loop contactor, system of pressurized tanks, and two different open surface tanks.

3.1. Pilot Pipe Loop System

The city of Fort Collins Municipal Water Treatment Facility allowed the use of their pilot pipe loop system for this study. The tracer was sampled after 14 major lengths to take advantage of a pre-existing tap in the system. The internal diameter of the piping was 0.15 m with a major length of 6.55 m and a minor length of 0.21 m measured from the outside of the joints. Figure 3.1 shows the pilot pipe-loop facility.

Figure 3.1. Pilot pipe-loop facility at Fort Collins Municipal Water Treatment Facility.

3.1.1. Pipe Loop System Computational Model Setup

Using ANSYS DesignModeler a model was created reflecting the sampling point after 14 major lengths as shown in Figure 3.2 (a). The model geometry was then meshed using ANSYS Meshing using the fluid dynamic automated procedure producing an initial unstructured tetrahedral mesh of approximately 895,000 cells shown in Figure 3.2 (b).
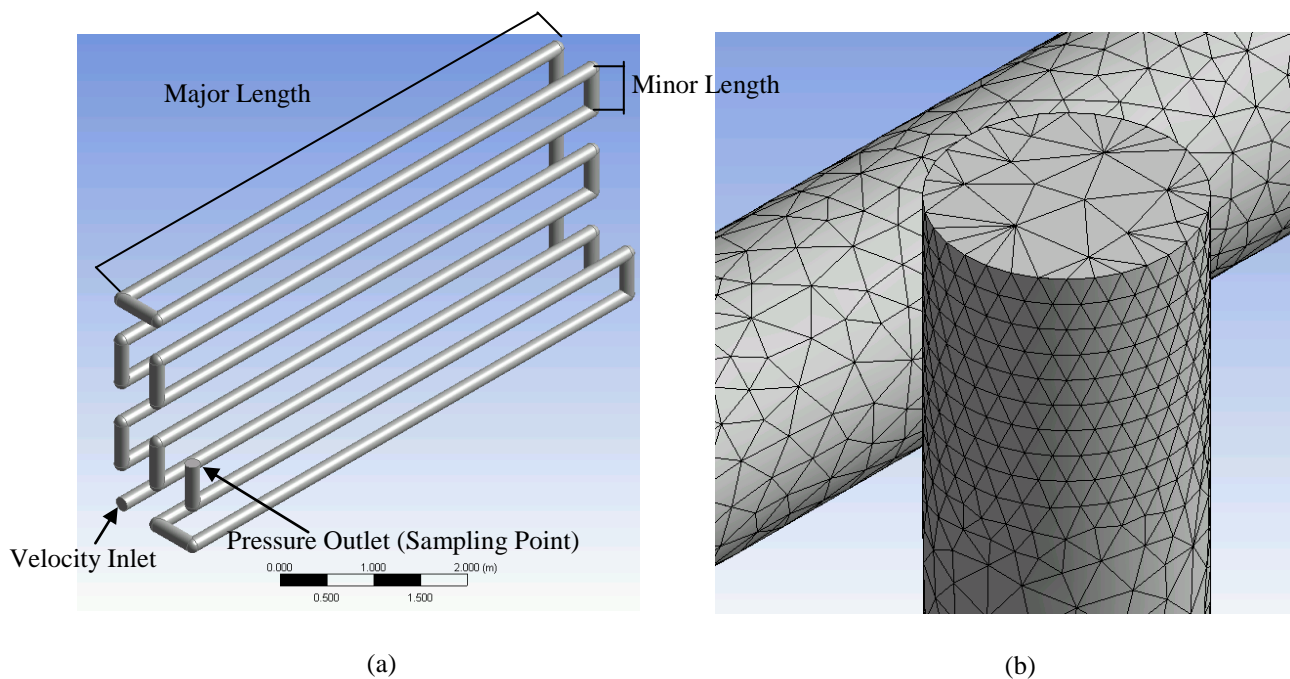

(a)

(b)

Figure 3.2. (a) Pipe loop geometry and (b) unstructured tetrahedral mesh for CFD analysis.

3.1.2. Pipe Loop System FLUENT Setup

This model was then imported into ANSYS FLUENT for setup. The boundary conditions on this system were an inlet velocity (which varied in magnitude depending on the analyzed flow rate), an outlet pressure, and a standard no-slip wall condition for the pipe wall. The turbulent boundary conditions were set to an intensity of 10 percent and hydraulic length of 1 m. As seen in chapter 4, these parameters produced a good correlation with experimental date and were kept constant for all models. The standard *k-ε* turbulence model was used with standard empirically derived model constants ($C_{1\varepsilon}$ = 1.44, $C_{2\varepsilon}$ = 1.92, C_{μ} = 0.09, σ_k = 1.0, and σ_{ε} = 1.3) developed by Jones and Launder (1972). For the solution methods, SIMPLE was used for the velocity-pressure coupling scheme which is described in detail in appendix B using the pressure-based segregated algorithm. The spatial discretization scheme was set to least squares cell based, standard discretization for the pressure term, and second order upwind for the momentum, turbulent kinetic energy, and turbulent dissipation rate terms. The solution was then initialized and run for a steady-state case until the convergence tolerance of 0.001 was met for continuity, *x*, *y*, and *z* velocities, turbulent kinematic energy *k*, and turbulent kinetic energy dissipation rate *ε*. All of the solution methods are described in further detail in appendix B.

This steady-state velocity field provided the basis from which the scalar was transported through the system. In order to analyze the scalar transport, a transient model was used given the converged steady-state velocity field as the initial conditions. Although, the velocity field changes through time, the major flow features are already developed. A user-defined function defining the scalar diffusivity (as discussed in Section 2.8, see e.g., equation 2.16) was introduced and the inlet concentration was set to a constant value of 1 (representing a non-dimensional concentration) to be progressed through time. Because the time step discretization was chosen to be first-order implicit, the solution was unconditionally stable regardless of time step size (discussed further in appendix B). The time step size would affect the accuracy of the solution in regards to scalar transport but was determined to produce the same results for a range of time step sizes from 0.1 to 10 s. For faster computational times, a time step size of 10 s was used throughout this study. To analyze the scalar transport characteristics, a monitor was created to determine the area-weighted average of the passive scalar at the system outlet.

3.1.3. Pipe Loop System Results and Conclusions

To further ensure solution convergence of the computational models, grid independence studies were performed, the full details of which are found in appendix C.

Figure 3.3 shows the contours of velocity magnitude displayed on the *xz*-plane through the pipe loop system operating at 0.001093 m³/s (or 16 gallons per minute (gpm) in English units).

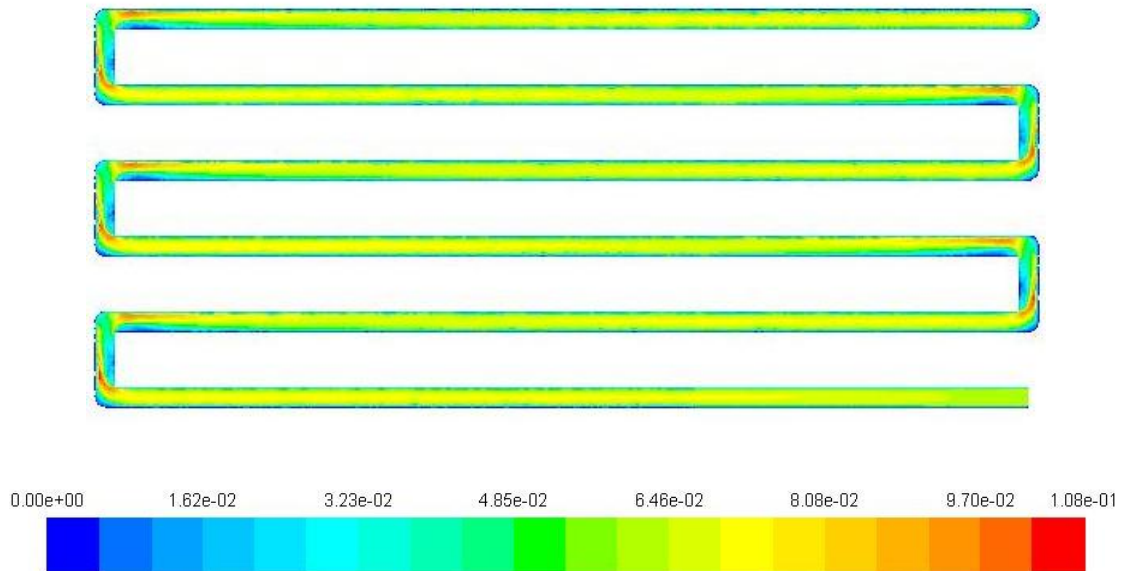**Figure 3.3. Contours of velocity magnitude (m/s) for pipe loop system operating at 0.001093 m³/s (16 gpm).**

Figure 3.4 shows an enlarged portion of the pipe loop system that clearly shows flow separation in the corners due to the inertia. As the developed flow field approaches the corner, it attempts to continue in the same direction due to its momentum but encounters a wall causing the flow to accelerate and separate along the inner wall of the corner. Less severe regions of acceleration and separation are seen as the flow re-enters a major length of the system due to the perturbed flow field. Once in the major length, the flow field returns to a fully developed profile relatively quickly.
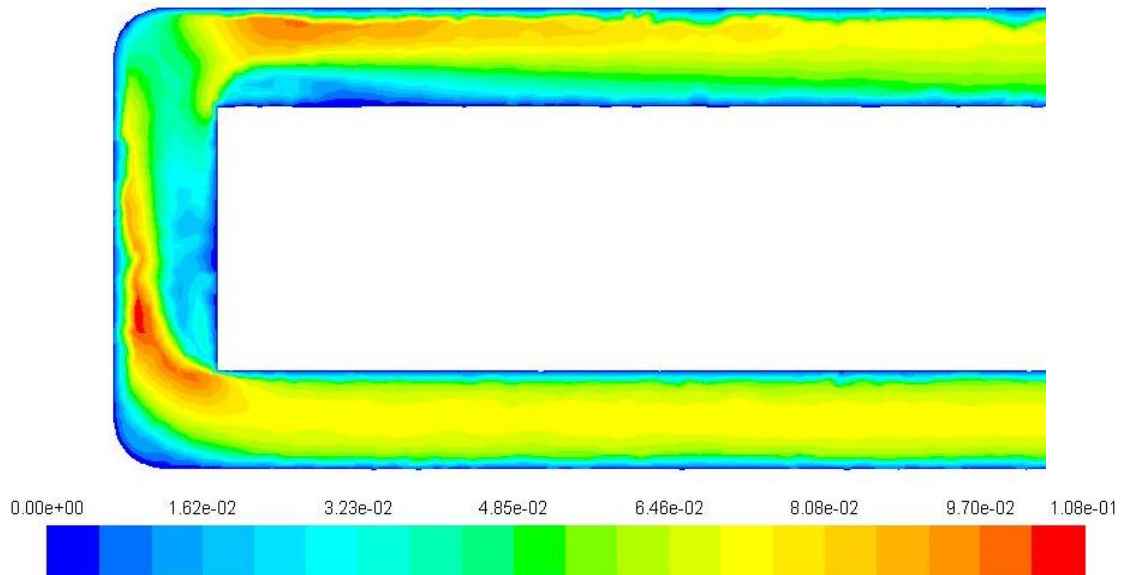

Figure 3.4. Contours of velocity magnitude (m/s) for a corner of the pipe loop system operating at 0.001093 m³/s (16 gpm).

Figure 3.5. shows the velocity vectors for the same portion of the pipe loop observed in Figure 3.4. The velocity vectors more clearly depict the regions of acceleration and recirculation.
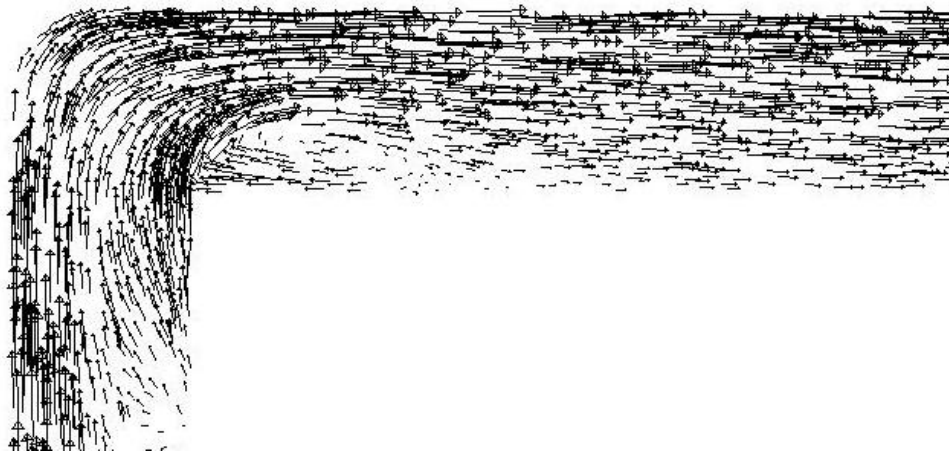

Figure 3.5. Velocity vectors for a corner of the pipe loop system operating at 0.001093 m^3/s (16 gpm).

Determining the amount of turbulent mixing in a system can also aid in evaluating the degree to which a system departs from plug flow behavior. The magnitude of the turbulent viscosity is a result of the turbulent mixing the system imparts through inlet/outlet configurations or flow features inducing regions of separation or recirculation. In the case of the pipe loop, the regions of separation and recirculation seen in Figure 3.5 correspond to the areas of higher dynamic turbulent viscosity μ_t as seen in Figure 3.6.

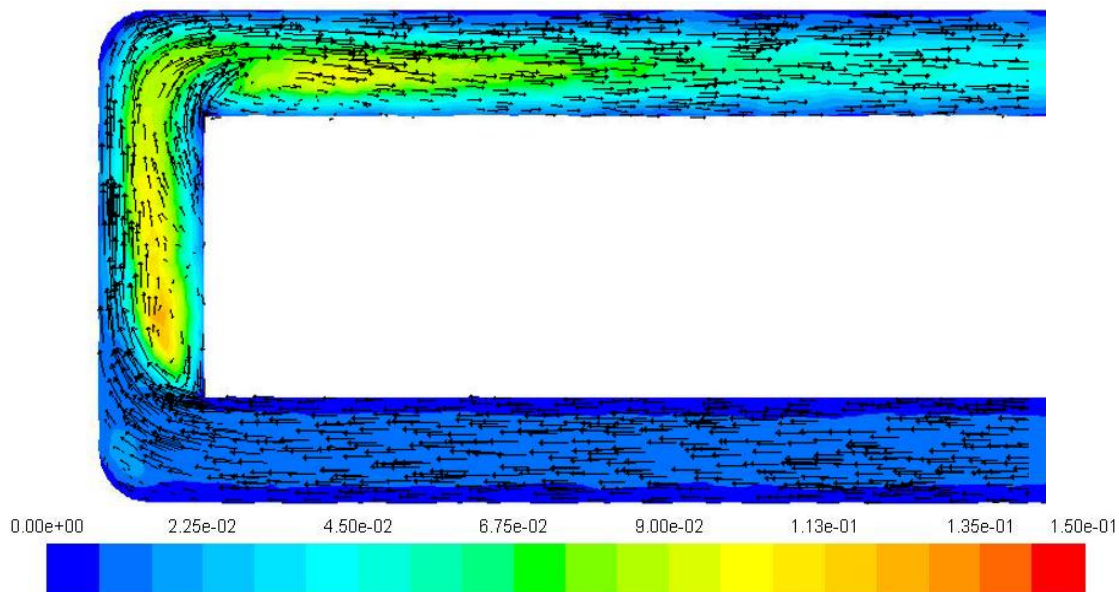**Figure 3.6. Contours of dynamic turbulent viscosity (kg/m-s) and velocity vectors for a corner of the pipe loop system operating at 0.001093 m^3/s (16 gpm).**

As observed in Figures 3.3, 3.4, 3.5, and 3.6, the dead zones are small in comparison to the regions dominated by advection. These flow dynamics lead to a system that is hydraulically efficient at mixing quantities (e.g., passive scalars, conservative tracers, or chlorine-containing species) through the system which is why pipe loops are considered ideal plug flow reactors. In the scalar transport model, the flow acceleration in the corners is seen to have a direct influence on the passive scalar transport through the system. The scalar field accelerates through the corners but evens out as the flow returns to a developed profile. Figures 3.7(a)-(h) depict the scalar field as it is transported through the pipe loop system for a flow rate of 0.001093 m³/s (16 gpm).
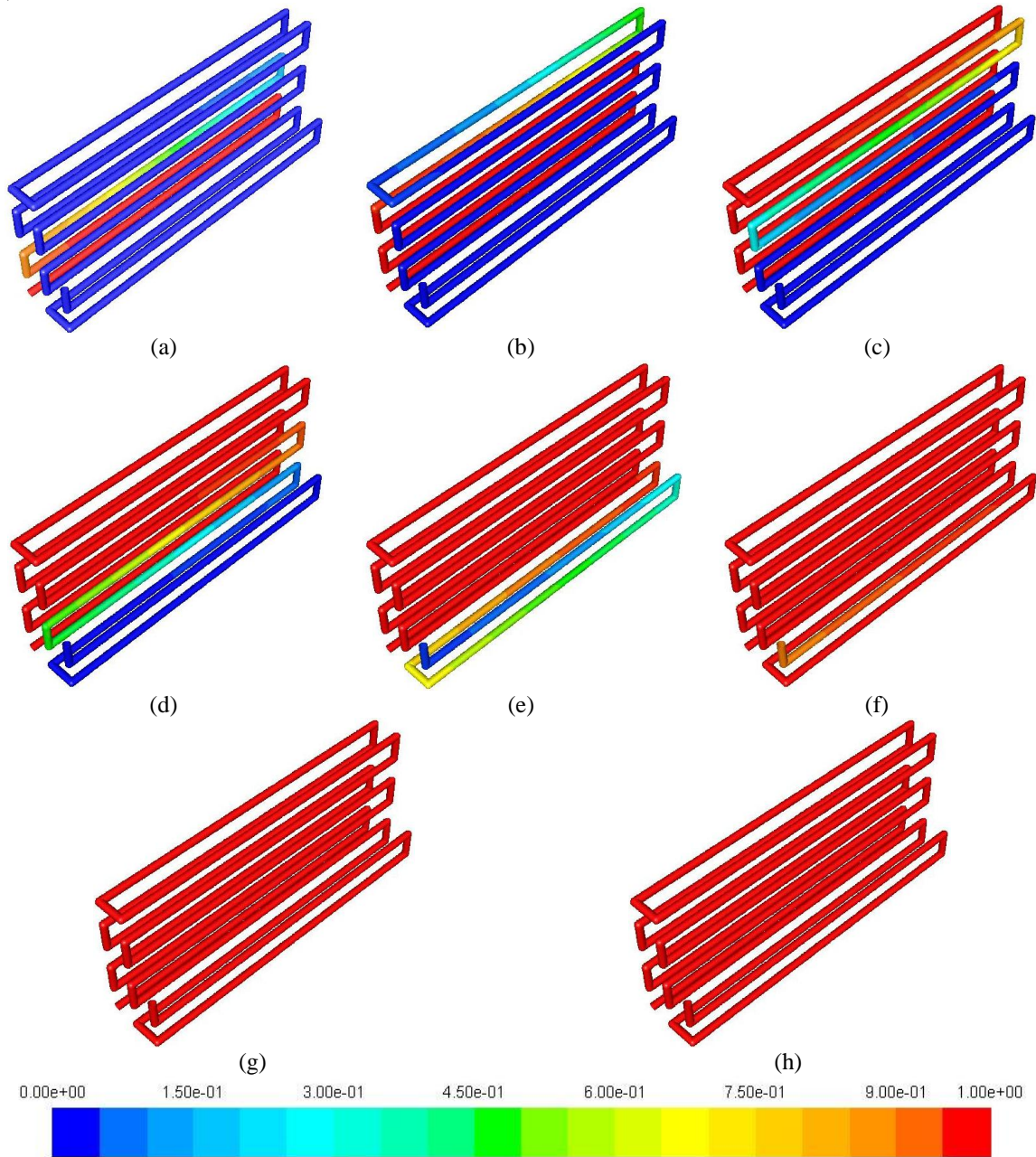

(a)   (b)   (c)

(d)   (e)   (f)

(g)   (h)

Figure 3.7. Contours of scalar concentration for pipe loop system operating at 0.001093 m³/s (16 gpm) for (a) t = 300 s, (b) t = 600 s, (c) t = 900 s, (d) t = 1200 s, (e) t = 1500 s, (f) t = 1800 s, (g) t = 2100 s, and (h) t = 2400 s.

3.2. Pressurized Tank Systems

This system was constructed at Colorado State University's hydraulics laboratory at the Engineering Research Center. The pressurized tank system was constructed using industry standard 0.3 m^3 (80 gallon) fiberglass tanks connected using 0.03175 m diameter schedule 80 PVC pipe and plumbed in a manner that allowed multiple flow arrangements to be analyzed without altering the footprint of the system. The system was analyzed for 1, 2, and 3 tanks in series, respectively, as shown in Figure 3.8. The footprint of this system was also altered by placing all 6 tanks in series to facilitate analysis of 4, 5, and 6 tanks in series.

Figure 3.8. Pressurized Series Tank System at CSU's ERC hydraulic laboratory.

The system was connected to a raw water supply fed from Horsetooth Reservoir in Fort Collins to the Engineering Research Center's hydraulic laboratory. The 3 series tank configuration was analyzed for 0.001262, 0.000946, 0.000631, and 0.000316 m^3/s (20, 15, 10, and 5 gpm). The 6 series tank configuration was analyzed for 0.001893, 0.001262, 0.000946, and 0.000631 m^3/s (30, 20, 15, and 10 gpm). A wide range of inlet pressures was observed depending on the desired flow rate. The inlet pressure for the maximum analyzed flow rate of 0.001893 m^3/s (30 gpm) was approximately 414 kPa (60 psi). The fiberglass tanks have a maximum pressure rating of 552 kPa (80 psi) and thus the system was limited via a pressure relief valve to 483 kPa (70 psi). Higher pressures were needed to drive flow through the systems as a result of the observed pressure losses discussed further in Subsection 3.2.2.3 and quantified through the hydraulic model presented in appendix D.

3.2.1. Pressurized Tank System Computational Model Setup

Using ANSYS DesignModeler the following models were created for the two footprints of 2 sets of 3 tanks in series and 6 tanks in series as seen in Figures 3.9(a) and (b), respectively.
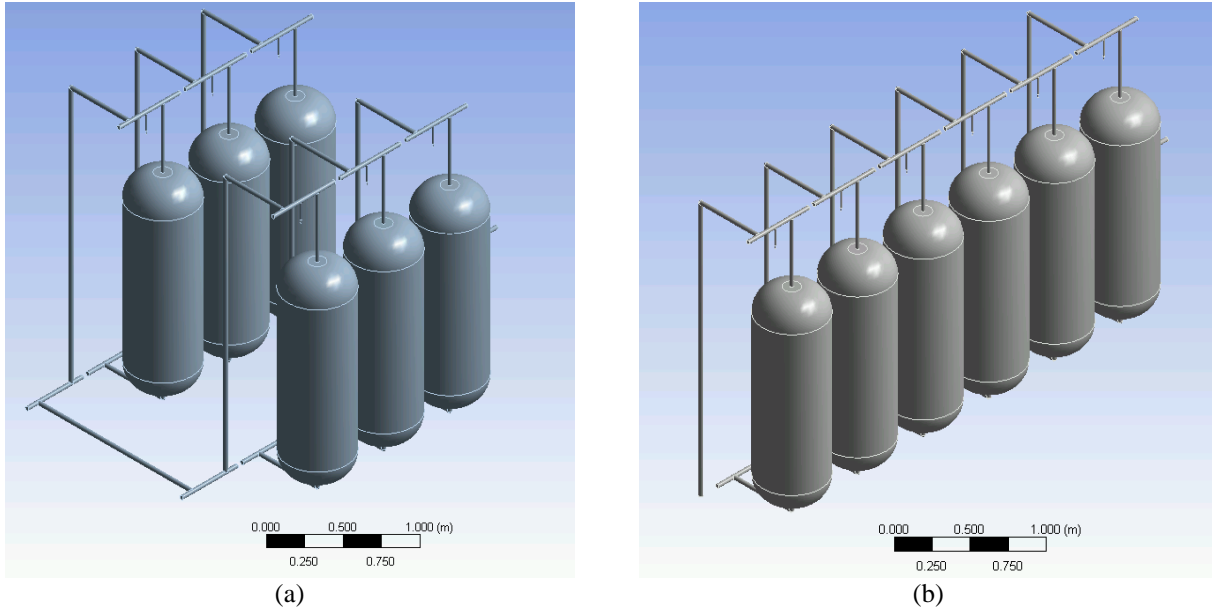
Figure 3.9. Pressurized tank configurations for (a) 3 series and (b) 6 series systems for CFD analysis.

The model with 2 sets of 3 tanks in series was meshed using ANSYS Meshing using the fluid dynamic automated procedure producing an unstructured tetrahedral mesh of 2,104,000 cells. The model of 6 tanks in series was meshed using the same procedure producing an unstructured tetrahedral mesh of 1,800,000 cells. Figure 3.10 displays a region of the unstructured tetrahedral mesh used for the pressurized tank systems.
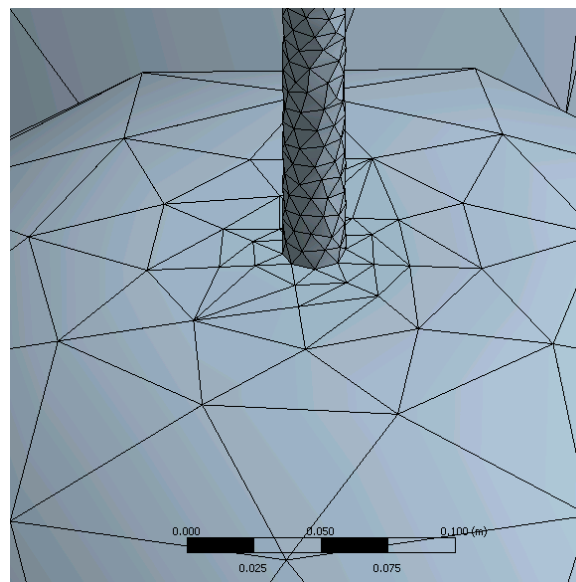

Figure 3.10. Unstructured tetrahedral mesh for pressurized tank systems.

3.2.2. Pressurized Tank System FLUENT Setup

The FLUENT setup for the pressurize tank system configuration followed the same procedure as described for the pipe loop system except the monitor for the area-weighted average of the passive scalar was varied depending on the number of tanks in series to be analyzed.

3.2.3. Pressurized Tank System Results and Conclusions

The grid independence studies for both of these systems can also be found in appendix C.

Figure 3.11 shows the contours of velocity magnitude for the 3 series tank system operating at 0.001262 m^3/s (20 gpm) about a *xz*-plane cut through the center of the tanks limiting the displayed maximum velocity to 1 m/s.
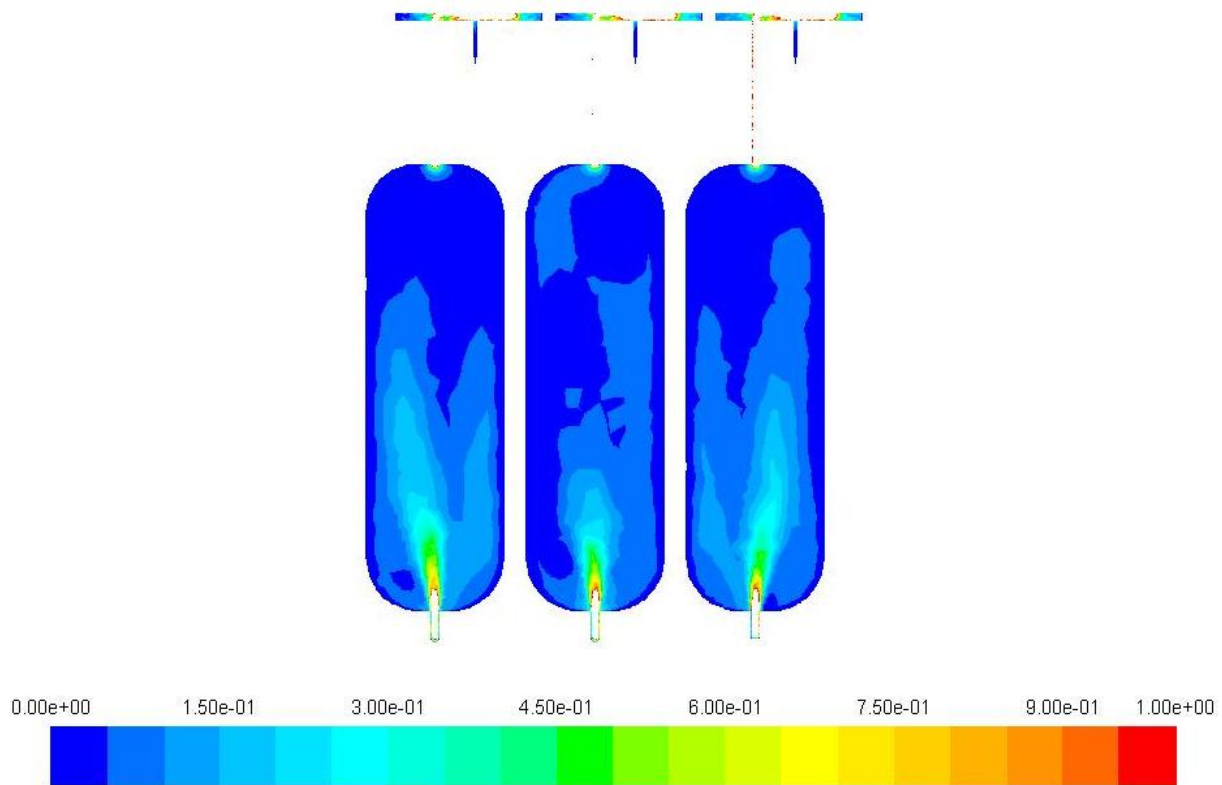
Figure 3.11. Contours of velocity magnitude (m/s) for the 3 series tank system operating at 0.001262 m^3/s (20 gpm).

The maximum velocities in the pressure tank systems occur at the entrance to the tanks where flow exits a small pipe into a larger tank carrying much of its momentum with it into the tank in the form of a jet. Figure 3.12 show the velocity vectors for the 3 tank system about the *xz*-plane through the center of the tanks.
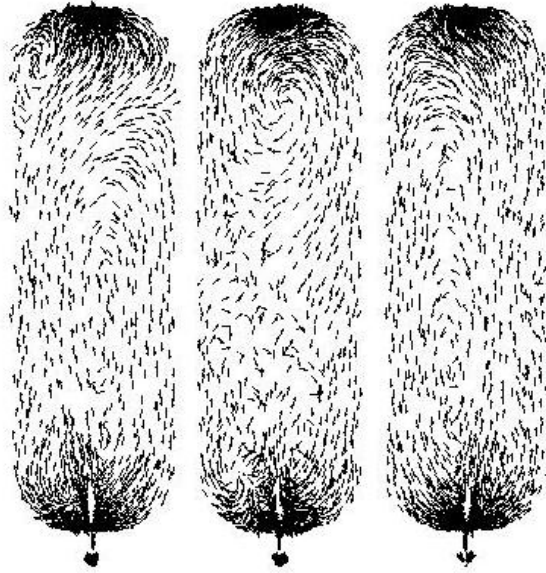
Figure 3.12. Velocity vectors for the 3 series tank system operating at 0.001262 m³/s (20 gpm).

To give a more complete picture of the velocity field, Figure 3.13 shows the velocity vectors about a *xy*-plane cut through the tanks 1 m from the bottom. These velocity vectors clearly show circulation regions around the perimeter, indicators of a swirling behavior in the tanks.

Figure 3.13. Velocity vectors for the 3 series tank system operating at 0.001262 m³/s (20 gpm).

Figure 3.14 displays the dynamic turbulent viscosity μ_t for the 3 tank system operating at 0.001262 m³/s (20 gpm) and limited to a displayed maximum value of 1.25 kg/m-s.
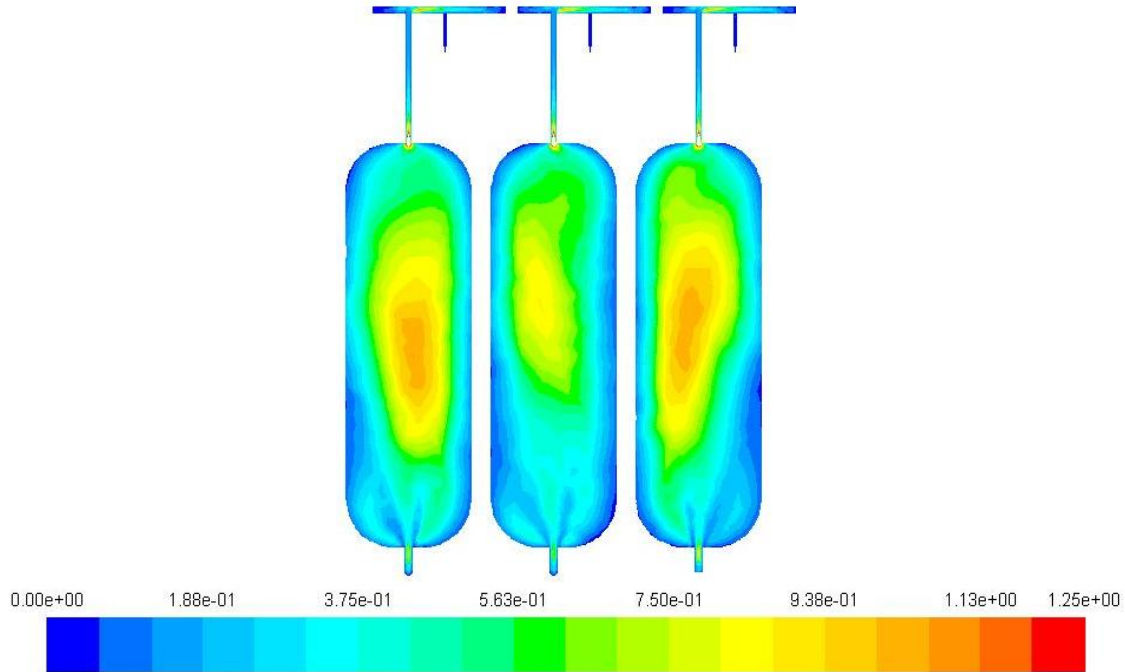
Figure 3.14. Contours of dynamic turbulent viscosity (kg/m-s) for the 3 series tank system operating at 0.001262 m³/s (20 gpm).

For the 3 series pressure tank system, the turbulent viscosity is more than three orders of magnitude large than the molecular viscosity of water in the system. These regions of higher turbulent viscosity correspond to the regions of higher mixing as observed through the velocity vectors in Figures 3.12 and 3.13.

Figures 3.15(a)-(h) display the contours of scalar concentration for the time-stepping transient solution to the RANS model as driven by the velocity field.
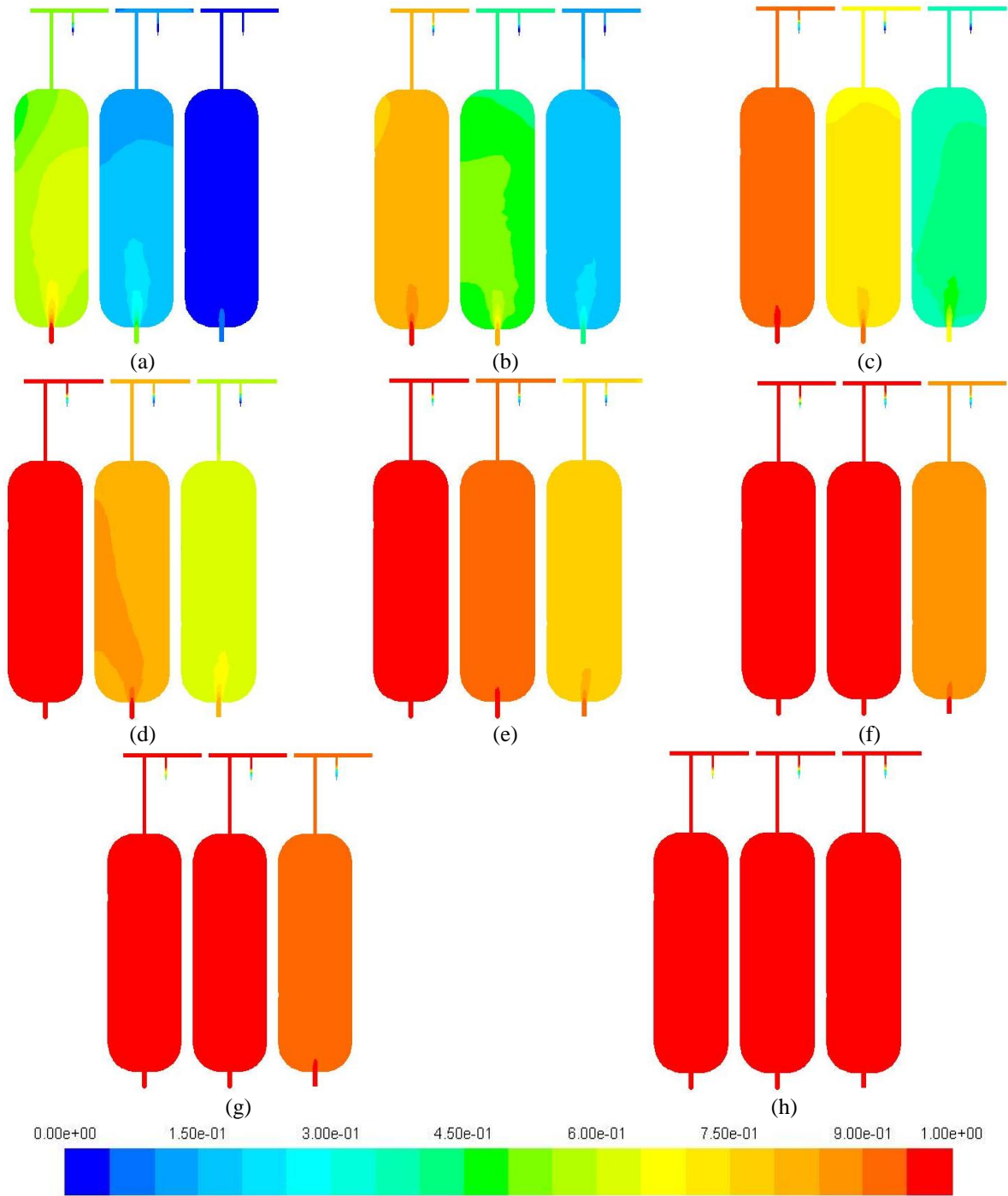
Figure 3.15. Contours of scalar concentration for 3 series tank system operating at 0.001262 m³/s (20 gpm) for (a) t = 250 s, (b) t = 500 s, (c) t = 750 s, (d) t = 1000 s, (e) t = 1250 s, (f) t = 1500 s, (g) t = 1750 s, and (h) t = 2000 s.

While it is known that the flow dynamics drive the transport of a passive scalar through a system, Figure 3.16 shows the scalar transport field for a time of 250 s overlain with the velocity vectors. It can be observed that areas of recirculation in the tank correspond to a lower value of scalar concentration. The scalar follows the flow path in the most direct route from the inlet to the outlet. While there are no true dead zones in these tanks, the spherical geometries at the tops and

bottoms of the tanks force mixing within the flow. The regions experiencing circulation increase in scalar concentration slower than the direct flow paths which lead to a system not nearly as efficient as the pipe loop system.

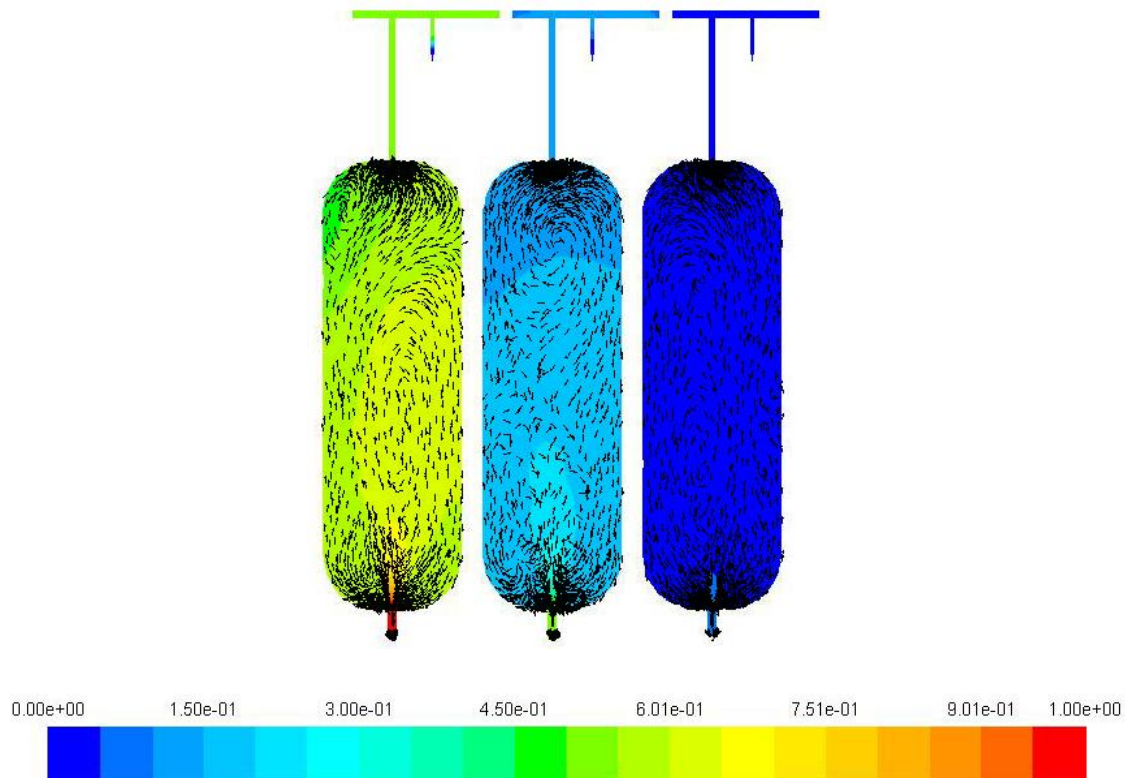**Figure 3.16. Scalar transport field at t = 250 s and velocity vectors for the 3 series tank system operating at 0.001262 m³/s (20 gpm).**

Figure 3.17 shows the contours of velocity magnitude for the 6 series tank system operating at 0.001893 m³/s (30 gpm) about a *xz*-plane cut through the center of the tanks limiting the maximum velocity to 1 m/s.
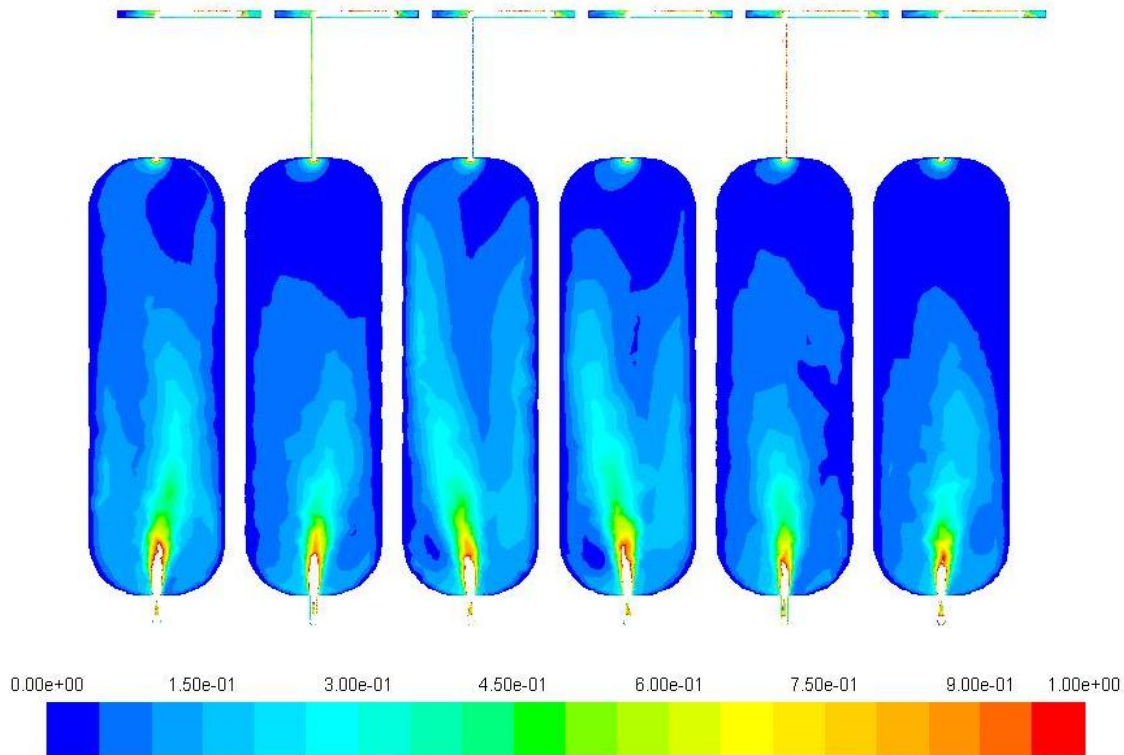
Figure 3.17. Contours of velocity magnitude (m/s) for the 6 series tank system operating at 0.001893 m³/s (30 gpm).

The highest velocity in these pressure tank systems is once again seen at the entrance to the tanks where flow exits a small pipe into a larger tank carrying much of its momentum with it into the tank in the form of a jet. Figure 3.18 shows the velocity vectors for the 6 tank system about the *xz*-plane through the center of the tanks. As seen with the 3 tank system, the 6 tank system exhibits the same general flow characteristics despite the more significant pressure losses observed by doubling the number of tanks in series.
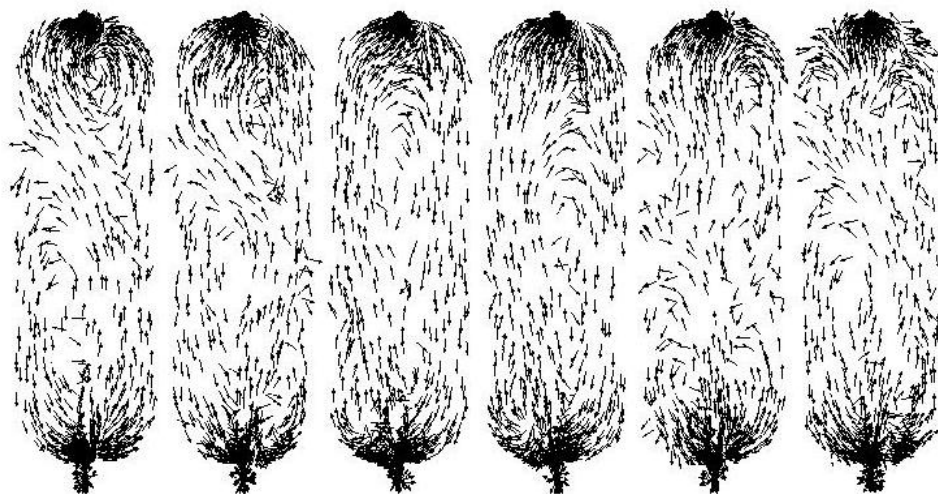
Figure 3.18. Velocity vectors for the 6 series tank system operating at 0.001893 m³/s (30 gpm).

Figure 3.19 displays the contours of turbulent dynamic viscosity for the 6 tank system limited to 2 kg/m-s.
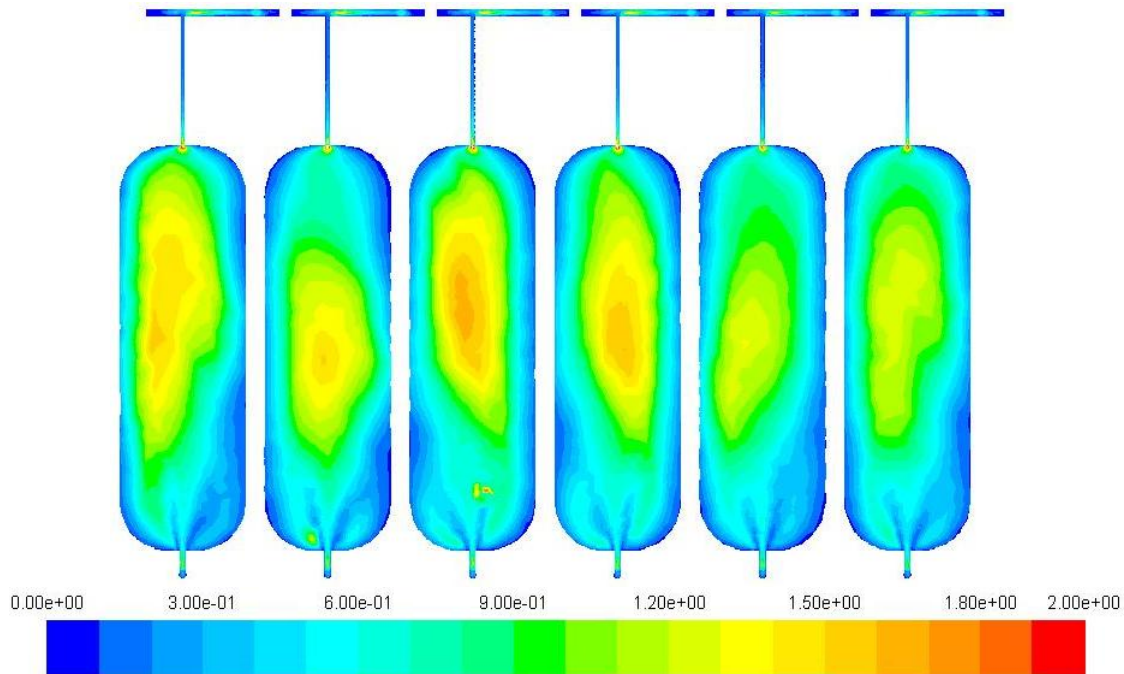
Figure 3.19. Contours of turbulent dynamic viscosity (kg/m-s) for the 6 series tank system operating at 0.001893 m³/s (30 gpm).

As expected, the increase in velocity within the same pressurized tanks resulted in intensified regions of turbulent mixing and associated higher values of turbulent viscosity. Figures 3.20 (a)-(h) display the contours of scalar concentration for the time-stepping transient solution to the RANS model as driven by the velocity field.
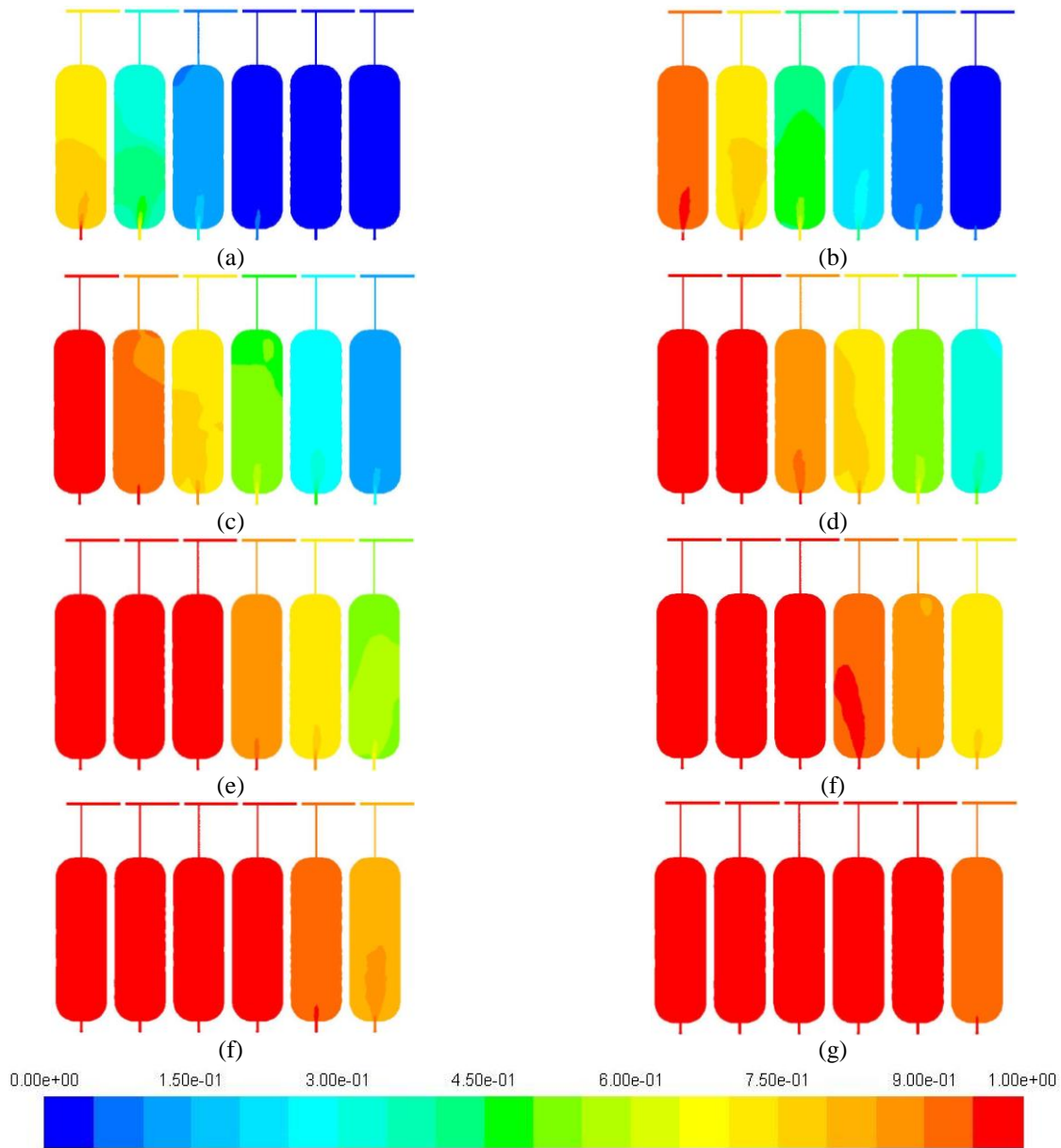
Figure 3.20. Contours of scalar concentration for 6 series tank system operating at 0.001893 m³/s (30 gpm) for (a) t = 250 s, (b) t = 500 s, (c) t = 750 s, (d) t = 1000 s, (e) t = 1250 s, (f) t = 1500 s, (g) t = 1750 s, and (h) t = 2000 s.

Figure 3.21 shows the scalar transport field for a time of 750 s and corresponding velocity vectors.
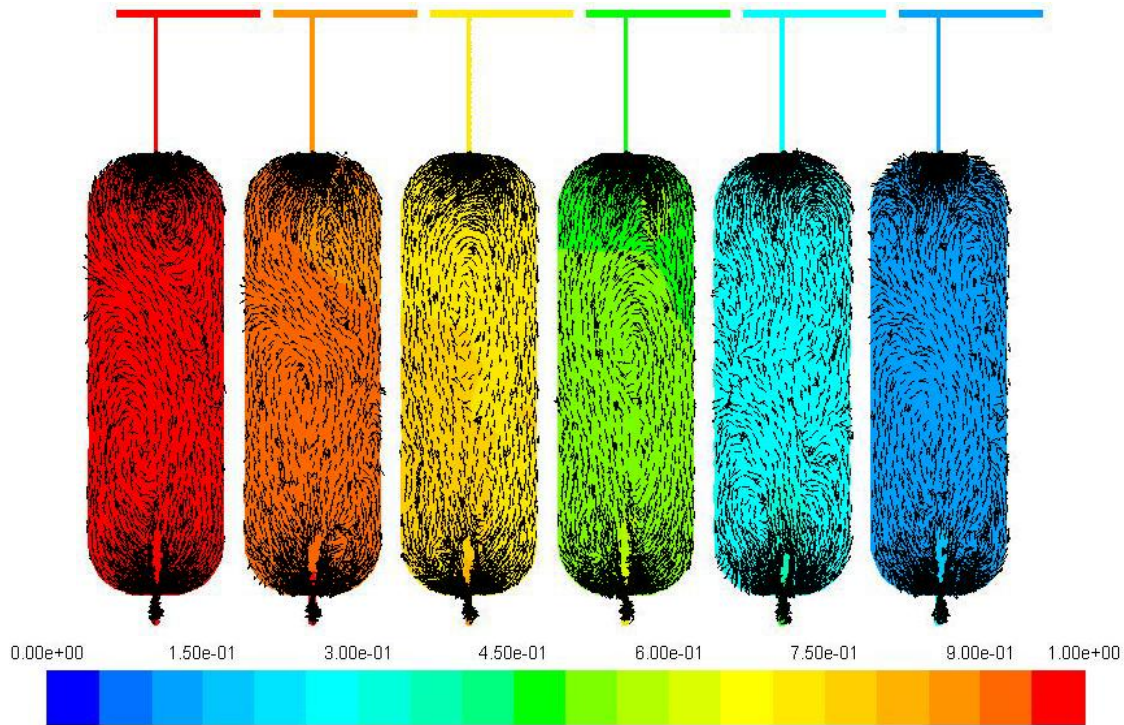
Figure 3.21. Scalar transport field at t = 750 s and velocity vectors for the 6 series tank system operating at 0.001893 m³/s (30 gpm).

Once again, the regions of lower scalar concentration in a given tank result from areas of recirculation.

3.3 Open Surface Tank Systems

These systems were constructed at Colorado State University's hydraulics laboratory at the Engineering Research Center. One system was comprised of a 1.89 m³ (or 500 gallon) capacity vertical polyethylene tank with an inlet comprised of a 90 degree end tilted 45 degrees from horizontal towards the bottom of the tank and a pressure-break outlet from the top of the tank as pictured in Figure 3.22 (a). The other system was comprised of a 1.99 m³ (or 525 gallon) capacity horizontal polyethylene tank with a similar inlet and outlet as described for the vertical tank and shown in Figure 3.22 (b).

<center>(a)   (b)</center>

Figure 3.22. (a) Vertical open surface tank system and (b) horizontal open surface tank system at CSU's ERC hydraulic laboratory.

3.3.1. Open Surface Tank Systems Computational Model Setup

Using ANSYS DesignModeler the following models were created for the two polyethylene tanks show in Figures 3.23 (a) and (b).
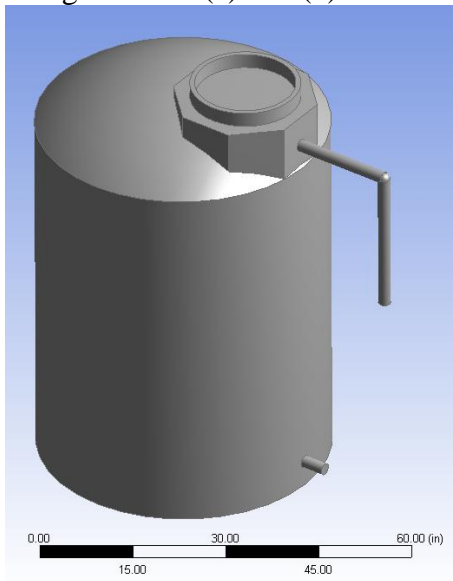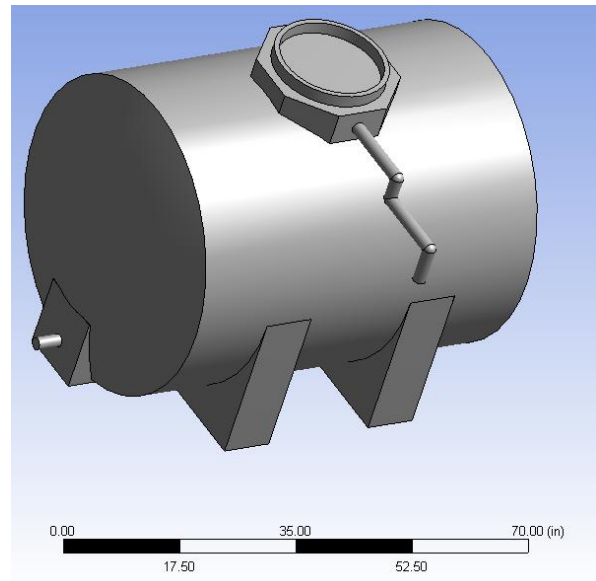
<center>(a)   (b)</center>

Figures 3.23. (a) Vertical open surface tank system and (b) horizontal open surface tank system model geometry for CFD analysis.

The differences between the prototype systems in Figures 3.22 (a) and (b) and the model geometry in Figures 3.23 (a) and (b) are evident. The simplifications in the model geometry are a result of the difficulty in meshing a model with all of the nuances of the physical systems which created steep gradients in cell size ultimately leading to divergence in the computational model. Removing some of the features that were not significant to the flow dynamics provided smoother transition in mesh elements leading to a stable solution to the respective problems. Figures 3.24

(a) and (b) show the unstructured tetrahedral meshes used for CFD analysis of the vertical and horizontal open surface tank systems.

(a)   (b)
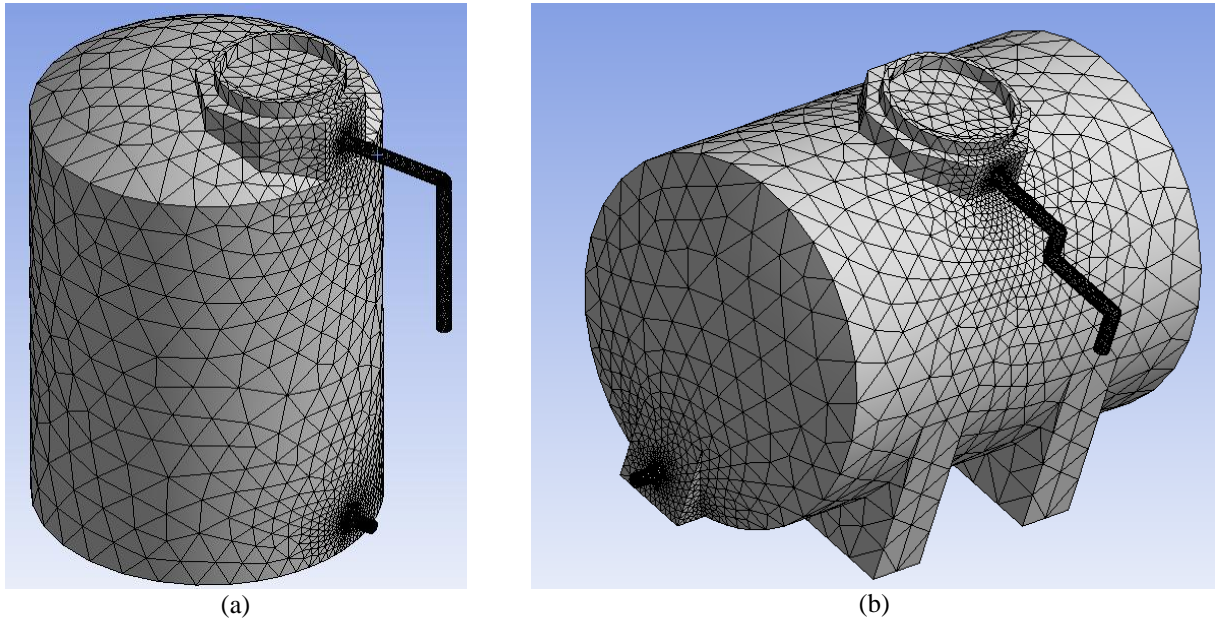
Figures 3.24. Unstructured tetrahedral mesh for (a) vertical and (b) horizontal open surface tank systems.

3.3.2. Open Surface Tank Systems FLUENT Setup

The FLUENT setup for the open surface tank system configurations followed the same procedure as described for the pipe loop system. Another simplification in modeling these open surface tanks was to model them as pressurized tanks which significantly lowered the complexity yet yielded accurate results as compared to the physical experiments.

3.3.3. Open Surface Tank Systems Results and Conclusions

While the major hydrodynamic features remained the same for all of the flow rates, 0.000315, 0.000631, and 0.000946 m^3/s (5, 10, and 15 gpm), they did vary in intensity. Figure 3.25 shows the contours of velocity magnitude for the vertical open surface tank system operating at 0.000946 m^3/s (15 gpm) on a *xz*-plane through the middle of the tank limited to 0.1 m/s. Limiting the maximum velocity allows for visualization of velocity contours through the entire tank and not just the inlet and outlets (by continuity the velocities in the inlet and outlet sections are considerably greater than in the tank).
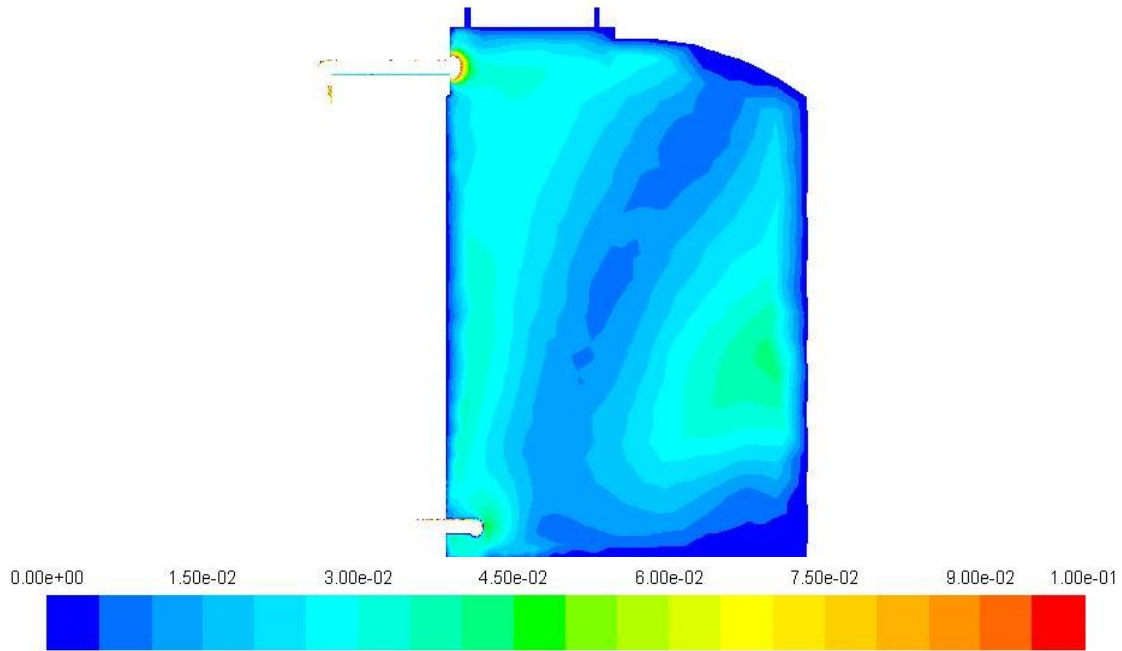
Figure 3.25. Contours of velocity magnitude (m/s) for vertical open surface tank system operating at 0.000946 m^3/s (15 gpm).

The exact nature of the highly three dimensional flow field induced by the inlet condition is difficult to perceive in a two-dimensional plane but it is evident that the left and right (as observed in Figure 3.25) encounter greater velocities while the center portion of the tank experiences lower velocities. Figures 3.26, 3.27, and 3.28 depict the velocity vectors on the same plane as pictured above, about a *xy*-plane cut through the tank 0.1 m from the bottom, and about a *xy*-plane cut through the tank 1.5 m from the bottom, respectively.
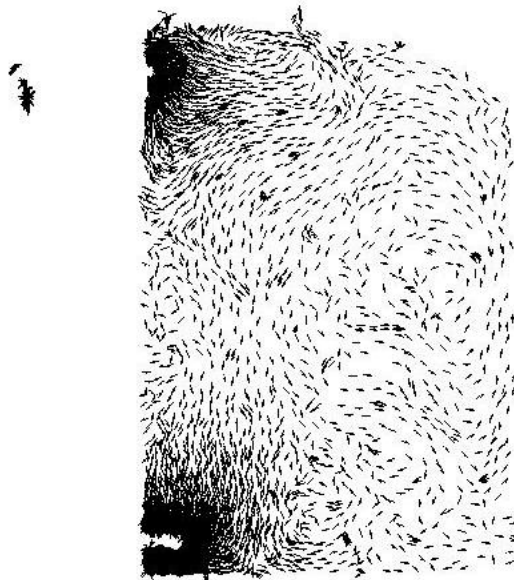
Figure 3.26. Velocity vectors for vertical open surface tank system operating at 0.000946 m^3/s (15 gpm).
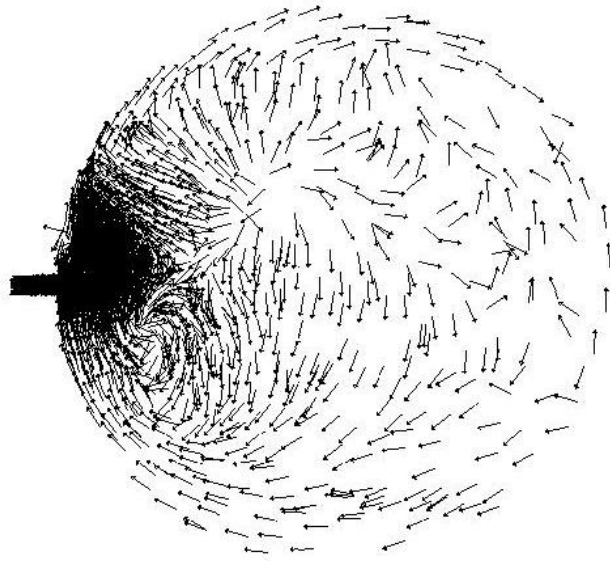
Figure 3.27. Velocity vectors for vertical open surface tank system operating at 0.000946 m³/s (15 gpm) about a xy-plane 0.1 m from the bottom surface.
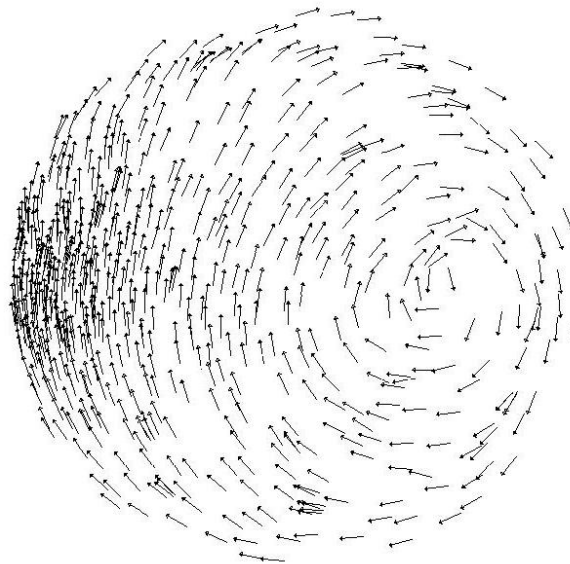
Figure 3.28. Velocity vectors for vertical open surface tank system operating at 0.000946 m³/s (15 gpm) about a xy-plane 1.5 m from the bottom surface.

Figure 3.26 shows distinct regions of circulation in the tank. Figure 3.27 shows chaotic velocity vectors resulting from the inlet configuration in the tank but the beginnings of a spiraling circulation are seen along the perimeter of the tank 0.1 m from the bottom of the tank. Figure 3.28 shows a clear clockwise circulation pattern has developed 1.5 from the bottom of the tank. There is also a region of recirculation, or dead zone, observed near the right wall of the tank in Figure 3.26 which corresponds closely to the lower region of velocity observed in Figure 3.25. Figure 3.29 shows the three-dimensional pathlines in the tank as transported by the velocity field from the inlet to the outlet and colored by residence time in the tank.
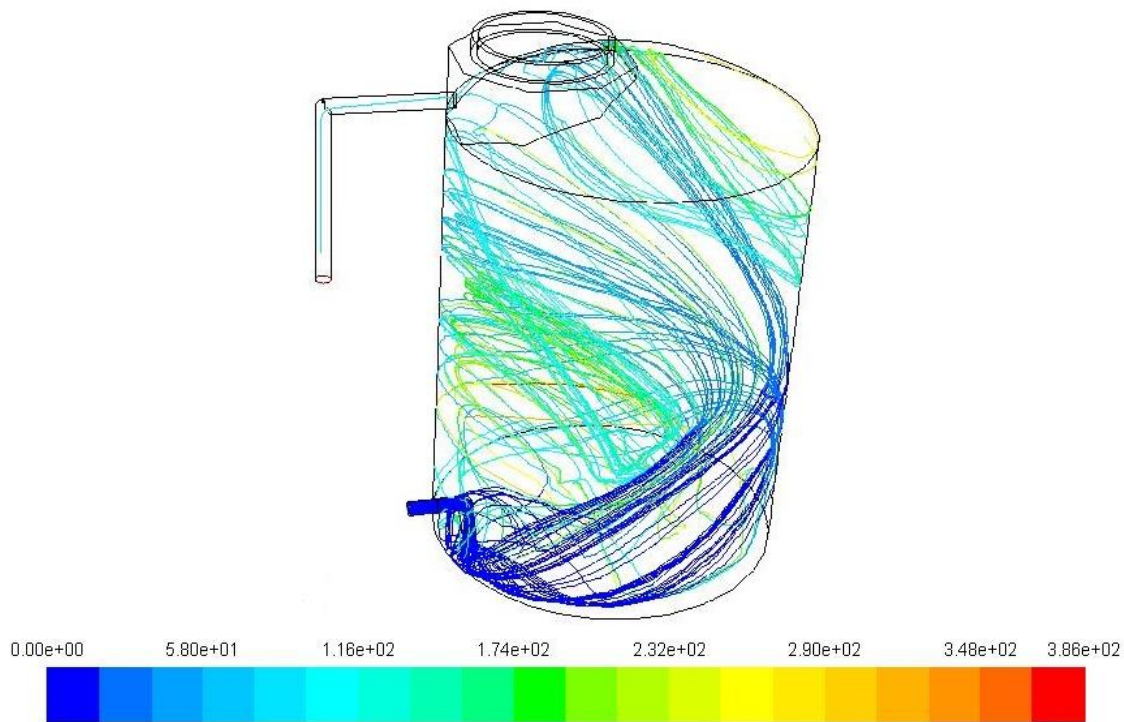
Figure 3.29. Three-dimensional pathlines of particle residence time (s) for vertical open surface system operating at 0.000946 m^3/s (15 gpm).

The three-dimensional pathlines gives a better overall visual representation of the flow field seen in Figure 3.25. The nature of the flow circulates around the perimeter of the tank in the *z*-direction towards the tank outlet. The simplification in analyzing this tank as a pressurized system allows for the flow to be deflected by the tanks upper surface inducing some additional turbulent mixing in the system. Yet the scalar transport characteristics over the analyzed flow rates compared closely to the physical tracer study results. As discussed with the pressurized tank systems, the regions of higher turbulent viscosity in the vertical open surface tank correspond to the areas of higher mixing as observed in the velocity vectors in Figures 3.26.

Figure 3.30 displays the contours of turbulent viscosity on a *xz*-plane through the center of the vertical open surface tank.
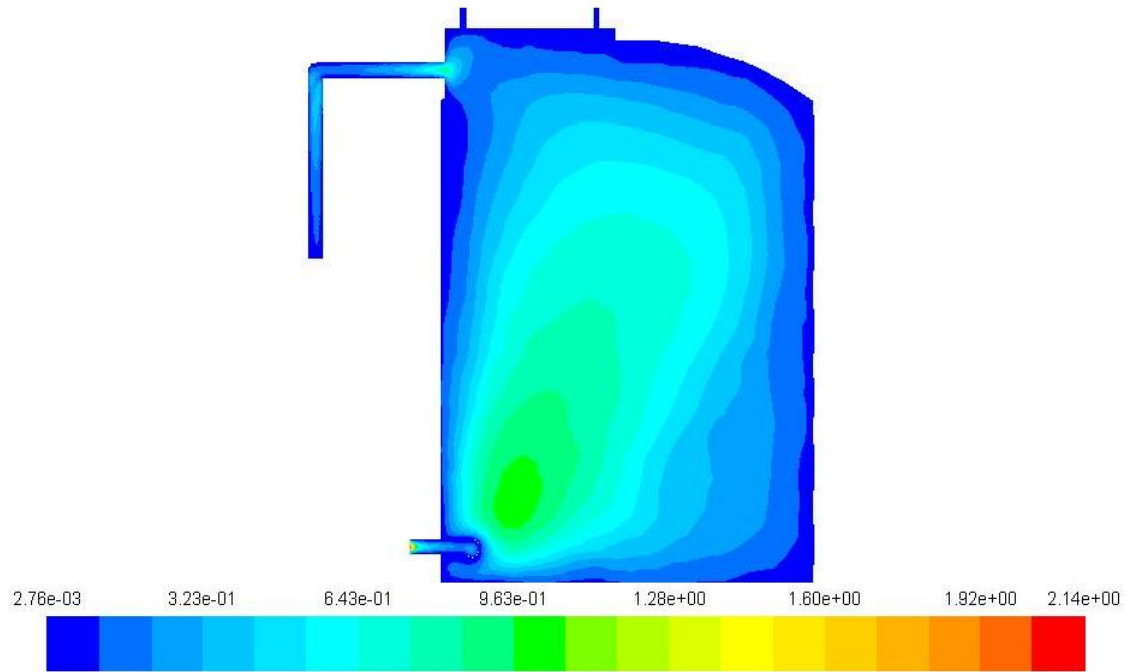
Figure 3.30. Contours of dynamic turbulent viscosity (kg/m-s) for the vertical open surface tank system operating at 0.000946 m³/s (15 gpm).

The values of higher turbulent viscosity correspond to the regions of greater mixing as observed in Figure 3.26.

Figures 3.31 (a)-(i) display the contours of scalar concentration for the time-stepping transient solution to the vertical open surface tank RANS model as driven by the highly three-dimensional velocity field.
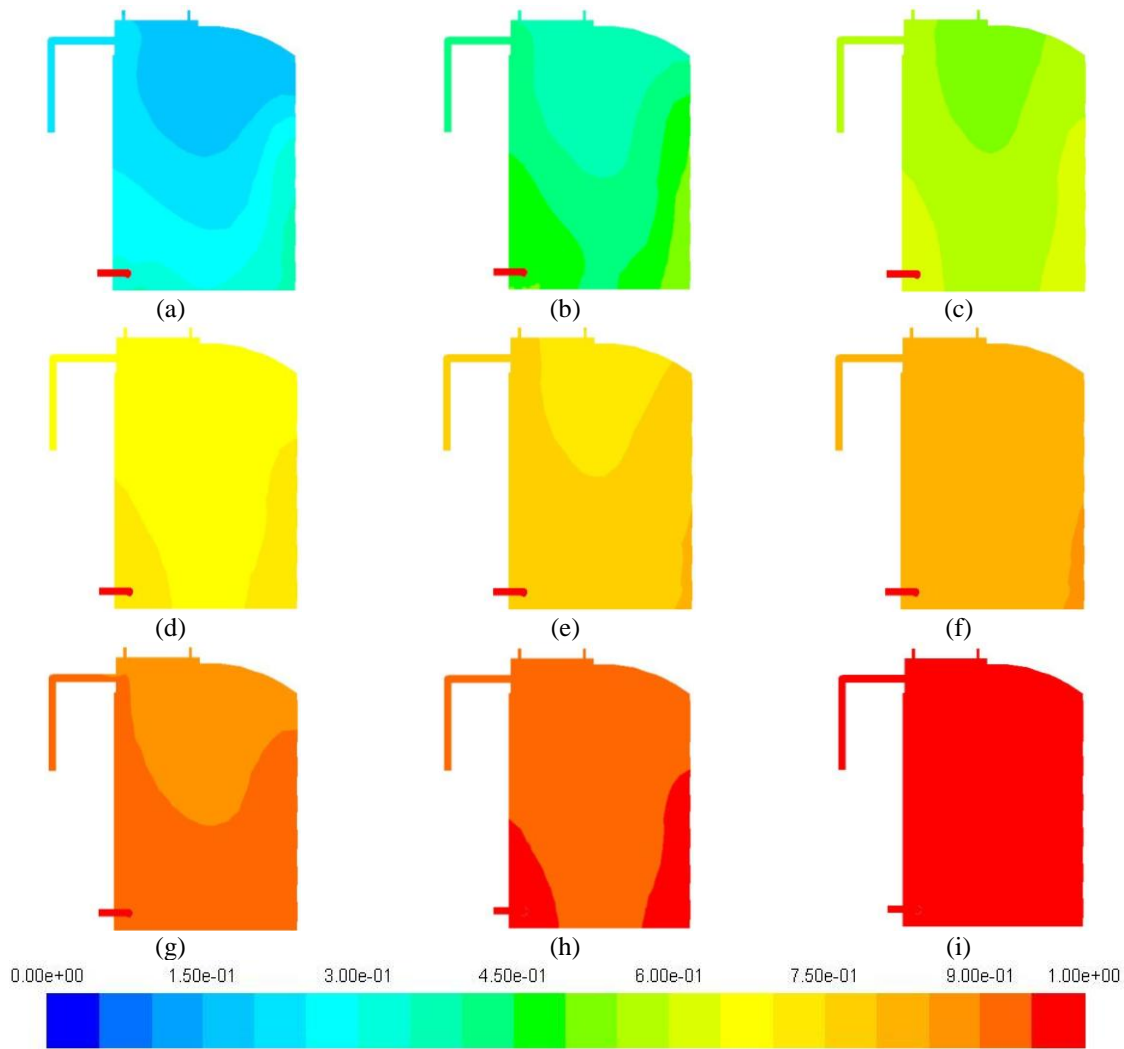
Figure 3.31. Contours of scalar concentration for vertical open surface tank system operating at 0.000946 m³/s (15 gpm) for (a) t = 600 s, (b) t = 1200 s, (c) t = 1800 s, (d) t = 2400 s, (e) t = 3000 s, (f) t = 3600 s, (g) t = 4800 s, (h) t = 6000 s, and (i) t = 7800 s.

The scalar concentration, as seen on the depicted *xz*-plane, increases around the perimeter of the tank first. It takes much longer for the scalar to increase in the center portion of the tank because of the large region of circulation.

Figure 3.33 shows the scalar concentration in the vertical open surface tank system for a time of 1800 s overlain with the velocity vectors.
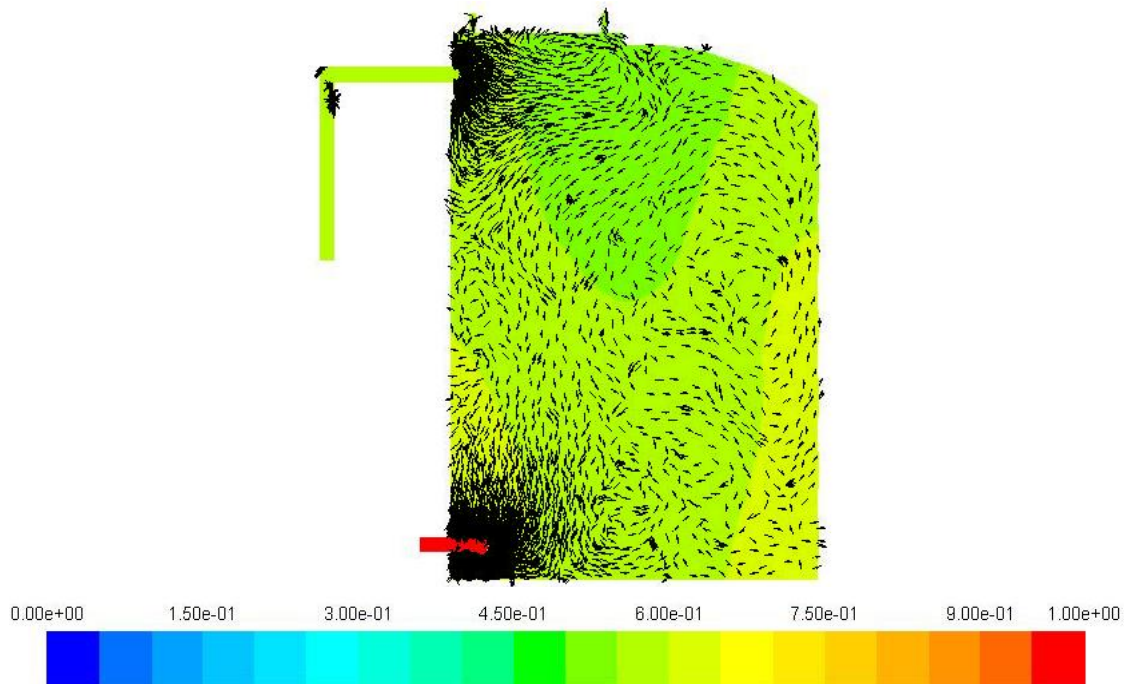
Figure 3.33. Scalar transport field at t = 1800 s and velocity vectors for vertical open surface tank system operating at 0.000946 m³/s (15 gpm).

It is more difficult to observe a relationship between the velocity vectors and scalar concentration about a *xz*-plane through the center of the tank. The scalar field is influenced greater by the flow circulation about the perimeter of the tank as observed in Figures 3.28, 3.29, and 3.30.

As in the vertical open surface tank, the major hydrodynamic features remained the same for all of the flow rates, 0.000315, 0.000631, and 0.000946 m³/s (5, 10, and 15 gpm), while varying in intensity. Figure 3.34 shows the contours of velocity magnitude for the horizontal open surface tank system operating at 0.000946 m³/s (15 gpm) on a *xz*-plane through the middle of the tank limited to 0.1 m/s.
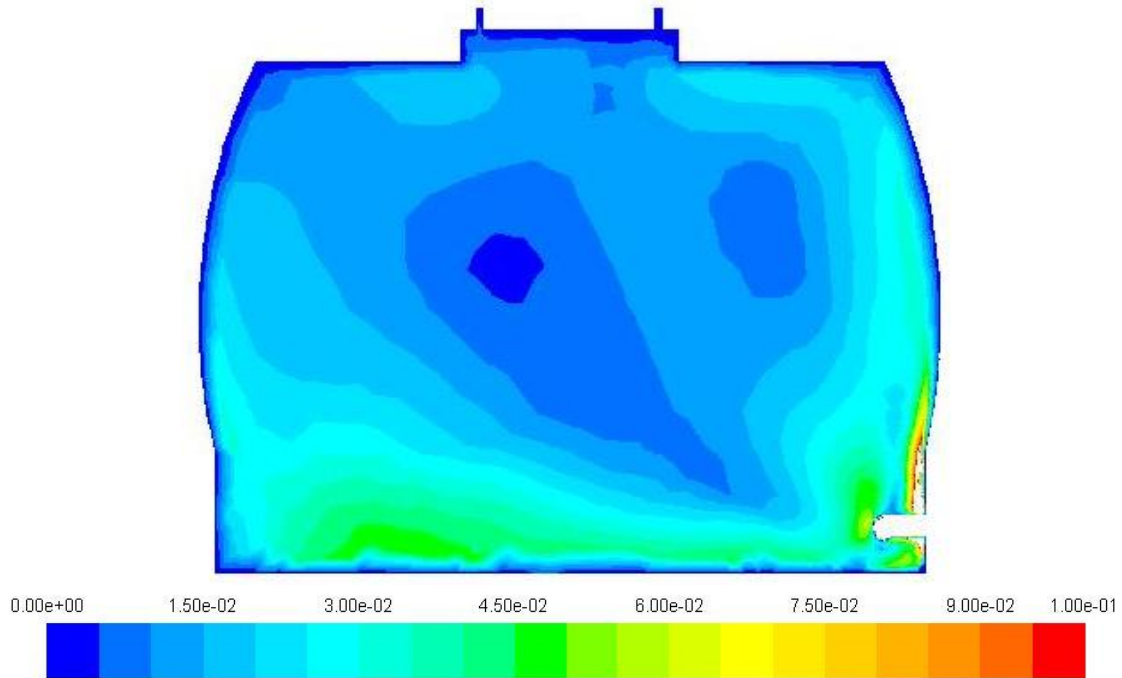
Figure 3.34. Contours of velocity magnitude (m/s) for horizontal open surface tank system operating at 0.000946 m³/s (15 gpm).

Figures 3.35 and 3.36 display the velocity vectors of the horizontal open surface tank operating at 0.000946 m³/s (15 gpm) about a *xz*-plane through the middle of the tank and a *xy*-plane 0.1 m from the bottom of the tank.
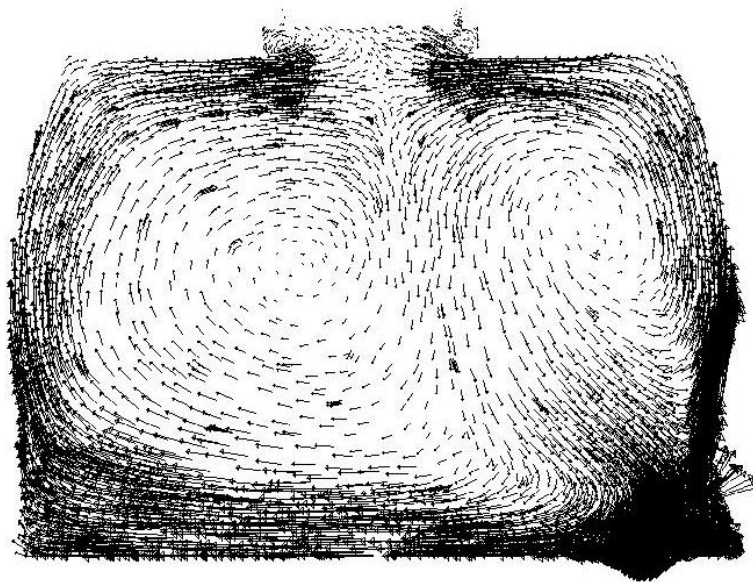
Figure 3.35 Velocity vectors for horizontal open surface tank system operating at 0.000946 m³/s (15 gpm).
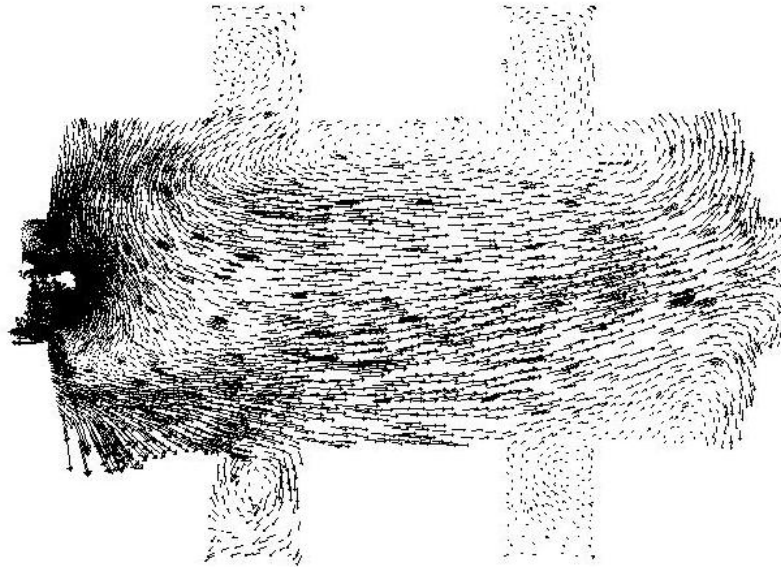
Figure 3.36. Velocity vectors for horizontal open surface tank system operating at 0.000946 m³/s (15 gpm) about a xy-plane 0.1 m from the bottom surface.

Figure 3.35 shows two distinct regions of circulation in middle of the tank about the xz-plane. Figure 3.36 shows chaotic velocity vectors resulting from the inlet configuration in the tank but the beginnings of a spiraling circulation are seen along the perimeter of the tank 0.1 m from the bottom of the tank and a clear flow path towards the far end of the tank where the flow begins to spiral upward around the perimeter of the tank. Figure 3.37 shows the three-dimensional pathlines in the tank as transported by the velocity field from the inlet to the outlet and colored by residence time in the tank.

| 0.00e+00 | 2.67e+02 | 5.33e+02 | 8.00e+02 | 1.07e+03 | 1.33e+03 | 1.60e+03 | 1.78e+03 |
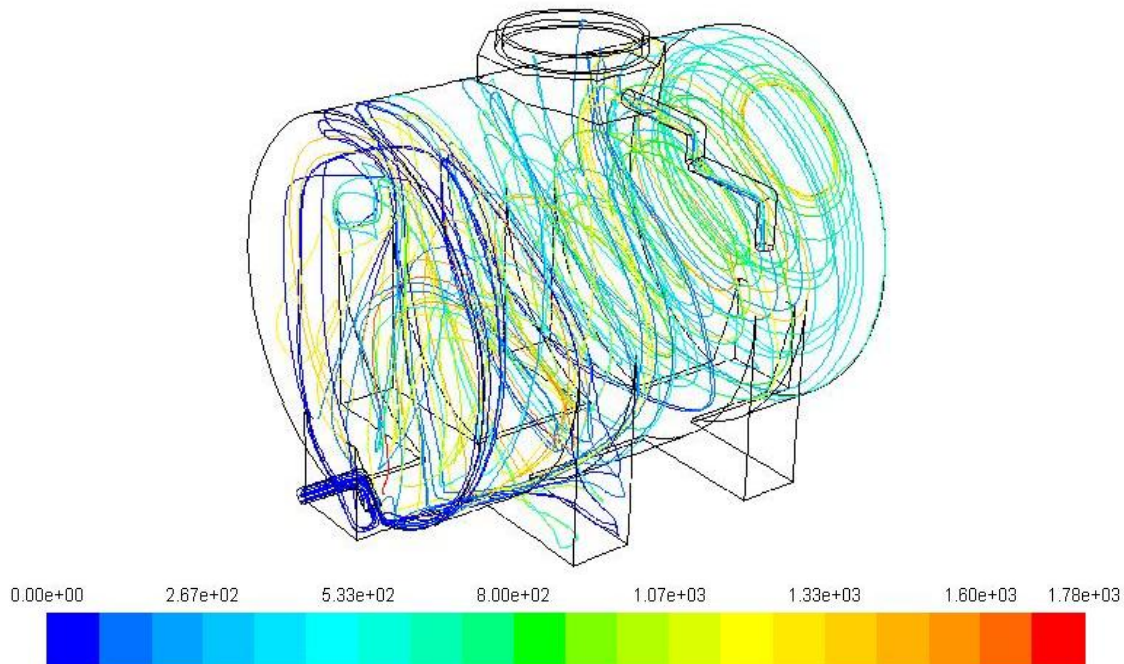
Figure 3.37. Three-dimensional pathlines of particle residence time (s) for horizontal open surface system operating at 0.000946 m³/s (15 gpm).

The three-dimensional pathlines give a better overall visual representation of the flow field seen in Figure 3.34 and the velocity vectors seen in Figures 3.35 and 3.36. The nature of the flow circulates around the perimeter of the tank in the *z*-direction towards the tank outlet.

Figure 3.38 displays the contours of turbulent dynamic viscosity on a *xz*-plane through the center of the tank.
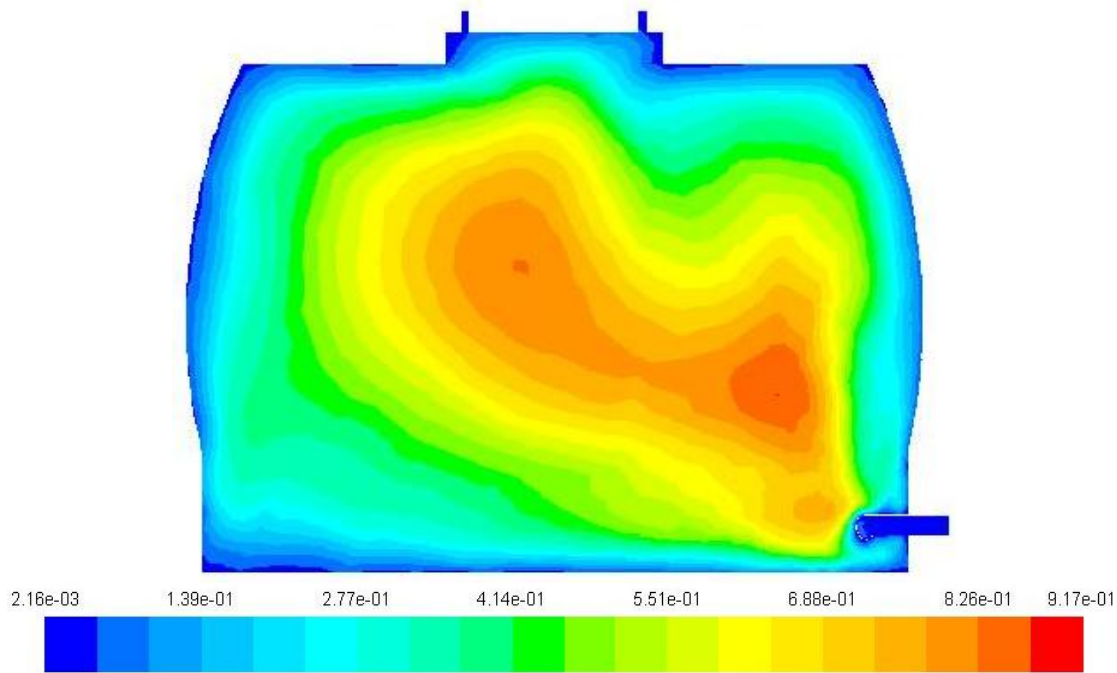
Figure 3.38. Contours of turbulent dynamic viscosity (kg/m-s) for the horizontal open surface tank system operating at 0.000946 m^3/s (15 gpm).

The simplification in analyzing this tank in a pressurized system allows the flow to be deflected by the tanks upper surface inducing some additional turbulent mixing in the system. Yet the scalar transport characteristics over the analyzed flow rates compared closely to the physical tracer study results discussed further in chapter 4.

Figures 3.39 (a)-(i) displays the scalar concentration field as a function of time for the horizontal open surface tank system.
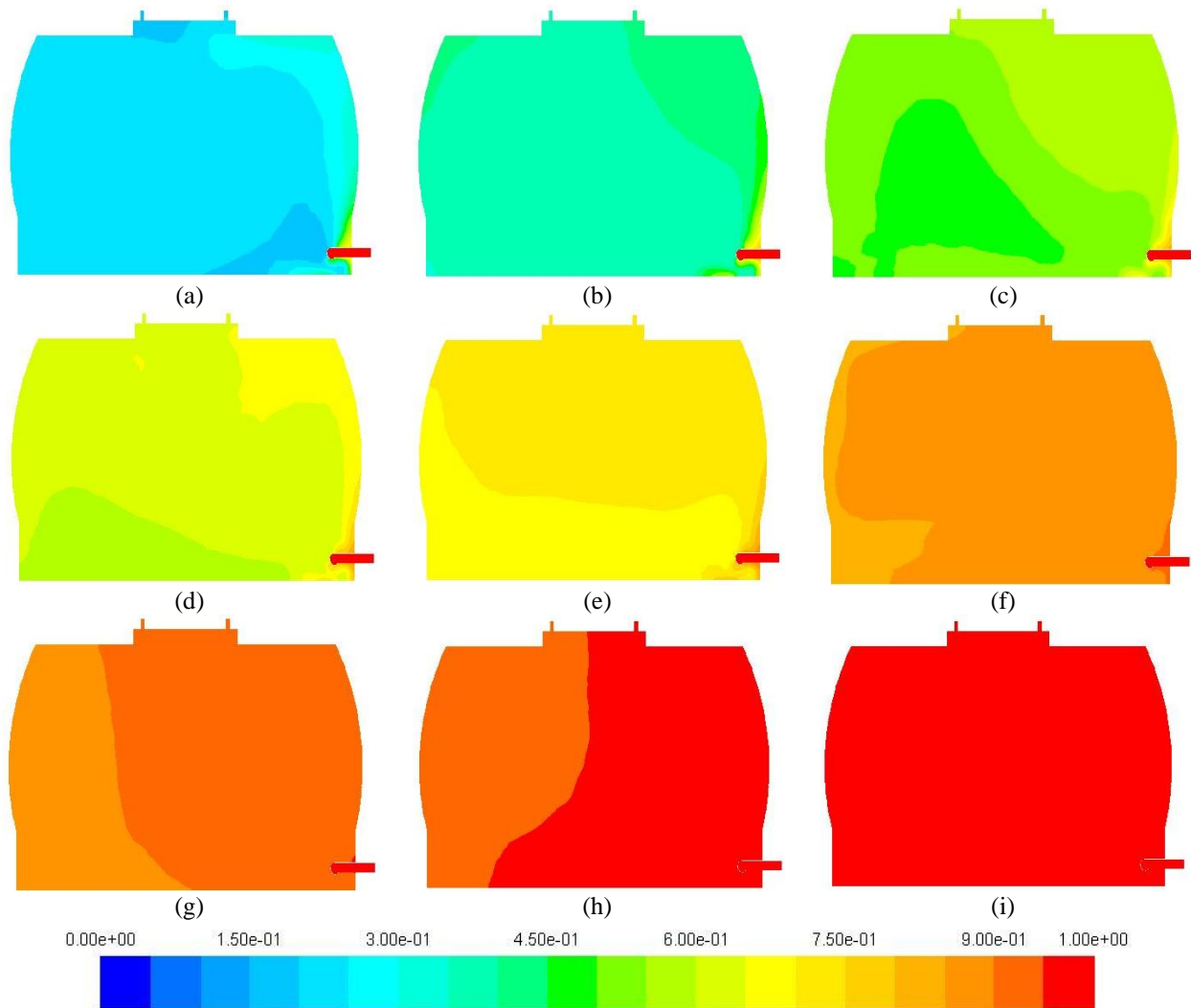
Figure 3.39. Contours of scalar concentration for horizontal open surface tank system operating at 0.000946 m³/s (15 gpm) for (a) t = 600 s, (b) t = 1200 s, (c) t = 1800 s, (d) t = 2400 s, (e) t = 3000 s, (f) t = 4800 s, (g) t = 6000 s, (h) t = 8400 s, and (i) t = 9600 s.

Figures 3.39(a)-(i) fail to show a clear pattern of scalar transport as with the series of pressurized tanks and vertical open surface tank systems. It is clear that the scalar concentration field takes a greater amount of time to interact with the left-hand-side portion of the tank (as pictured above). This effect is largely due to the location of the system outlet in the center portion of the tank (e.g., see Figure 3.24 (b)) and the more chaotic flow field as observed in Figure 3.37.

Figure 3.40 shows the scalar transport field for a time of 1800 s overlain with the velocity vectors.
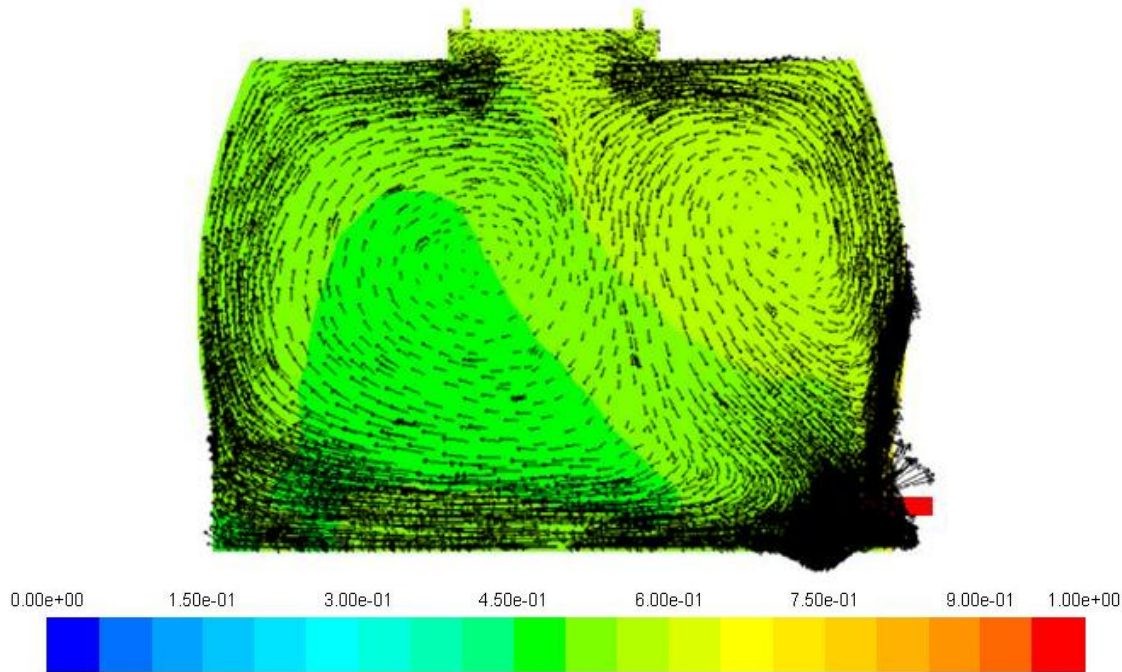
Figure 3.40. Scalar transport field at t = 1800 s and velocity vectors for horizontal open surface tank system operating at 0.000946 m³/s (15 gpm).

The regions of lower scalar concentration in the horizontal tank are a result of the flow recirculation in that region and not a direct path. Again, as in the case of the vertical open surface tank, the highly three-dimensional flow field drives the scalar field and cannot be easily observed on any one given plane through the system.

3.4. Conclusions

Pipe loop systems have traditionally been considered ideal plug flow reactors because of their large length to width ratio. The pipe loop system in this study is clearly dominated by advective forces as shown in the system velocity fields and scalar transport properties. The regions of separation and recirculation are relatively small in comparison to the entire system. The maximum magnitude of turbulent viscosity (approximately 0.15 kg/m-s) was relatively small in comparison to the maximum turbulent viscosities observed in the other systems in this study again showing the dominance of advective forces over mixing and diffusive forces. The system was analyzed only for turbulent flows (Reynolds numbers of approximately 5800 and 2900) and would likely have a different behavior for purely laminar flow conditions, although such low flows would be well below the requirements for any public water system.

The Water Quality Control Division of CDPHE designated the analyzed pressure tank systems as viable small public water disinfection systems. Chapter 4 will focus on the hydraulic efficiency of these systems but the hydrodynamics already show a significant departure from the plug flow behavior seen in the pipe loop system. While there are no clear dead zones in the tanks as observed in baffled tanks, there are significant areas of recirculation as indicated by the velocity vector and contours of turbulent viscosity. The observed scalar transport through the system does

indicated some short circuiting as the concentration front reaches the tank outlet before the concentration reaches a steady-state. The difficulty in visualizing the entirety of the scalar transport about a two-dimensional plane is the three-dimensional nature of the flow through these systems as observed in the velocity vectors in Figures 3.12 and 3.13. A single pressurized tank would likely not be an adequate disinfection system, but a series of these tanks would yield a sufficient system mimicking the behavior of baffles in a large tank as will be seen in chapter 4.

The open surface tank systems displayed the most highly three-dimensional flow fields amongst all of the systems in this research. This condition was a result of the inlet configurations in the tanks. There were apparent regions of recirculation in the center of each of the tanks designated by lower velocities and higher turbulent viscosities. The three-dimensional pathlines showed a clearer picture of the flow field for each of the respective systems which governed the flow of the passive scalar field through the systems. As these open surface tanks are an ongoing field of study not included in the scope of this research, they will be analyzed using a free surface model to more fully analyze the flow characteristics as influenced by the inlet configuration. The goal of this further research will be to increase the hydraulic efficiency of these large open surface tanks by altering the inlet configuration to more evenly distribute the flow at the inlet resulting in a lower region of the tank to promote uniform mixing and drive to flow towards plug flow conditions.

4. Physical Evaluation of Systems from Tracer Studies

Hydraulic efficiency is an important component in the design and operation of disinfection systems, particularly chlorine contact tanks, considering the potential carcinogenic products formed in the chlorination process. Improving the hydraulic efficiency of a system allows for a smaller dose of disinfectant to be used thus reducing the formation of potential carcinogens (Singer 1994 and Wang *et al*. 2003). Most contact tanks have an uneven flow path, inducing regions of recirculation or stagnation, commonly known as dead zones (Wang & Falconer 1998) shown throughout the CFD model results in chapter 3.

In order to evaluate the efficiency of contact tanks for disinfection purposes, the United States Environmental Protection Agency (USEPA) has established the practice of assigning tanks a baffle factor (*BF*) (USEPA 2003). The contact time of the disinfectant with the water in the tank is taken to be t_{10}, which is the time for 10 percent of the inlet concentration to be observed at the outlet. These quantities are typically obtained through tracer studies of an established system using conductivity measurements or tracer analysis using fluoride or lithium. *BF* is the ratio of t_{10} to *TDT* and ranges from a value of 0.1 representing an unbaffled tank with significant short-circuiting to an upper bound value of 1.0 representing ideal plug flow conditions as described by the Interim Enhanced Surface Water Treatment Rule (USEPA 2003).

In addition, the Morrill Index (*MI*), used as a measure of hydraulic efficiency in Europe, evaluates the amount of diffusion in a system based on the ratio t_{90}/t_{10} (USEPA 1986 and Teixeira & Siqueira 2008). The USEPA's practice of assigning *BFs* assumes that a system can achieve plug flow through the use of *TDT*s. The research presented in this chapter shows that a better measure of hydraulic efficiency must include the complete flow dynamics of the system since it is the flow dynamics that governs the transport of a tracer from the inlet to outlet through time (Stamou & Noutsopoulos 1994). This is usually depicted by a residence time distribution (RTD) or flow through curve (FTC), obtained by plotting the system's effluent concentration over time, as shown for example in Figure 4.1.
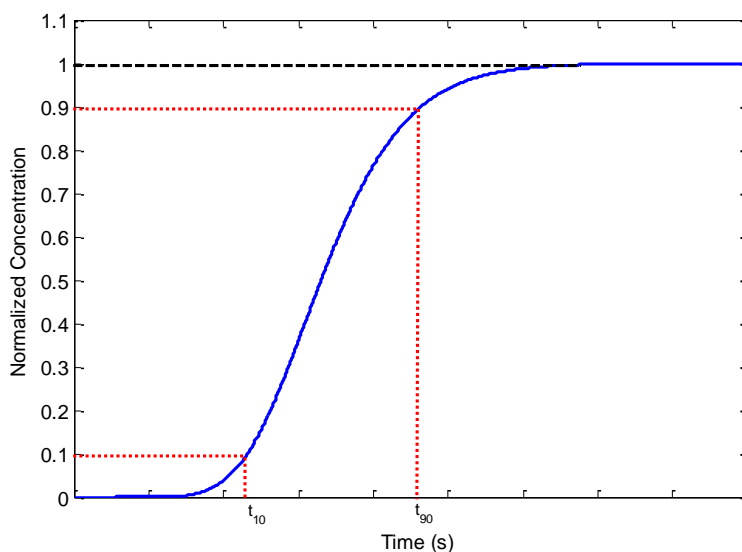

Figure 4.1. Residence time distribution (RTD) curve for an arbitrary disinfection system.

As previously discussed in chapter 2, the shape of the RTD curve provides insight to the nature of the flow in the system (Stamou 2002). However, current practice only uses the rising limb, or rather the t_{10} value, from the RTD curve and compares it to a *TDT* value unrelated to the actual flow in the system. This methodology often leads to a *BF* that overestimates the system's actual hydraulic efficiency, as shown throughout the results in this study. The results evaluating the four disinfection systems are discussed in detail, providing the basis for a better evaluation methodology of hydraulic efficiency based on the ratio of t_{10} to t_{90} obtained from the RTD curves.

4.2. Experimental Methods

To validate the usage of CFD for analysis of these small public water disinfection systems, conservative tracer analysis was performed on each of these systems at a minimum of two flow rates. A detailed standard operating procedure (SOP) was developed for the conservative tracer analysis of these systems and can be found in its entirety in appendix A. Lithium (lithium chloride) was selected as the primary conservative tracer in this study due to the low background levels found in raw water. Fluoride (sodium fluoride) was used as a secondary conservative tracer due to its wide use in industry and the ability for on-site analysis whereas lithium sample must be analyzed using mass spectrometry or inductively coupled plasma-atomic emission spectroscopy (used by Colorado State University's Soils and Water Laboratory for analysis). A stock solution was mixed so that the maximum concentration of lithium and fluoride in the system effluent was 0.04 and 1 mg/L, respectively, as to not exceed the maximum contaminant levels. Lithium is not currently regulated under USEPA regulations and while fluoride is regulated, the 1 mg/L concentration falls well below the 4 mg/L maximum level. The main concern with fluoride was to keep the concentration under the typical range for potable water in the city of Fort Collins.

For the systems constructed at the hydraulics laboratory at Colorado State University's Engineering Research Center, conductivity tracer studies were also performed using sodium chloride to provide a clear estimate for the sampling protocol for lithium and fluoride tracers. These conductivity studies were not used for validating the CFD models due to the fluctuations in source conductivity beyond the control of the experiment. On occasion, the quantity of sodium chloride added to the stock solution under high flow rates often yielded an over-saturated solution which often precipitated out and caused an uneven inlet concentration. While this situation was not ideal, the results were clear enough to accurately develop a sampling protocol. Appendix B contains a SOP for performing conductivity studies using sodium chloride (or similar salt) and an online conductivity meter.

After mixing the appropriate quantity of stock solution for the tested flow rate, the solution was connected to a dual-control electronic chemical injection pump (LMI P151-392BI) to be fed into the system upstream of a static mixer to aid in the even mixing of the tracer (or chlorine-containing species in an actual system). Samples were taken from the appropriate points in the system at the specified times to be sent to the Soil and Water Laboratory for analysis. For some of the tracer studies, sufficient sample quantities were collected to perform on-site analysis using atomic absorption of a colorimeter (HACH Fluoride Pocket Colorimeter) with SPADNS 2

(Arsenic-free) Fluoride Reagent AccuVac Ampules commonly used in field analysis of water treatment facilities.

4.3. Comparison of scalar transport results for CFD models and physical tracer studies

4.3.1. Pipe Loop System

The tracer study analyzed flow rates of 0.000505 and 0.001093 m^3/s (8 and 16 gpm), respectively. Table 4.1 presents the results of the pipe loop analysis which show that the *BF* values are consistently higher than the t_{10}/t_{90} values by approximately 10 percent.

Table 4.1. Results of CFD model and tracer study analysis of pilot pipe-loop facility.

Analysis	Q (m^3/s)	t_{10} (s)	t_{90} (s)	TDT (s)	BF	t_{10}/t_{90}
CFD Model	0.000505	3234	3774	3360	0.96	0.86
	0.001093	1584	1890	1680	0.94	0.84
Tracer Study	0.000505	3120	3786	3360	0.93	0.82
	0.001093	1536	1950	1680	0.91	0.79

Figures 4.2(a) and (b) show a comparison of RTD curves for the tracer study and CFD model results for two different flow rates. The CFD model and lithium tracer RTD curves correlated closely, as observed in Figures 4.2(a) and (b), thus validating the CFD analysis for three-dimensional scalar transport on the specified pipe-loop configuration.

(a)

(b)
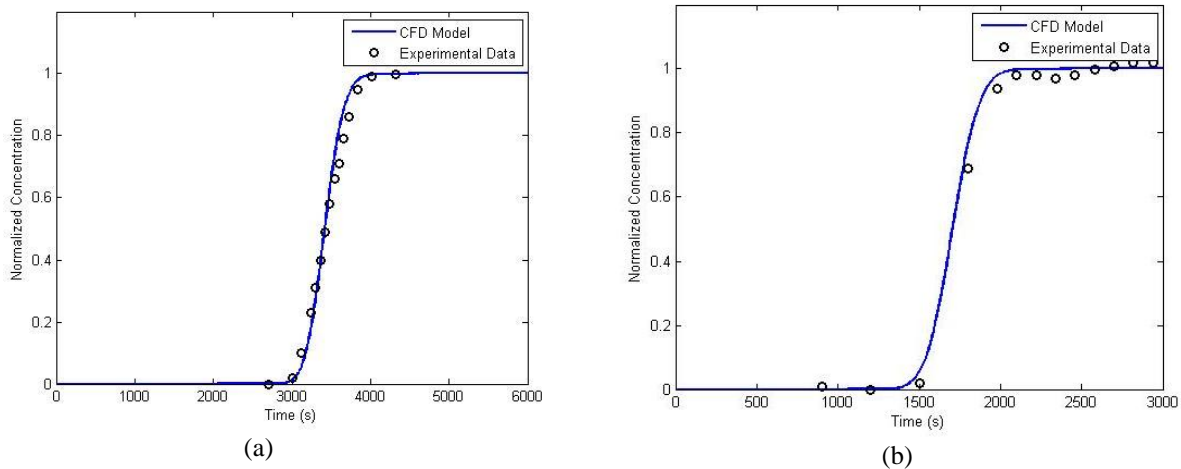
Figure 4.2. Comparison of CFD model and tracer study RTD curves for pipe loop facility for (a) 0.000505 m^3/s (8 gpm) and (b) 0.001093 m^3/s (16 gpm).

4.3.2. Pressurized Tank System

The tracer study analyzed flow rates of 0.000631, 0.000946, and 0.001262 m^3/s (or 10, 15, and 20 gpm) for 1, 2, and 3 tanks in series, respectively. Figures 4.3 (a), (b) and (c) show the comparison of RTD curves for the tracer study and the CFD model results for 1, 2, and 3 tanks in series at a flow rate of 0.000946 m^3/s, respectively. The CFD model and lithium tracer RTD

curves again correlated closely, as observed in Figures 4.3 (a), (b), and (c), thus validating the CFD analysis for three-dimensional scalar transport on the specified pressurized tank configuration.

(a)

(b)

(c)

Figure 4.3. Comparison of CFD model and tracer study RTD curves for 0.000946 m³/s (15 gpm) through (a) 1 tank, (b) 2 tanks and (c) 3 tanks in series.

For the 4, 5, and 6 series tank system, flow rates of 0.001893, 0.001262, 0.000946, and 0.000631 m³/s (30, 20, 15, and 10 gpm) were analyzed. Figures 4.4 (a), (b), and (c) present a comparison of the tracer study and CFD model study results for a flow rate of 0.001893 m³/s (30 gpm) for 4, 5, and 6 series tank systems, respectively.
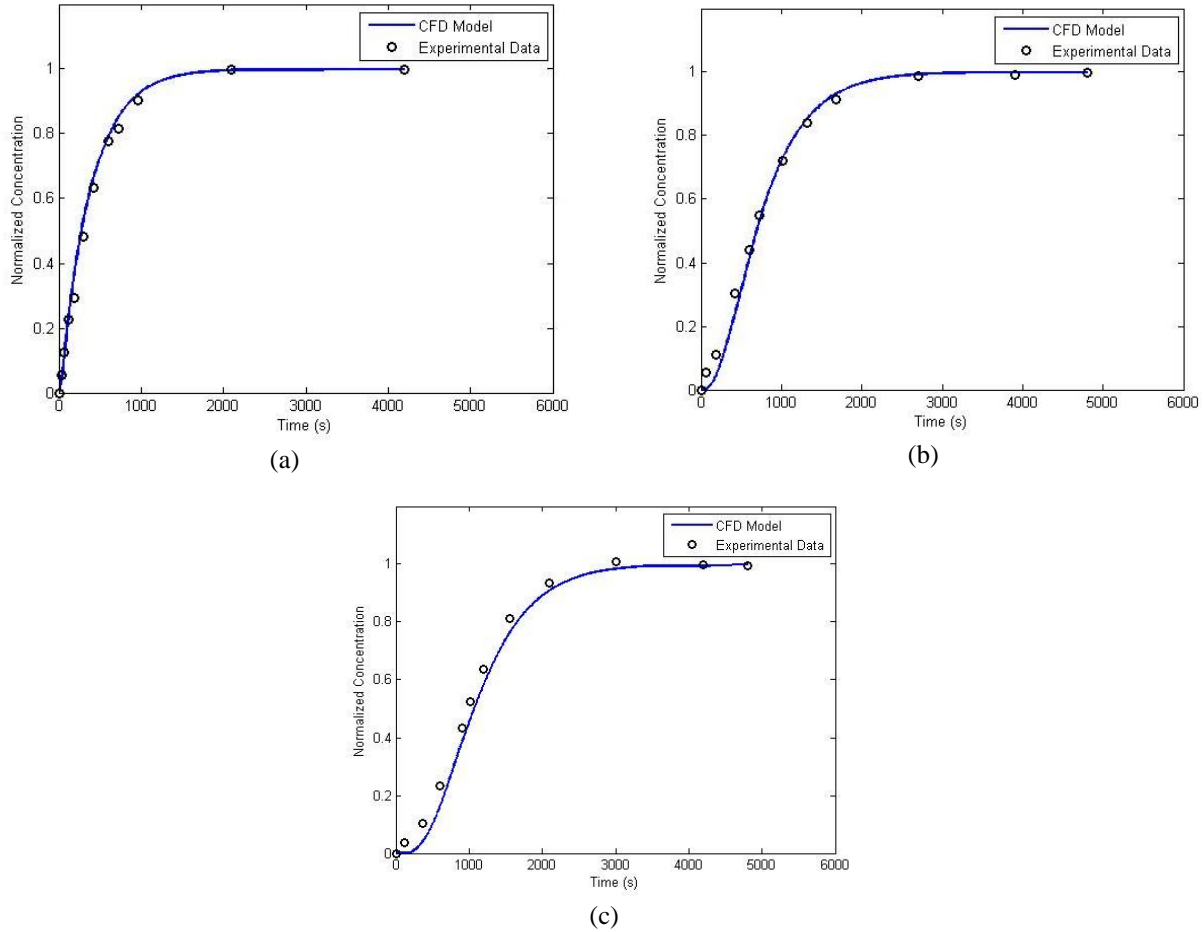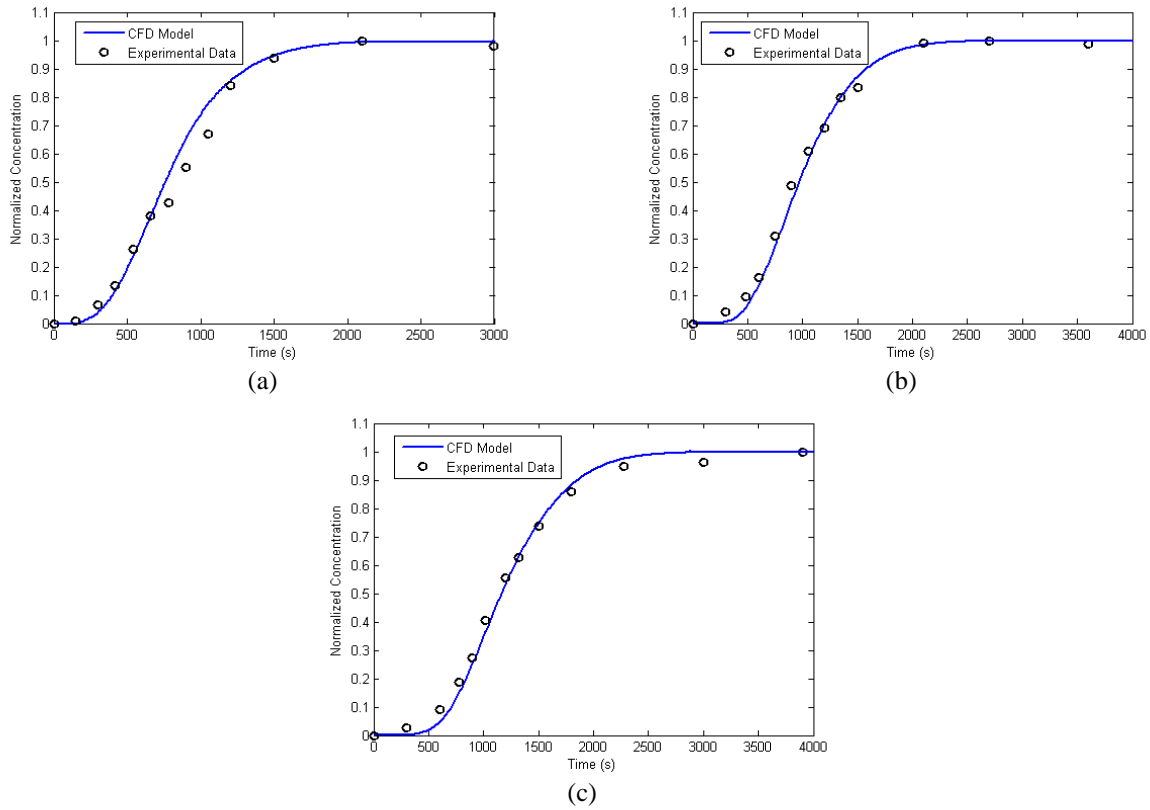
Figure 4.4. Comparison of CFD model and tracer study RTD curves for 0.0.001893 m^3/s (30 gpm) through (a) 4 tanks, (b) 5 tanks and (c) 6 tanks in series.

Table 4.2 contains the data resulting from physical tracer studies and CFD models for all of the series pressure tank systems.

Table 4.2. Results of CFD model and tracer study analysis of series tank system.

Analysis	No. of Tanks in Series, N_T	Q (m³/s)	t_{10} (s)	t_{90} (s)	TDT (s)	BF	t_{10}/t_{90}
CFD Model	1	0.000316	155	2354	1000	0.16	0.07
	1	0.000631	108	1212	498	0.21	0.09
	1	0.000946	60	870	336	0.19	0.07
	1	0.001262	54	624	252	0.22	0.09
	2	0.000316	730	4271	2000	0.36	0.17
	2	0.000631	354	2106	1002	0.36	0.17
	2	0.000946	252	1506	666	0.38	0.17
	2	0.001262	210	1062	498	0.42	0.20
	3	0.000316	1670	6185	3000	0.56	0.27
	3	0.000631	744	3078	1500	0.50	0.24
	3	0.000946	498	2046	1002	0.50	0.24
	3	0.001262	378	1548	750	0.50	0.24
	4	0.000631	1207	3931	2000	0.60	0.31
	4	0.000946	80	2594	1333	0.60	0.31
	4	0.001262	601	1988	1000	0.60	0.30
	4	0.001893	401	1328	667	0.60	0.30
	5	0.000631	1634	4659	2500	0.65	0.35
	5	0.000946	1101	3106	1667	0.66	0.35
	5	0.001262	846	2378	1250	0.68	0.36
	5	0.001893	566	1582	833	0.68	0.36
	6	0.000631	2105	5505	3000	0.70	0.38
	6	0.000946	1396	3665	2000	0.70	0.38
	6	0.001262	1042	2738	1500	0.69	0.38
	6	0.001893	713	1869	1000	0.71	0.38
Tracer Study	1	0.000316	90	2963	1000	0.09	0.03
	1	0.000631	48	1266	498	0.10	0.04
	1	0.000946	48	948	336	0.14	0.05
	1	0.001262	30	684	252	0.12	0.04
	2	0.000316	446	3487	2000	0.22	0.13
	2	0.000631	300	2496	1002	0.30	0.12
	2	0.000946	162	1608	666	0.24	0.10
	2	0.001262	168	1110	498	0.34	0.15
	3	0.000316	989	6027	3000	0.33	0.16
	3	0.000631	510	3048	1500	0.34	0.17
	3	0.000946	354	1944	1002	0.35	0.18
	3	0.001262	258	1530	750	0.34	0.17
	4	0.000946	546	2430	1333	0.41	0.22
	4*	0.001262	246	1920	1000	0.25	0.13
	4	0.001893	360	1380	667	0.54	0.26
	5	0.000946	774	2808	1667	0.46	0.28
	5*	0.001262	384	2400	1250	0.31	0.16
	5	0.001893	486	1752	833	0.58	0.28
	6	0.000946	1044	3576	2000	0.52	0.29
	6*	0.001262	336	2346	1500	0.22	0.14
	6	0.001893	618	2016	1000	0.62	0.30

*Lithium results were skewed because of a significant residual left in the system from a prior tracer study and are thus unreliable.

Additional figures presenting the comparison of CFD and tracer study results for the pressurized tank systems can be found in appendix G.

Figures 4.5 (a) and (b) show the hydraulic efficiency versus the number of tanks in series over the system for the CFD models and tracer studies, respectively.
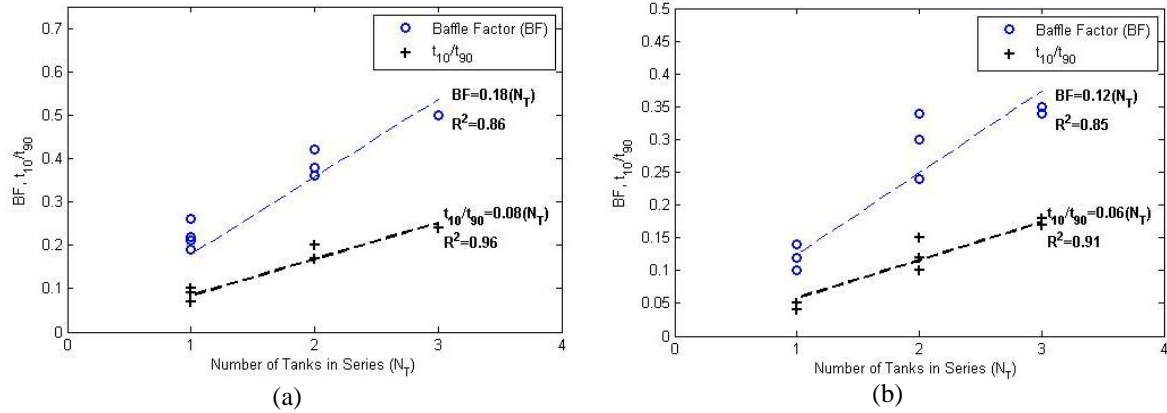
Figure 4.5. Comparison of *BF* and t_{10}/t_{90} values for (a) CFD model and (b) tracer study for 3 pressurized series tank system.

Figures 4.5 (a) and (b) also show a linear regression curve fit to each series of data points and their corresponding equations and coefficients of determination, R^2, with a *y*-intercept of zero. Despite the differences in the *BF* and t_{10}/t_{90} values of the computational model and tracer study results, the curve fits in Figures 4.5 (a) and (b) show a linear scale-up in the hydraulic efficiency with an increase of the number of tanks in series. Furthermore, Figures 4.5 (a) and (b) show that the *BF* values overestimate the hydraulic efficiency described by t_{10}/t_{90} by approximately 100 percent for both cases.

Figures 4.6 (a) and (b) display the average values of *BF* and t_{10}/t_{90} for the CFD model and tracer studies as compared to the linear regression curve fit developed for the 3 series tank system.
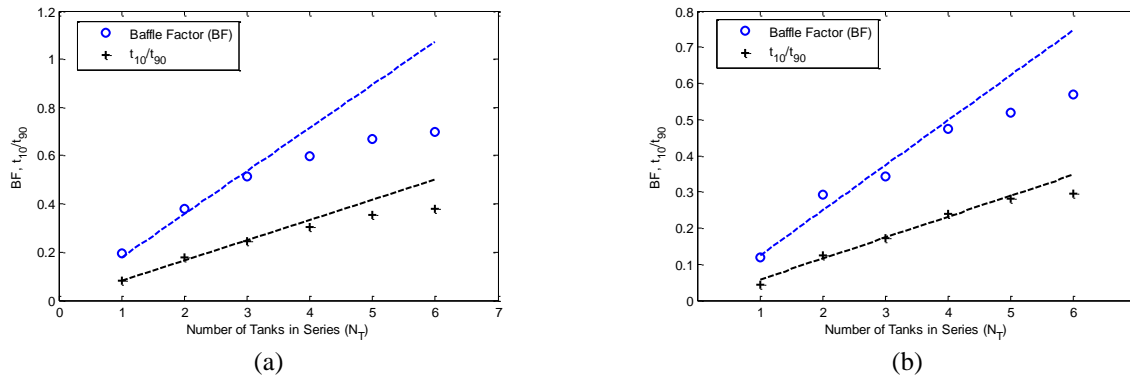
Figure 4.6. Comparison of *BF* and t_{10}/t_{90} values for (a) CFD model and (b) tracer study for 6 pressurized series tank system.

These figures show that a linear increase in hydraulic efficiency breaks down after approximately 4 tanks in series. Additionally, adding another tank into the system after 4 tanks only provides a minimal gain in efficiency but still adds a significant amount of pressure loss to the system as observed in chapter 3. If the pressure head of a source is questionable, it is

important to maximize system efficiency while reducing pressure losses allowing for adequate flow through the system.

4.3.3. Open Surface Tank Systems

The tracer study analyzed flow rates of 0.000316, 0.000631, and 0.000946 m^3/s (or 5, 10, and 15 gpm) for both the vertical and horizontal open surface tank systems. Figures 4.7 (a), (b) and (c) show the comparison of RTD curves for the tracer study and the CFD model results for the vertical open surface tank over the range of analyzed flow rates. Figures 4.8 (a), (b) and (c) show the comparison of RTD curves for the tracer study and the CFD model results for the horizontal open surface tank over the range of analyzed flow rates.

(a)   (b)

(c)
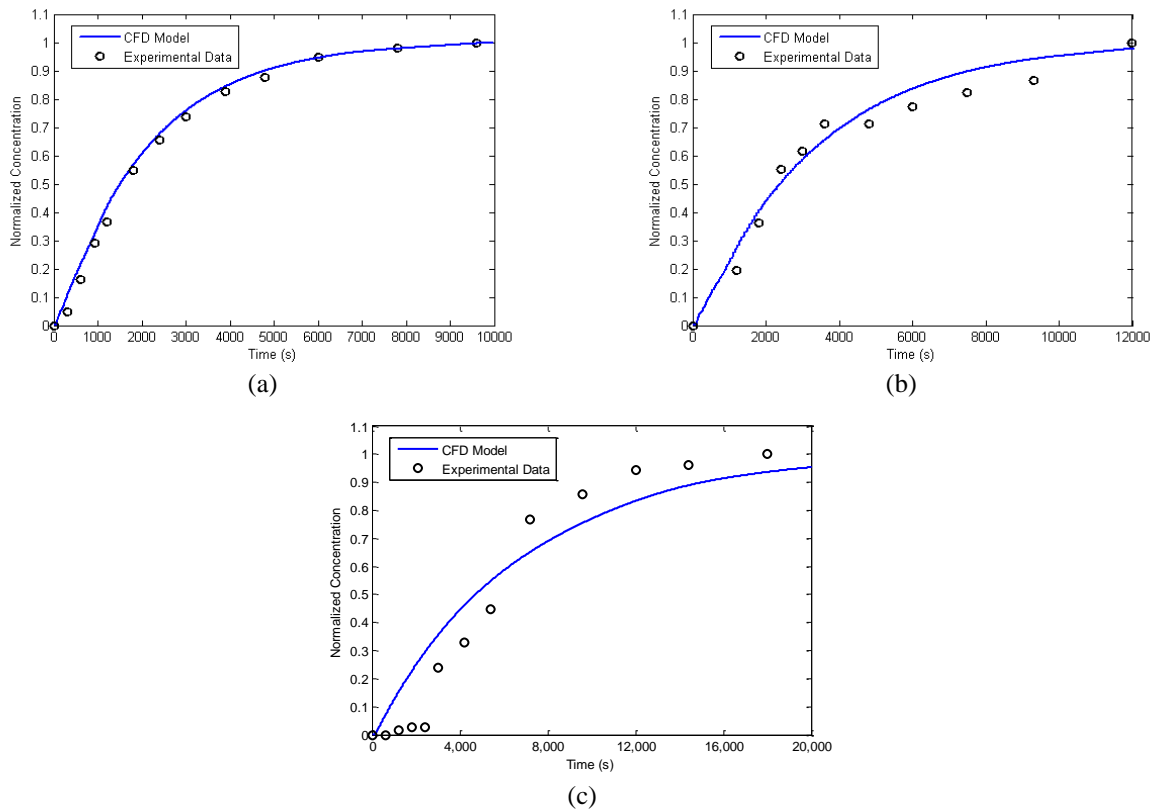
Figure 4.7. Comparison of CFD model and tracer study RTD curves for vertical open surface tank system operating at (a) 0.000946 (15 gpm), (b) 0.000631 (10 gpm), and (c) 0.000316 m^3/s (5 gpm).
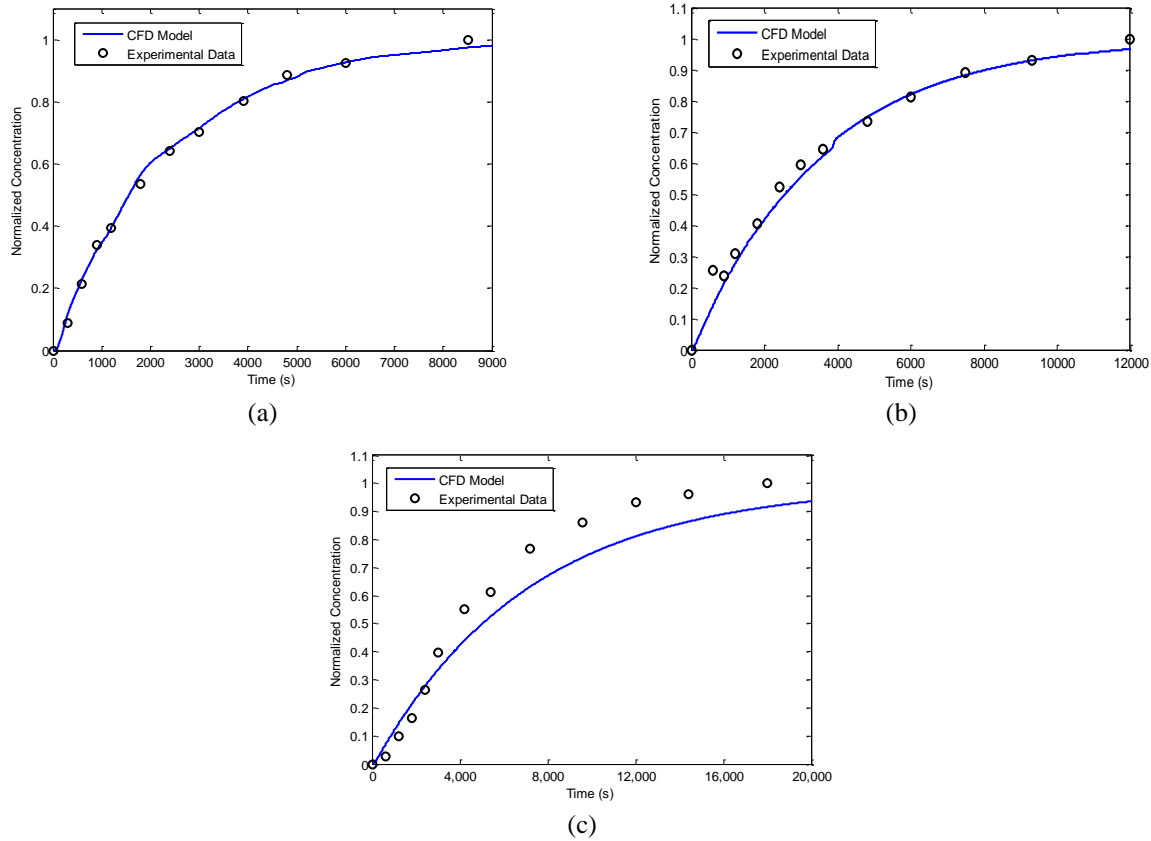
Figure 4.8. Comparison of CFD model and tracer study RTD curves for horizontal open surface tank system operating at (a) 0.000946 (15 gpm), (b) 0.000631 (10 gpm), and (c) 0.000316 m³/s (5 gpm).

The CFD model and lithium tracer RTD curves again correlated well with the 0.000946 and 0.000631 m³/s (15 and 10 gpm) for both the vertical and horizontal open surface tank systems, as observed in Figures 4.7 (a) and (b) and Figures 4.8 (a) and (b). For all 0.000316 m³/s (5 gpm) cases, the CFD model followed the trend of the experimental data but did not match their magnitude. These results show that the pressurized treatment of these open surface tank systems begins to break down around 0.000631 m³/s. In a pressurized model of these systems, the flow is allowed to interact with the top portions of each tank which induces greater recirculation and causes that passive scalar to reside longer in the computational models than in the physical models.

Tables 4.3 and 4.4 show the data analysis of the vertical and horizontal open surface tanks. These results also show that the *BF* values are consistently higher than the t_{10}/t_{90} values

Table 4.3. Results of CFD model and tracer study analysis of vertical open surface tank system.

Analysis	Q (m^3/s)	t_{10} (s)	t_{90} (s)	TDT (s)	BF	t_{10}/t_{90}
	0.000946	436.8	5168.0	2000	0.22	0.08
Tracer Study	0.000631	616.7	10002.0	3000	0.21	0.06
	0.000316	1260.6	10793.1	6000	0.21	0.12
	0.000946	293.9	4793.2	2000	0.15	0.06
CFD Model	0.000631	446.6	7588.3	3000	0.15	0.06
	0.000316	815.2	15040.0	6000	0.14	0.05

Table 4.4. Results of CFD model and tracer study analysis of horizontal open surface tank system.

Analysis	Q (m^3/s)	t_{10} (s)	t_{90} (s)	TDT (s)	BF	t_{10}/t_{90}
	0.000946	327.9	5253.3	2100	0.16	0.06
Tracer Study	0.000631	380.6	7882.5	3150	0.12	0.05
	0.000316	1193.7	10910.8	6300	0.19	0.11
	0.000946	271.3	5267.9	2100	0.13	0.05
CFD Model	0.000631	428.5	8073.0	3150	0.14	0.05
	0.000316	852.6	16689.2	6300	0.14	0.05

4.4. Discussion

While estimates can be made about a systems efficiency based on the *BF* guidelines (USEPA 1986), a tracer study and resulting RTD curve or combination of a CFD model and validation tracer study are the only ways to evaluate the respective hydraulic efficiencies of the systems. As seen in this study, even the detention time in a pipe loop, listed as a perfect plug flow contactor by the USEPA, departs from a perfect step function. A full RTD curve is a clear indicator of the internal flow dynamics of a system; whether it be a short-circuited flow, plug flow, or somewhere in between (Stamou 2002 and Lyn & Rodi 1990). There are many contributing factors for this departure of the flow such as boundary layer turbulence, flow separation, entry and exit conditions, and buoyancy forces due to stratification. As a result, the t_{10}/t_{90} values for all three systems discussed in this study are consistently lower than the values for the *BF*. Because the *BF* formulation assumes that a perfect plug flow can be achieved in every system, it, therefore, inherently overestimates the hydraulic efficiency. For example, systems of the same volume can have differing geometries yet have the same *TDT* for a given flow rate. Clearly, large unbaffled rectangular tanks and long pipe contactors have differing flow dynamics and should not have their efficiencies evaluated based on the same idealized *TDT,* which assumes plug flow conditions. This simple illustration presents a major flaw in the USEPA's methodology through failing to make a clear distinction between the hydraulic efficiency and *BF* of a contact tank in the *LT1ESWTR Disinfection Profiling and Benchmarking Manual*.

Because a disinfection system with a sufficiently large length-to-width ratio asymptotically approaches ideal plug flow behavior, the *BF* values did not differ as significantly from the t_{10}/t_{90} values in the pipe loop contactor as they did in the pressurized and baffled tank systems. As the length-to-width ratio decreases, the difference in *BF* and t_{10}/t_{90} values increases due to diffusion and other flow phenomena (e.g., flow separation and recirculation). This also results in a further departure from the ideal plug flow assumption inherent in the *BF* formulation of a purely

advective system. Furthermore, the results of the CFD models and tracer studies suggest that the ratio of t_{10} to t_{90} is a more appropriate measure of hydraulic efficiency. The values of t_{10} and t_{90} are obtained from the RTD curve which as previously mentioned is a direct indicator of the flow dynamics in the system, thus eliminating any ambiguity associated with the *TDT*. The *MI* evaluates the amount of diffusion in a system based on the ratio t_{90}/t_{10} with a lower bound value of 1.0 representing pure advection (ideal plug flow) but is convoluted in that there is no upper limit to describe the amount of diffusion in the system (Kothandaraman *et al*. 1973). In contrast, the quantity t_{10}/t_{90} gives the ratio of advective to diffusive actions with an upper bound value of 1.0 representing pure advection and a lower bound value of zero representing (at least in theory) pure diffusion. In this manner, t_{10}/t_{90} presents a straightforward ratio from which one can easily deduce the influence of advective and diffusive forces on the system similar to the Peclet number which is a measure of the advection to diffusion effects in a fluid transport system and is given by

$$Pe = \frac{UL}{\kappa}$$
(4.1)

where U is a characteristic velocity scale of the flow, L is a characteristic length scale, and κ is molecular diffusivity. A high Peclet number would imply a system which is dominated by advection and vice versa for a system dominated by diffusion. Hence, the ratio of t_{10}/t_{90} can in fact be considered as a form of the Peclet number expressed here as a time scale ratio.

As with any disinfection system, a more efficient system requires less contact time for a given amount of chlorine-containing species to achieve a certain level of log-inactivation. While the USEPA guidelines have proven adequate for use in contact tank systems, this study has shown that *BFs* only provide a partial assessment of the hydraulic efficiency, making use of only the rising limb of the RTD curve, and thus tend to overestimate the hydraulic efficiency of the disinfection system. On the other hand, the t_{10}/t_{90} ratio provides a better measure of the hydraulic efficiency of any disinfection system since it takes into account the actual flow and scalar transport dynamics in a given system by utilizing a substantial portion of the RTD curve of a given system.

5. Pre-Engineered Systems

Based on the experimental studies and CFD models results, a 4-tank pressurized series tank system was determined to be the optimal pre-engineered system. A pressurized tank system allows for use of readily available supplies, requires minimal construction and maintenance, provides a relatively good hydraulic efficiency, and has a relatively low pressure drop across the system. The *BF* for this prescribed system is 0.5.
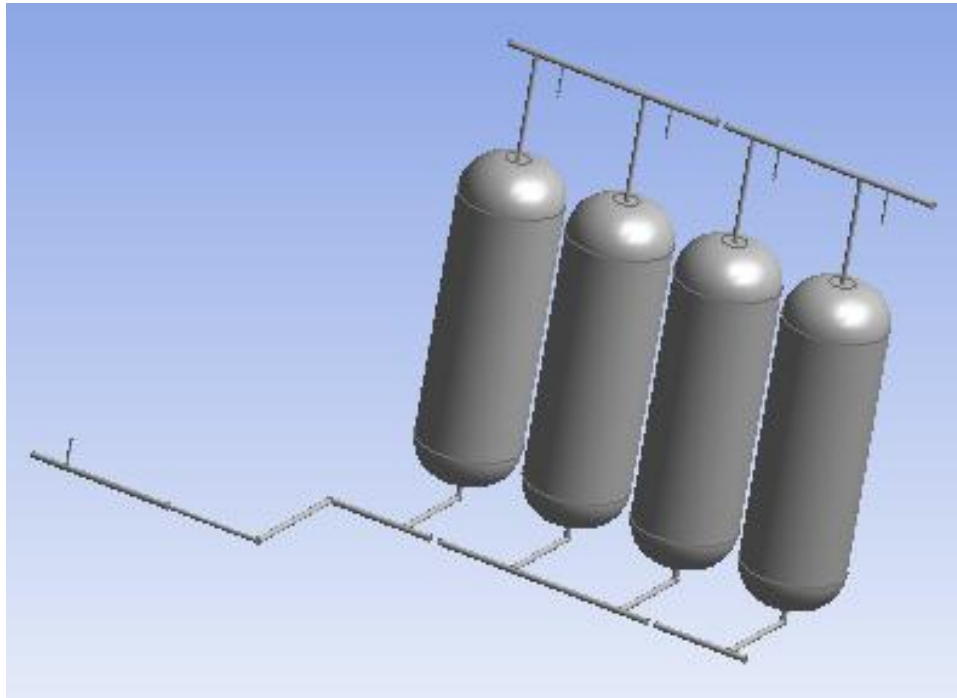
Figure 5.1. 4 Series pressurized tank system

Figure 5.1 displays the computational model of 4 pressurized tanks in series suggested as a pre-engineered system from this body of research. This system meets the appropriate 4-log inactivation when operated under proper conditions as described in the following subsections.

5.1. System Disinfection Analysis

5.1.1. Log Inactivation Procedure

This section provides a basic review of the log inactivation methodology as well as an evaluation of the 4 series pressurized tank system. The log inactivation calculation procedure is described in detail in the *LT1ESWTR Disinfection Profiling and Benchmarking Technical Guidance Manual*. This brief overview of the log inactivation calculation procedure serves only to highlight the major steps. It is important to note the disinfection capabilities of chlorine are greatly influenced by solution strength, age, temperature, pH, and presence of metal catalysts (Gordon *et al*. 1993, 1995). Figure 5.2 shows the available fraction of free chlorine as a function of pH for a temperature of 20ºC.
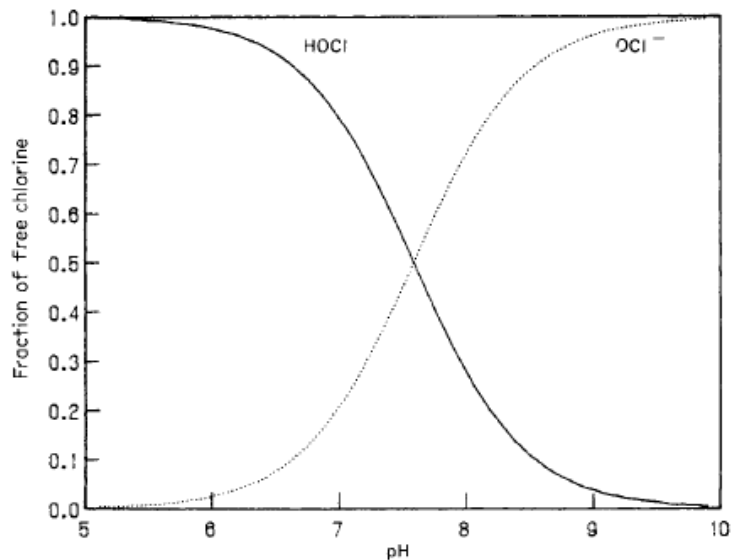
Figure 5.2. Fraction of free chlorine as a function of pH for water at 20° C (Letterman 1999).

As observed in Figure 5.2, chlorine disassociates into hypochlorous acid (HOCl) and hypochlorite (OCl⁻) as pH increases. There is an exponential decrease in the available fraction of free chlorine in the form of hypochlorous acid as pH increases. Hypochlorous acid is much more effective at disinfection as compared to hypochlorite and for this reason, inflows must have a pH less than 10 for small systems in the state of Colorado as determined by CDPHE.

Log inactivation describes the percentage of microorganisms inactivated in the disinfection process in a specific environment. For example, 4-log inactivation translates to 99.99% of the microorganisms of interest inactivated. The disinfection capability of a system is influenced by disinfection concentration, temperature, pH, and disinfectant type. The CT (min-mg/L) methodology, where CT is the product of the disinfectant concentration C (mg/L) and the contact time T (also referred to as t_{10}), is commonly used in evaluating the disinfection effectiveness of a system.

1. **Calculate Detention Time**
   a. Calculate Theoretical Detention Time (TDT)

   $$TDT = V/Q$$

TDT	= theoretical detention time (minutes)
V	= volume, based on low water level (gallons)
Q	= peak hourly flow (gpm)

   b. Calculate Actual Detention Time (T)

   $$T = TDT \ x \ BF$$

T	= actual detention time (minutes)
TDT	= theoretical detention time (minutes)
BF	= baffling factor (as described in Table 1.1)

2. **Calculate CT$_{CALC}$**

$$CT_{CALC} = C \ x \ T$$

CT_{CALC} = concentration time, calculated value (min-mg/L)
C = residual disinfection concentration (mg/L)
T = actual detention time (minutes)

3. Calculate *Giardia lamblia* log inactivation
a. Determine CT required for *Giardia lamblia* 3-log reduction ($CT_{99.9}$) using EPA tables and WTP information

Table 5.1. $CT_{99.9}$ values for 3-log inactivation of *Giardia lamblia* (CDPHE 2009)

Chlorine Conc. (mg/L)	Temperature <= 0.5°C							Temperature = 5°C							Temperature = 10°C						
	pH							pH							pH						
	<=6.0	6.5	7	7.5	8	8.5	9	<=6.0	6.5	7	7.5	8	8.5	9	<=6.0	6.5	7	7.5	8	8.5	9
<=0.4	137	163	195	237	277	329	390	97	117	139	166	198	236	279	73	88	104	125	149	177	209
0.6	141	168	200	239	286	342	407	100	120	143	171	204	244	291	75	90	107	128	153	183	218
0.8	145	172	205	246	295	354	422	103	122	146	175	210	252	301	78	92	110	131	158	189	226
1.0	148	176	210	253	304	365	437	105	125	149	179	216	260	312	79	94	112	134	162	195	234
1.2	152	180	215	259	313	376	451	107	127	152	183	221	267	320	80	95	114	137	166	200	240
1.4	155	184	221	266	321	387	464	109	130	155	187	227	274	329	82	98	116	140	170	206	247
1.6	157	189	226	273	329	397	477	111	132	158	192	232	281	337	83	99	119	144	174	211	253
1.8	162	193	231	279	338	407	489	114	135	162	196	238	287	345	86	101	122	147	179	215	259
2.0	165	197	236	286	346	417	500	116	138	165	200	243	294	353	87	104	124	150	182	221	265
2.2	169	201	242	297	353	426	511	118	140	169	204	248	300	361	89	105	127	153	186	225	271
2.4	172	205	247	298	361	435	522	120	143	172	209	253	306	368	90	107	129	157	190	230	276
2.6	175	209	252	304	368	444	533	122	146	175	213	258	312	375	92	110	131	160	194	234	281
2.8	178	213	257	310	375	452	543	124	148	178	217	263	318	382	93	111	134	163	197	239	287
3.0	181	217	261	316	382	460	552	126	151	182	221	268	324	389	95	113	137	166	201	243	292

Chlorine Conc. (mg/L)	Temperature = 15°C							Temperature = 20°C							Temperature = 25°C						
	pH							pH							pH						
	<=6.0	6.5	7	7.5	8	8.5	9	<=6.0	6.5	7	7.5	8	8.5	9	<=6.0	6.5	7	7.5	8	8.5	9
<=0.4	49	59	70	83	99	118	140	36	44	52	62	74	89	105	24	29	35	42	50	59	70
0.6	50	60	72	86	102	122	146	38	45	54	64	77	92	109	25	30	36	43	51	61	73
0.8	52	61	73	88	105	126	151	39	46	55	66	79	95	113	26	31	37	44	53	63	75
1.0	53	63	75	90	108	130	156	39	47	56	67	81	98	117	26	31	37	45	54	65	78
1.2	54	64	76	92	111	134	160	40	48	57	69	83	100	120	27	32	38	46	55	67	80
1.4	55	65	78	94	114	137	165	41	49	58	70	85	103	123	27	33	39	47	57	69	82
1.6	56	66	79	96	116	141	169	42	50	59	72	87	105	126	28	33	40	48	58	70	84
1.8	57	68	81	98	119	144	173	43	51	61	74	89	108	129	29	34	41	49	60	72	86
2.0	58	69	83	100	122	147	177	44	52	62	75	91	110	132	29	35	41	50	61	74	88
2.2	59	70	85	102	124	150	181	44	53	63	77	93	113	135	30	35	42	51	62	75	90
2.4	60	72	86	105	127	153	184	45	54	65	78	95	115	138	30	36	43	52	63	77	92
2.6	61	73	88	107	129	156	188	46	55	66	80	97	117	141	31	37	44	53	65	78	94
2.8	62	74	89	109	132	159	191	47	56	67	81	99	119	143	31	37	45	54	66	80	96
3.0	63	76	91	111	134	162	195	47	57	68	83	101	122	146	32	38	46	55	67	81	97

b. Calculate Giardia lamblia Log Inactivation

Giardia Log Inactivation = 3 log x ($CT_{CALC}/CT_{99.9}$)

$$CT_{CALC}\qquad = \text{concentration time, calculated value (min-mg/L)}$$
$$CT_{99.9}\qquad = \text{concentration time to inactivate 3 log of Giardia (min-mg/L)}$$

4. **Calculate virus log inactivation**
     a. Determine CT required for Virus 4 log reduction (CT99.99)

Table 5.2. $CT_{99.99}$ values for 4-log inactivation of viruses (CDPHE 2009)

Temperature °C	pH	
	6-9	10
0.5	12	90
5	8	60
10	6	45
15	4	30
20	3	22
25	2	15

     b. Calculate Virus Log Inactivation

$$\textit{Virus Log Inactivation} = 4 \log x \, (CT_{CALC}/CT_{99.99})$$

$$CT_{CALC}\qquad = \text{concentration time, calculate value (min-mg/L)}$$
$$CT_{99.99}\qquad = \text{concentration time to inactivate 4 log of virus (min-mg/L)}$$

5.1.2 Pre-engineered system log inactivation analysis results

The following systems sufficiently meet the 4-log inactivation standard for a temperature range of 7°C to 12°C and pH range of 6-9 with associate chlorine residual as specified.

Table 5.3. Viable system configuration for 0.7 mg/L chlorine residual

Pressurized Tank Systems	Temp. (C)	7 to 12	Free Chlorine Residual	0.7 mg/L
Operational Flow Rate (gpm)	Number of Tanks in Series		Volume of Tanks (gal)	
5	4		120, 80	

For example, the above table shows that for a chlorine residual of 0.7 mg/L, 4 – 120 or 80 gallon tanks may be used in series to appropriately create a system capable of 4-log inactivation with an operational flow rate of 5 gpm. The following tables contain the same information over the spectrum of chlorine residual from 0.8 mg/L to 1.2 mg/L.

Table 5.4. Viable system configuration for 0.8 mg/L chlorine residual

Pressurized Tank Systems	Temp. (C)	7 to 12	Free Chlorine Residual	0.8 mg/L
Operational Flow Rate (gpm)	Number of Tanks in Series		Volume of Tanks (gal)	
5	4		120, 80	

Table 5.5. Viable system configuration for 0.9 mg/L chlorine residual

Pressurized Tank Systems	Temp. (C)	7 to 12	Free Chlorine Residual	0.9 mg/L
Operational Flow Rate (gpm)	Number of Tanks in Series		Volume of Tanks (gal)	
5	4		120, 80	

Table 5.6. Viable system configuration for 1.0 mg/L chlorine residual

Pressurized Tank Systems	Temp. (C)	7 to 12	Free Chlorine Residual	1.0 mg/L
Operational Flow Rate (gpm)	Number of Tanks in Series		Volume of Tanks (gal)	
5	4		120, 80	
10	4		120	

Table 5.7. Viable system configuration for 1.1 mg/L chlorine residual

Pressurized Tank Systems	Temp. (C)	7 to 12	Free Chlorine Residual	1.1 mg/L
Operational Flow Rate (gpm)	Number of Tanks in Series		Volume of Tanks (gal)	
5	4		120, 80	
10	4		120	

Table 5.8. Viable system configuration for 1.2 mg/L chlorine residual

Pressurized Tank Systems	Temp. (C)	7 to 12	Free Chlorine Residual	1.2 mg/L
Operational Flow Rate (gpm)	Number of Tanks in Series		Volume of Tanks (gal)	
5	4		120, 80	
10	4		120	

5.2. System Supplies

This subsection provides example components for the described 4 series pressurized tank system. Figure 5.3 displays an example schematic of a 3 series pressurized tank system will all components labeled.
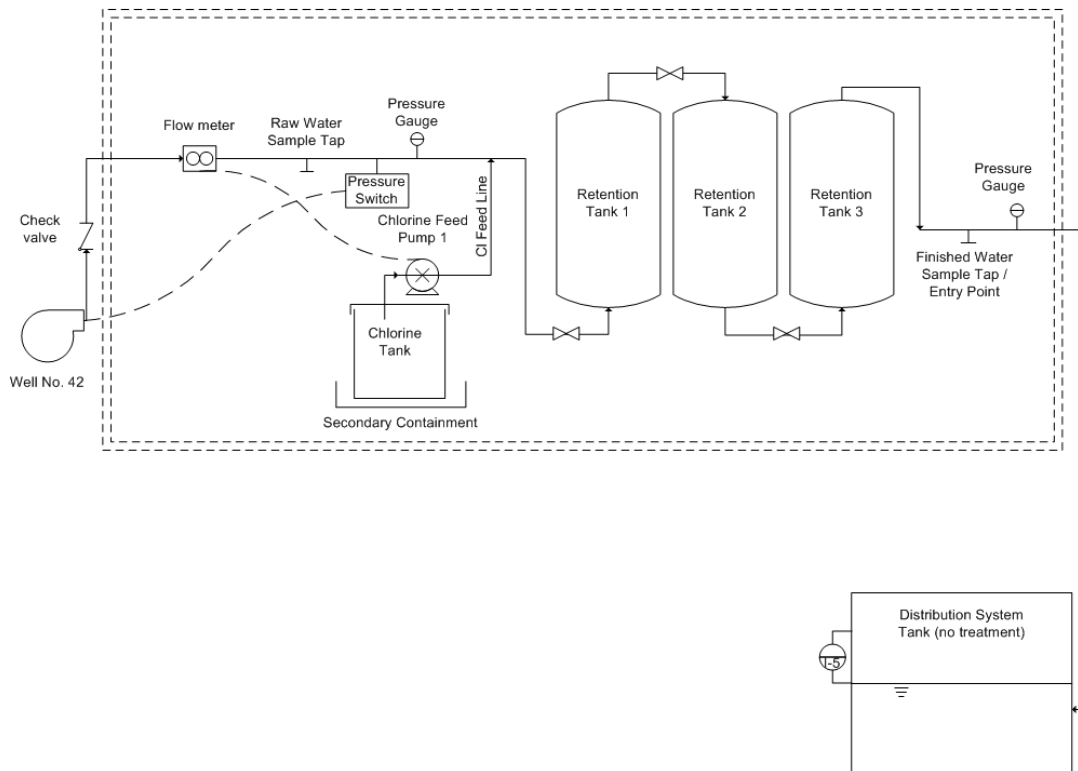
Figure 5.3. Schematic for an example small public water system

5.2.1. Flow Meters

The flow meter for the system should be rated to within $\pm$ 5% accuracy and capable of measuring flows up to 40 gpm. A flow meter is preferred in this application as opposed to a water meter which is of questionable accuracy in a flow metering application.

5.2.2. Pressure Gauges

Gauges should be capable of measuring pressures up to 100 psig with accurate resolution. Any standard liquid-filled gauges are suitable for this application.

5.2.3. Chlorine Feed Pump

Chemical feeds pumps are used to deliver the chlorine solution into the system. The feed rate is a function of the system flow rate and residual concentration desired. The following equation can be used to determine the capacity of the chemical feed pump required.

$$System\ Flow\ Rate\ (gpm) \times Required\ Dosage\ \left(\frac{mg}{L}\right) \times 1440\frac{min}{day}$$
$$\times Solution\ Strength\ \left(\frac{mg}{L}\right) = Feed\ Pump\ Output\ (gpd)$$

The required dosage and solution strength can also be measured in ppm as long as their units are kept consistent. Any diaphragm chemical feed pump capable of meeting the maximum rated feed output is acceptable. A pre-built chemical feed skid (such as those offered by USA Blue Book) should also be incorporated to provide a calibration column and pressure gauge to ensure the metering pump's rated pressure is not exceeded.

5.2.4. Chlorine Supply Tank

The chlorine supply tank should provide adequate storage for 3 to 4 days at most. This ensures the chlorine remains active. Any polyethylene chemical storage tank is suitable for this application.

5.2.5. Retention Tanks

The retention tanks for use in the describe system are fiberglass pressure tanks from 80 to 120 gallons in capacity (without bladders). These tanks should have fittings at the top and bottoms of the tank for flow to pass from bottom to top or vice-versa (as direction was not determined to have an effect on system efficiency). Figures 5.4 (a) and (b) show two examples of these fiberglass pressure tanks.

Well Mate (a)

Flexcon (b)

Available from USA Blue Book and Aqua Science

Available from Aqua Science

Figure 5.4. (a) Well Mate and (b) Flexcon fiberglass pressure tanks

These tanks are ideal because of their relatively small footprint. These tanks can also be arranged to fit any footprint and then plumbed in series.

5.2.6. Distribution System Tank

A distribution system tank provides a predetermined amount of storage in the event of maintenance of unexpected downtime in the system. Any polyethylene storage tank is suitable for this purpose.

5.2.7 Other Supplies

The plumbing in this system should be comprised of Schedule 80 PVC piping (including valves and taps).

6. Summary and Conclusions

6.1. Summary of Research

The research performed in this study validated the use of CFD analysis, specifically the use of a finite volume code invoking a time-stepping RANS formulation with a standard k-ε turbulence model, for analysis of passive scalar transport through small public water disinfection systems. Systems included a pipe loop system, series of pressurized tanks, and vertical and horizontal open surface tank systems. This research was used to propose a 4 series pressurized tank pre-engineered system.

Chapter 3 provided the hydrodynamic analysis of the prescribed systems as well as detailed descriptions of the unique flow characteristics influencing the nature of scalar transport for each of the systems. Chapter 4 follows up on chapter 3 by interpreting the data obtained from the scalar transport through use of RTD curves. Chapter 4 also challenges the common misconception that the USEPA's *BF* classification system is synonymous with hydraulic efficiency and suggested that the ratio t_{10}/t_{90} might be a better measure of hydraulic efficiency as compared to those found in literature. Chapter 5 provides basic log inactivation calculations for a disinfection system as well as the details of the proposed pre-engineered system.

6.2. Major Conclusions

The pipe loop system was dominated by advective force yet did not exhibit the predicted ideal plug flow behavior. This result leads to the conclusion that plug flow is an idealized flow characteristic which can only be asymptotically approached. The pipe loop system is an ideal disinfection system that will require a significant footprint area to obtain an adequate capacity.

The series of pressurized tank systems exhibited significant turbulent mixing in the interior region of each tank but were similar to baffles in a rectangular tank in that the more tanks added in series, the greater degree of efficiency the system obtained. A system of 4 tanks in series yielded the maximum return in hydraulic efficiency.

The open surface tanks were the least efficient systems with significant short-circuiting and regions of recirculation. The inlet configuration in each of these two tanks greatly influenced the flow dynamics and subsequent scalar transport. By more evenly distributing the inflow, the hydraulic efficiency is likely to increase, which is the subject of future research.

In evaluating hydraulic efficiency, it was concluded that the ratio t_{10}/t_{90} was the best indicator of advective and diffusive forces. While it is clear that this measure of hydraulic efficiency will not replace the baffle factor classification system used by the USEPA for contact tank design based on the billions of dollars of infrastructure built under this assumption, it should be used in combination to provide a better evaluation of these small systems. Small public water systems often lack the resources to provide adequate monitoring of the free chlorine residual in the system. In such systems, t_{10}/t_{90} is more appropriate in the design calculations.

6.3. Recommendations

The following recommendations are made for the continuing research on the small public water disinfection systems

- Analyze the open surface tank system using an open surface CFD model. While the pressurized model assumption gave an adequate representation of the systems operating at higher flow rates, it failed to capture the true flow dynamics and scalar transport properties at the lowest flow rate.

- Alter the inlet configurations of the open surface tank system and analyze the effect on the systems hydraulic efficiency. It is hypothesized that distributing the influent in a more even fashion will increase the system efficiency. After validating an open surface CFD model, concepts will be modeled to evaluate their performance before constructing and analyzing its behavior in the physical system. This research has the potential to produce further pre-engineered systems to improve the hydraulic efficiency of these commonly used open surface tank systems.

REFERENCES

Fluent Inc. *FLUENT 6.3 User's Guide*. **2006**. Ann Arbor, MI.

Gordon, G.; Adam, L. C.; Bubnis, B. P.; Hoyt, B.; Gillette, S. J.; Wilczak, A. Controlling the formation of chlorate ion in liquid hypochlorite feedstocks, *J. AWWA*. **1993**, 85 (9): 89–97.

Gordon,G.; Adam, L.C.; Bubnis, B. P. Minimizing chlorate ion formation, *J. AWWA*. **1995**, 87 (6): 97–106.

Gualtieri, C. Numerical simulation of flow and tracer transport in a disinfection contact tank. *Hydraulic and Environmental Engineering Department Girolamo Ippolito*, **2003**.

Hannoun, I.A.; Boulos, P.F.. Optimzing distribution storage water quality: a hydrodynamic approach, *Appl. Math. Model.* **1997**, 21: 495-502.

Hannoun, I.A.; Boulos, P.F.; List, E.J. Using hydraulic modeling to optimize contact time, *J. AWWA*, **1998**, 90 (8): 77-87.

Hart, F. L.; Allen, R.; Dialesio, J.; Dzialo, J. Modifications improve chlorine contact chamber performance. Part II, *Water & Sewage Works*. **1975**, 122 (10): 88–90.

Hart, F. L. Improved hydraulic performance of chlorine contact chamber, *J. Water Pollut. Control Fed.* **1979**, 51 (12): 2868–2875.

HDR Engineering, Inc. Safe Drinking Water Act Update: Looking Back - A Century of Change, March **1999**.

Jones, W.P.; Launder, B.E. The prediction of laminarization with a two-equation model of turbulence, *Int. J. Heat Mass Transfer*, **1972**, 15: 301-314.

Kothandaraman, V.; Southerlan, H.L.; Evans, R.L. Performance characteristics of chlorine contact tanks, *Journal (Water Pollution Control Federation)*. **1973**, 45 (4): 611-619.

Letterman, R. D, ed. *Water Quality and Treatment*, 5th ed., American Water Works Association, McGraw-Hill: New York, **1999**.

Levenspiel, O; Smith, W. K. Notes on the diffusion-type model for the longitudinal mixing of fluids in flow, *Chem. Eng. Sci.* **1957**, 6: 227-233.

Levenspiel, O. *Chemical reaction engineering*, 2nd Ed., Wiley: New York, **1972**.

Lyn, D.A.; Rodi, W. Turbulent measurements in model settling tank, *J. Hydraulic Eng.* **1990**, 116 (1): 3-21.

Marske, D. M.; Boyle, J. D. Chlorine contact tank design—A field evaluation, *Water & Sewage Works*, **1973**, 120 (1): 71–77.

Pope, S.B. *Turbulent Flows*; Cambridge University Press: Cambridge, U.K., **2000**.

Rebhun, M., and Argaman, Y. Evaluation of hydraulic efficiency of sedimentation basins, *J. Sanit. Eng. Div.* **1965**, 91 (5): 37–45.

Sawyer, C. M., and King, P. H. The hydraulic performance of chlorine contact tanks, *Proc., 24th Industrial Waste Conf.* **1969**, Purdue Univ., West Lafayette, 1151–1168.

Shiono, K.; Teixeira, E.C. Turbulent characteristics in a baffled contact tank, *J. Hydraulic Res*. **2000**, 38 (4): 271-271.

Singer, P.C. Control of disinfection by-products in drinking water, *J. Environ. Eng*. **1994**, 120 (4): 727-744.

Stamou A. I.; Adams, E. A.; Rodi, W. Numerical modelling of flow and settling in primary rectangular clarifiers, *J. Hydr. Res.,* IAHR, **1989**. 27(5): 665-682.

Stamou A. I. On the prediction of flow and mixing in settling tanks using a curvature modified k-ε model, *Applied Mathematical Modelling,* **1991**. 15: 351-358.

Shiono, K.E.; Teixiera, E.C.; Falconer, R.A. *Turbulent measurements in chlorine contact tank*, The 1st international conference on water pollution: Modeling, measuring, and predicting, Southampton, UK: **1991**, 519-531.

Stamou, A.I.; Noutsopoulos, G. Evaluating the Effect of Inlet Arrangement in Settling Tanks Using the Hydraulic Efficiency Diagram, *Water SA*. **1994**, 20 (1), 77-83.

Stamou, A.I. Verification and application of a mathematical model for the assessment of the effect of guiding walls on hydraulic efficiency of chlorination tanks, *J. Hydroinformatics.* **2002**, 4: 245-254.

Stamou, A.I. Improving the hydraulic efficiency of water process tanks using CFD models, *Chem. Eng. Process*. **2008**, 47: 1179-1189.

Stamou, A.I.; Theodoridis, G.; Xanthopoulos, K. Design of secondary settling tanks using a CFD model, *J. Environ. Eng.*, **2009**, 135 (7): 551-561.

Stovin, V.R.; Saul, A.J. A computational fluid dynamics (CFD) particale tracking approach to efficiency prediction. *Water Sci. Technol.* **1998**, 37: 285-293.

Teefy, S.M., ed. *Tracer Studies in Water Treatment Facilities: A Protocol and Case Studies*, American Water Works Association Research Foundation: Denver, **1996**.

Teixeira, E. C. Hydrodynamic processes and hydraulic efficiency of chlorine contact units, Ph.D. thesis, Dept. of Civil Engineering, Univ. of Bradford, Bradford, U.K, **1993**.

Teixeira, E.; Siqueira, R. Performance Assessment of Hydraulic Efficiency Indexes, *J. Environ. Eng*. **2008**, 134 (10), 851-859.

Templeton, M.R.; Hofmann, R.; Andrews, R.C. Case study comparisons of computational fluid dynamics (CFD) modelling versus tracer testing for determining clearwell residence times in drinking water treatment, *J. Environ. Eng.,* **2006**. 5 (6): 529-536.

Thirumurthi, D. A break-through in the tracer studies of sedimentation tanks, *J. Water Pollut. Control Fed.* **1969**, 41 (11): R405–R418.

Trussell, R. R.; Chao, J.L. Rational design of chlorine contact facilities, *J. Water Pol. Control Fed.* **1977**, 49 (7): 659–667.

United States Environmental Protection Agency, USEPA. Design manual: municipal wastewater disinfection. **1986.** EPA:625:1-86:021. USEPA Office of Res. and Dev., Cincinnati, OH.

United States Environmental Protect Agency, USEPA. Report of the National Drinking Water Advisory Council Small Systems Implementation Working Group. **2000,** EPA 816-R-00-012, Office of Water, Washington, D.C.

United States Environmental Protect Agency, USEPA. Disinfection profiling and benchmarking guidance manual. **2003,** EPA 815-R-99-013, Office of Water, Washington, D.C.

United States Environmental Protect Agency, USEPA. The Ground Water Rule (GWR) Implementation Guidance. **2009,** EPA 816-R-09-004, Office of Water, Washington, D.C.

United States Environmental Protection Agency, USEPA. Small Systems and Capacity Development; http://water.epa.gov/type/drink/pws/smallsystems/basicinformation.cfm#challenges, **2010**.

Venayagamoorthy, S.K.; Stretch, D.D. On the turbulent Prandtl number in homogeneous stably stratified turbulence, *J. Fluid Mech*. **2010**, 644: 359-369.

Wang, H.; Falconer, R.A. Simulating disinfection processes in chlorine contact tanks using various turbulence models and high-order accurate difference schemes, *Water Res*. **1998**, 32 (5): 1529-1543

Wang, H.; Shao, X.; Falconer, R.A. Flow and transport simulation models for prediction of chlorine contact flow-through curves, *Water Res*. **2003**, 75 (5): 455-471.

Wilson, J.M.; Venayagamoorthy, S.K. Evaluation of hydraulic efficiency of disinfection systems based on residence time distribution curves, *Environ. Sci. Technol.,* **2010**, 44 (24): 9377-9382.

Wilson, J.M. Evaluation of flow and scalar transport characteristics of small public drinking water disinfection systems using computational fluid dynamics, Masters thesis, Dept. of Civil and Environmental Engineering, Colorado State University, U.S. **2011**.

Wilson, J.M.; Venayagamoorthy, S.K. *Hydraulics and mixing efficiency of small public water disinfection systems*, ASCE/EWRI World Environmental and Water Resources Congress, 22-27 May 2011, Palm Springs, CA: **2011**.

Xu, Q.; Venayagamoorthy, S.K. *Hydraulic efficiency of baffled disinfection contact tanks*, 6th International Symposium on Environmental Hydraulics, 23-25 June 2010, Athens: **2010**, 1041-1046.

Xu, Q. Internal hydraulics of baffled disinfection contact tanks using computational fluid dynamics, Masters thesis, Dept. of Civil and Environmental Engineering, Colorado State University, U.S. **2010**.

APPENDIX A

Standard Operating Procedure (SOP) for conservative tracer analysis of small public water disinfection systems

PURPOSE
The purpose of this SOP is to layout a protocol for tracer studies on small scale contact tank facilities.

SUMMARY
The SOP describes the step necessary to perform a tracer study using lithium and fluoride conservative tracers on small water systems. There are two most common methods of tracer addition employed in water treatment evaluations: the step-dose method and the slug-dose method. In general, the step-dose procedure offers the greatest simplicity. However, both methods are theoretically equivalent for determining T_{10}. While either method is acceptable for conducting drinking water tracer studies, each has distinct advantages and disadvantages with respect to tracer addition procedures and analysis of results. The choice of the method may be determined by site-specific constraints. If possible, tracer studies should be conducted on each segment to determine the T_{10} for each segment. In order to minimize the time needed to conduct studies on each segment, the tracer studies should be started at the last segment of the treatment train prior to the first customer and completed with the first segment of the system. Conducting the tracer studies in this order will prevent the interference of residual tracer material with subsequent studies.

RELATED SOPs
None

HEALTH AND SAFETY

Lithium Chloride (LiCl)

Hazards
Potential Acute Health Effects: Hazardous in case of skin contact (irritant), of eye contact (irritant), of ingestion, or inhalation.
Potential Chronic Health Effects:
CARCINOGENIC EFFECTS: Not available
MUTAGENIC EFFECTS: Mutagenic for mammalian somatic cells. Mutagenic for bacteria and/or yeast.
TERATOGENIC EFFECTS: Classified POSSIBLE for human
DEVELOPMENTAL TOXICITY: Classified Reproductive system/toxin/female, Reproductive system/toxin/male [POSSIBLE].
Repeated or prolonged exposure is not known to aggravate medical condition

First Aid
Eye Contact: Get medical attention immediately. Flush eyes with plenty of water for at least 15 minutes, occasionally lifting the upper and lower eyelids.
Skin Contact: Get medical attention immediately. Immediately wash skin with soap and water for at least 15 minutes and remove contaminated clothing. Wash clothing before reuse.
Serious Skin Contact: Wash with soap and cover the contaminated skin with an anti-bacterial cream. Seek immediate medical attention.
Inhalation: Remove from exposure to fresh air immediately. If breathing is difficult, give oxygen. Get medical attention if symptoms appear.
Ingestion: Get medical attention immediately. Do not induce vomiting. If the victim is conscious and alert, give 2-4 cupfuls of milk or water. Never give anything to an unconscious person.

Accidental Release Measures
Dispose of spilled solid in waste disposal container and clean surface with water avoiding skin contact.

Sodium Fluoride (NaF)

Hazards
Potential Acute Health Effects: Hazardous in case of skin contact (irritant), of eye contact (irritant, corrosive), of ingestion, or inhalation. Slightly hazardous in case of skin contact (corrosive). Severe over-exposure can result in death.
Potential Chronic Health Effects:
CARCINOGENIC EFFECTS: A4 (Not classifiable for human or animal) by ACGIH, 3 (Not classifiable for human) by IRAC
MUTAGENIC EFFECTS: Mutagenic for mammalian somatic cells. Mutagenic for bacteria and/or yeast.
TERATOGENIC EFFECTS: Not available
DEVELOPMENTAL TOXICITY: Not available
The substance may be toxic to kidneys, lungs, the nervous system, heart, gastrointestinal tract, cardiovascular system, bones, teeth.
Repeated or prolonged exposure to the substance can produce target organs damage. Repeated exposure to a highly toxic material may produce general deterioration of health by an accumulation in one or many human organs.

First Aid
Eye Contact: Get medical attention immediately. Flush eyes with plenty of water for at least 15 minutes, occasionally lifting the upper and lower eyelids.
Skin Contact: Get medical attention immediately. Immediately wash skin with soap and water for at least 15 minutes and remove contaminated clothing. Wash clothing before reuse.
Serious Skin Contact: Wash with soap and cover the contaminated skin with an anti-bacterial cream. Seek immediate medical attention.
Inhalation: Remove from exposure to fresh air immediately. If breathing is difficult, give oxygen. Get medical attention if symptoms appear.
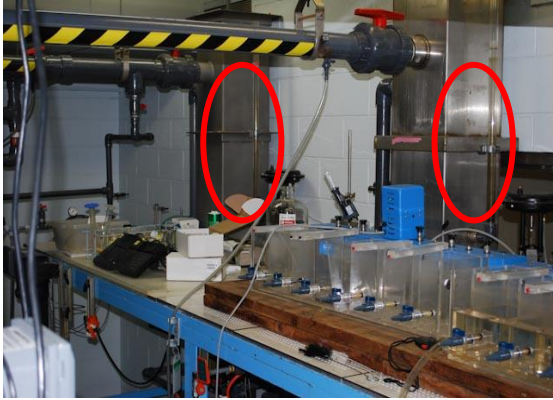Serious Inhalation: Evacuate the victim to a safe area as soon as possible. Loosen tight clothing such as a collar, tie, belt, or waistband. Get immediate medical attention.
Ingestion: Get medical attention immediately. Do not induce vomiting. If the victim is conscious and alert, give 2-4 cupfuls of milk or water. Never give anything to an unconscious person.

Accidental Release Measures
Use appropriate tools to put spilled solid in waste disposal container.

PROCEDURE	
STEP NUMBER/NAME	**VISUAL AID**
1. Adjust flow rate for first desired analysis	**Picture**

Adjust flow rate using PID controller or other control device	 PID Controller Interface
2. Verify flow rates	**Picture**
Verify the flow meter readings using drawdown columns	 Drawdown columns
3. Verify system volume and calculate HRT	**N/A**
Perform measurements as necessary. $$HRT = \frac{Volume}{Flow\ rate}$$	
4. Develop Sampling Protocol	**N/A**

The sampling protocol is largely dependent on the type of system analyzed 1. For a pipe loop configuration (ie. plug flow), the sampling interval should be 30 seconds within $\pm$ 5 minutes of HRT and 5 minutes within $\pm$ 20 minutes of HRT 2. For baffled basin (ie. series tank), the sampling interval should be 5 minutes within $\pm$ 30 minutes of HRT and 10 minutes within $\pm$ 60 minutes of HRT 3. For open basin, the sampling interval should be 10 minutes with $\pm$ 90 minutes of HRT	
4. Determine injection and sampling points	**Pictures**

The injection point will be comprised of a 3/8 inch quick-connect fitting to accept the effluent hose from the injection pump.	Injection Point
The sampling point should be easily accessible and contain a quarter-turn valve for ease of sampling	Sampling Point
5. Determine background levels	**N/A**
Sample water prior to any tracer injection to determine the tracer solution concentration	
6. Set and calibrate injection pump	**Picture**

- Fill bulk container with deionized water and attach to injection pump - Attach effluent hose from injection pump to the system injection point - Open valve to fill the calibration column, then close the valve - Set pump stroke to 100 and speed to 80 - Turn pump on - Open valve from calibration column to pump - Time the drop in the column over a determine volume - Turn off pump - Calculate injection flowrate	 Calibration Column Injection pump
7. Prepare bulk tracer solution	**Pictures**
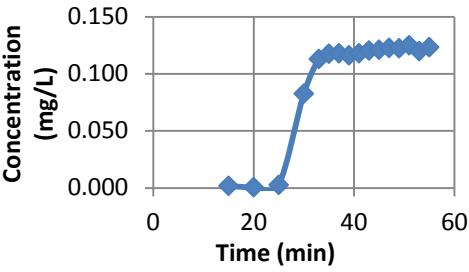
• Determine the volume of tracer solution needed • $Volume_{tracer} = Mean\ Resonance\ Time \times Injection\ Pump\ Rate$ • Add the dry masses of *LiCl* and *NaF* to the determined volume of water in 7 and mix thoroughly	 Tracer Compounds in dry bulk form
8. Determine the mass of *LiCl* added to tracer solution	**N/A**
• Assume a system maximum of 0.04 mg/L based on background levels • $\frac{0.04\ mg\ Li}{L} \times Volume_{system} = mass_{Li}$ • $mass_{LiCl} = mass_{Li} \times \frac{42.394\ g\ LiCl}{6.941\ g\ Li}$	
9. Determine the mass of *NaF* added to tracer solution	**N/A**
• Assume a system maximum of 1.00 mg/L based on background levels • $\frac{mg\ F}{L} \times Volume_{system} = mass_F$ • $mass_{NaF} = mass_F \times \frac{41.99\ g\ NaF}{18.998\ g\ F}$	
10. Add the dry masses of *LiCl* and *NaF* to the determined volume of water in 7 and mix thoroughly	**N/A**
11. Attach bulk tracer solution to injection pump	**N/A**
Attach the bulk tracer solution container to the inject pump and ensure that the valves are open allowing flow into the system	
12. Turn on injection pump	**N/A**

Allow 2 minutes to pass before beginning to time for the sampling protocol. This allows for the DI water used to calibrate the pump to be flushed from the system	
13. Determine maximum tracer concentration in system	**Picture**
Sample at an intermediated point in the system well past the time estimated for the full concentration of the tracer to pass. This sample will provide the maximum tracer concentration in the system.	 Intermediate Sampling Point
14. Sample according to protocol	**N/A**
- Label containers appropriately - Place adequate sample in test tube for laboratory analysis of lithium - Place adequate sample in open container for on-site analysis of fluoride	
15. Analyze fluoride using Colormeter	**Pictures**

• Place an adequate amount of DI water in an open container • Insert AccuVac sample and break off glass tip • Turn on colormeter • Program – 28 – enter • Remove colormeter cover, insert DI water AccuVac sample, replace cover, and press zero • Place new AccuVac into sample container, break off glass tip, press timer – enter on colormeter • When alarm sounds, remove colormeter cover, insert AccuVac sample, replace cover, press read, and record reading • Repeat steps for remaining samples	New AccuVac Filled AccuVac AccuVac Samplers DR890 Colormeter
16. Review results	**Plot**
Analyze colormeter fluoride results to ensure samples captured tracer breakthrough (RTD curve)	
17. Adjust sampling protocol (if necessary)	**See Figure in 16.**
If the RTD curve or a significant portion of the RTD curve are not captured, adjust the sampling to protocol	
18. Repeat step 3-18 (if necessary)	**See Figure in 16.**

Repeat these steps until an accurate RTD curve is captured	
19. Repeat steps 1-18	**N/A**
Repeat steps 1-18 for all considered flow rates	

APPENDIX B

Standard Operating Procedure (SOP) for conductivity analysis of small public water disinfection systems

PURPOSE
The purpose of this SOP is to layout a protocol for conductivity studies on small-scale contact tank facilities.

SUMMARY
The SOP describes the steps necessary to perform a conductivity study using NaCl on small water system using a step-dose method of introduction. There are two most common methods of tracer addition employed in water treatment evaluations: the step-dose method and the slug-dose method. In general, the step-dose procedure offers the greatest simplicity. However, both methods are theoretically equivalent for determining T_{10} and the determination of methods is often site specific depending upon available resources.

RELATED SOPs
Tracer Study Procedure (04-08-10)

HEALTH AND SAFETY
Sodium Chloride (NaCl) **Hazards** May cause eye irritation. Not believed to present a significant hazard to health.

PROCEDURE	
STEP NUMBER/NAME	**VISUAL AID**
1. Adjust flow rate for first desired analysis	**(a) Rotameter and (b) Water meter**
Verify the flow rate using rotameter (if available) and/or water meter. Note: The accuracy of the rotameter is 2% of the full scale (or +/- 0.4 gpm) whereas the accuracy of the water meter is unknown	(a) (b)
2. Verify system volume and calculate HRT	**N/A**
Perform measurements as necessary. $$HRT = \frac{Volume}{Flow\ rate}$$	
3. Determine injection and sampling points	**(a) Injection point and (b) sampling point**
The injection point is located immediately upstream of the static mixer and has a quarter-turn valve for operational ease. The sampling point is located immediately after the tank in consideration. Flexible tubing transports the flow to the bottom of the apparatus pictured in figure (b) and allows for the conductivity probe to be fully submerged.	 (a) (b)
4. Determine background levels	**N/A**

Turn on the conductivity meter and press [mode] until the [°C] is blinking indicating that the temperature compensated mode is turned selected. Place the conductivity probe in the sampling apparatus and open the sample tap allowing flow to pass over the probe. Record the baseline conductivity reading. Leave this assembly as is to record the conductivity measurements subsequent to step 9.	
5. Set and calibrate injection pump	**(a) Calibration column and (b) injection pump**
• Fill bulk container with water and attach to injection pump • Attach effluent hose from injection pump to the system injection point • Open valve to fill the calibration column, then close the valve • Set pump stroke to 100 and speed to 80 • Turn pump on (using the breaker switch on the electrical plug outlet) • Open valve from calibration column to pump • Time the drop in the column over a determine volume • Turn off pump • Calculate injection flowrate	(a) (b)
7. Prepare salt (NaCl) solution	**N/A**
For systems up to 550 US gallons, add 100 grams of NaCl to 1 gallon of water or until the stock solution reaches a conductivity of approximately 40 mS. Ensure that the NaCl is thoroughly mixed and does not accumulate significantly at the bottom of the stock solution bottle.	

8. Attach salt solution to injection pump	**N/A**
Attach the salt solution container to the injection pump and ensure that the valves are open allowing flow into the system. Turn on the injection pump allowing the salt solution to recirculate into the container until all air has been flushed from the system. Turn injection pump off.	
9. Attach injection pump to the system and begin conductivity study	**Injection pump assembly connected to system inlet**
Insert the feed line from the injection pump assembly into the system inlet. Open the valve. Simultaneously turn on the injection pump and start a timer, as the time is needed to incrementally record the conductivity readings to produce an RTD curve of the system.	
10. Record conductivity measurements	**N/A**
Record the conductivity readings and corresponding time of reading as appropriate. The system has effectively reached a steady state when readings vary +/- 0.1 μS over a 5-minute period. Note: Temperature readings are not necessary as the meter is in the temperature compensated mode.	
11. Repeat step 7-10 for same flow rate	**N/A**

For consistency, ensure that the data from a minimum of 2 runs compare closely before testing the system at a different flow rate and/or different configuration.
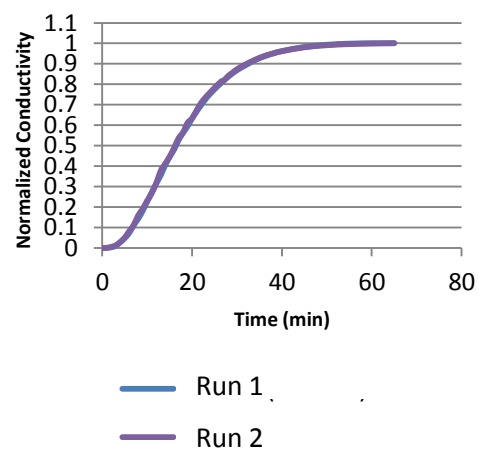
APPENDIX C

Additional results for pressurized tank systems

This appendix contains additional plots showing the comparison of CFD and physical tracer study results depicting through RTD curves for both the 3 and 6 series pressurized tank systems. As mentioned in the text, the results for the tracer test for the 6 series system operating at 0.000946 m^3/s were skewed because of a residual left in the system. The results of this error can be observed in Figures F.4 (a), (b), and (c).
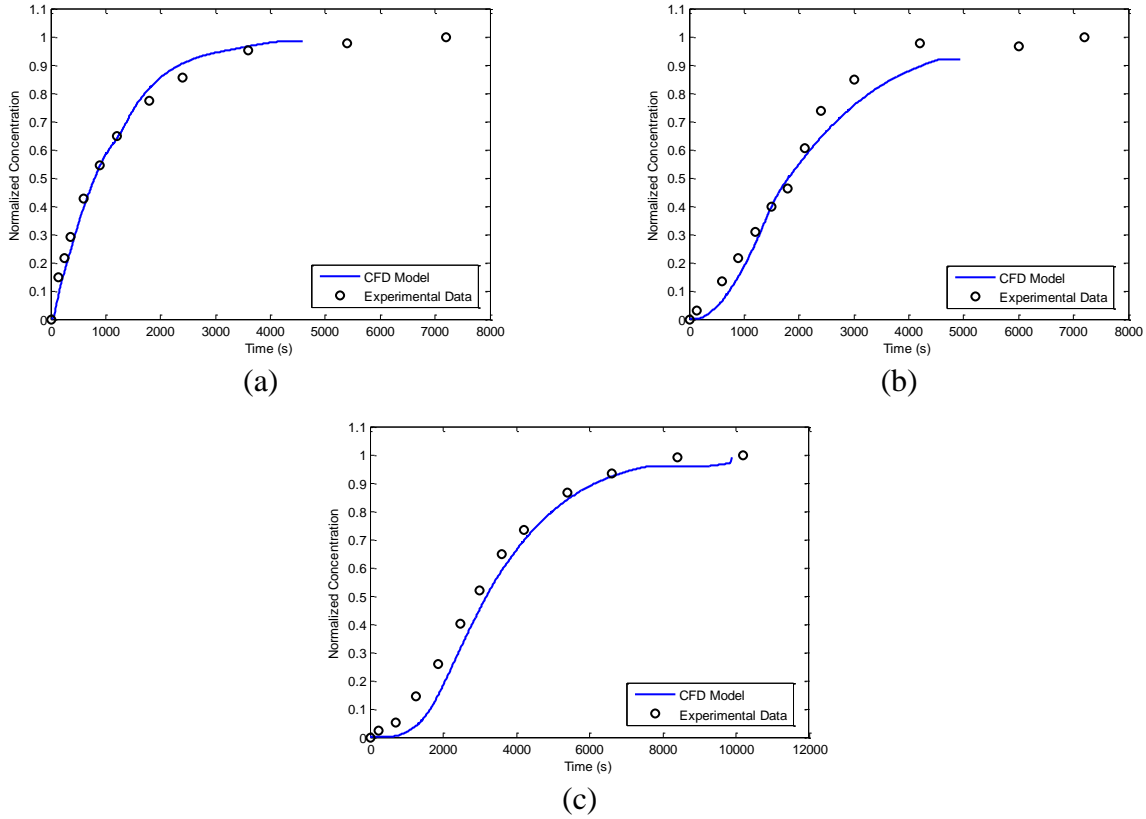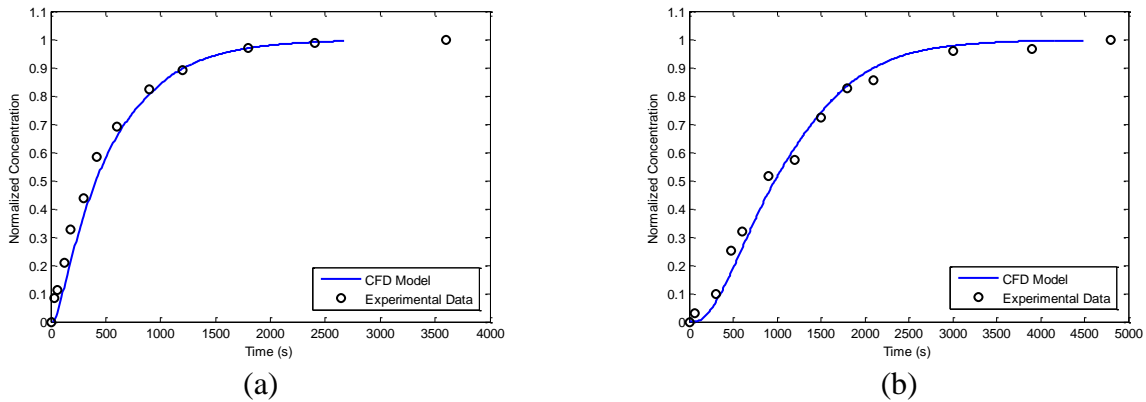

(a)

(b)

(c)

Figure F.1 Comparison of CFD model and tracer study RTD curves for 0.000316 m^3/s (5 gpm) through (a) 1 tank, (b) 2 tanks and (c) 3 tanks in series.

(a)

(b)

(c)

Figure F.2 Comparison of CFD model and tracer study RTD curves for 0.000631m^3/s (10 gpm) through (a) 1 tank, (b) 2 tanks and (c) 3 tanks in series.

(a)

(b)

(c)

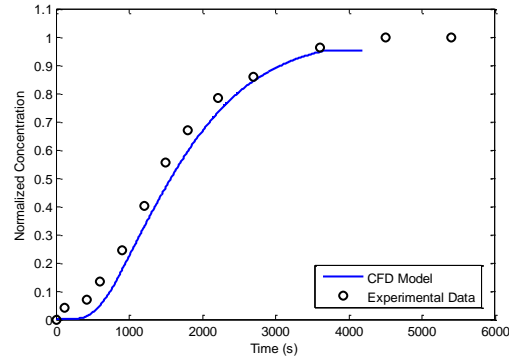**Figure F.3 Comparison of CFD model and tracer study RTD curves for 0.001262 m^3/s (20 gpm) through (a) 1 tank, (b) 2 tanks and (c) 3 tanks in series.**

(a)

(b)

(c)

Figure F.4 Comparison of CFD model and tracer study RTD curves for 0.000946 m^3/s (15 gpm) through (a) 4 tanks, (b) 5 tanks and (c) 6 tanks in series.

(a)

(b)

(c)

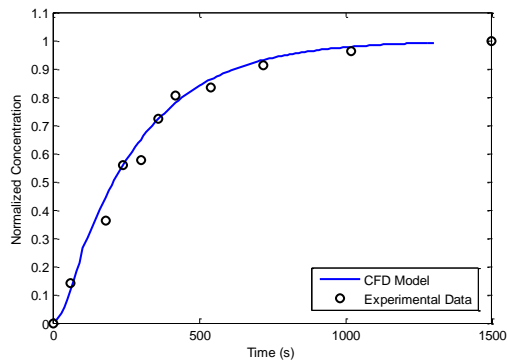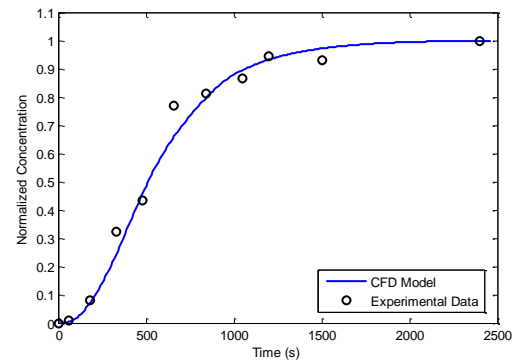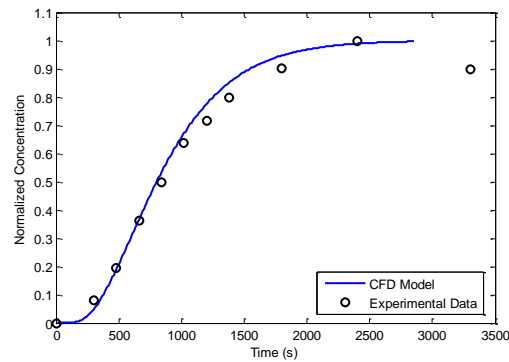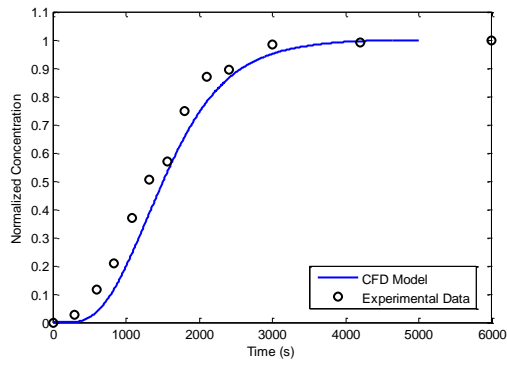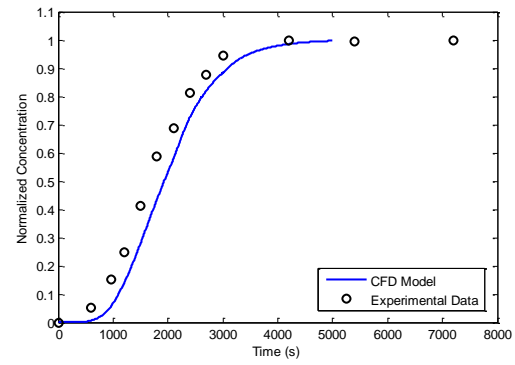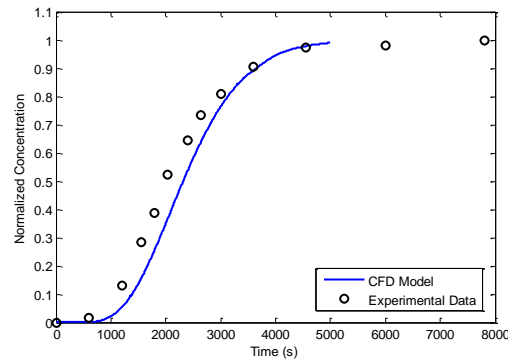**Figure F.5 Comparison of CFD model and tracer study RTD curves for 0.001262 m³/s (20gpm) through (a) 4 tanks, (b) 5 tanks and (c) 6 tanks in series**

APPENDIX D

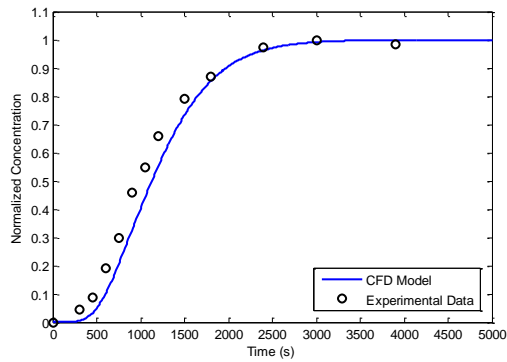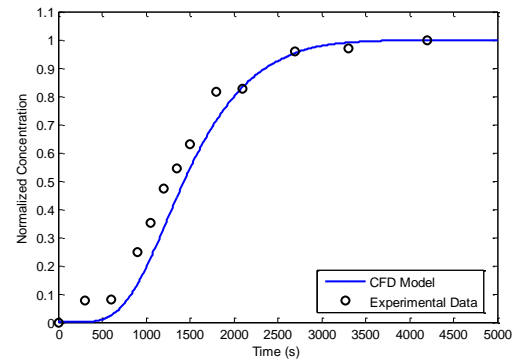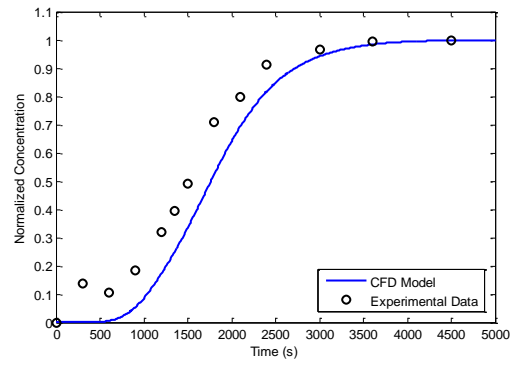Application for Drinking Water Construction Approval
Application Form: Transient Non-Community, Sodium hypochlorite for disinfection and contact time treatment only

Application for Drinking Water Construction Approval
Application Form: Transient Non-Community, Sodium hypochlorite for disinfection and contact time treatment only

Background:

Regulation: Article 11.1.2 (b) of *the Colorado Primary Drinking Water Regulations* states that "No person shall commence construction of any new water works, or make improvement to or modify the treatment process of an existing waterworks, or initiate the use of a new source, until plans and specifications for such construction, improvements, modifications or use have been submitted to, and approved by the Department."

Design Criteria: The Water Quality Control Division (Division) Engineering Section reviews potable water design for conformance with the *State of Colorado Design Criteria for Potable Water Systems* (Design Criteria). A copy of the Design Criteria is available at:
http://www.cdphe.state.co.us/wq/engineering/pdf/DesignCriteriaPotableWaterSystem.pdf

TNC GW Application:

Applicability: The following application applies to transient, non-community (TNC) water systems utilizing sources classified as groundwater (GW) only. Furthermore, the application only applies for treatment facilities that use sodium hypochlorite treatment only to comply with the *Colorado Primary Drinking Water Regulations* (e.g., a proposed treatment system that includes a greensand filter and chemical feed system for iron and manganese removal cannot use this form).

Instructions: All design submittals need to have a minimum of:
- Application for Construction Approval Form
- Project Information (G1-7)
- Completed application sections in proposed project scope – state "not applicable" if not in project scope (S1-8, T1-16,)
- Signature Sheet with owner/representative signature and local health signature
- Appendices (e.g., Floodplain Certification, Raw Water Quality Analysis Results)

If the submitted design is missing any of the above sections or the application and/or appendices are incomplete, Division staff will return the application to be completed and/or notify the applicant in writing on Division letterhead of any missing information. Under these circumstances the application will be put on hold until the applicant submits the requested information.

Please note: The application is intended to help facilitate design submittal for TNC GW systems utilizing sodium hypochlorite treatment only with the Division design approval process and is not meant to supersede the Design Criteria requirements. Therefore; if the submitted design does not meet the requirements of the State of Colorado's *Design Criteria for Potable Water Systems* then Division staff will notify the applicant in writing on Division letterhead of any missing information and the applicant will need to resubmit. The form has the applicable Design Criteria section referenced.

Colorado Department of Public Health and Environment
Water Quality Control Division
4300 Cherry Creek Drive South, B2
Denver, Colorado 80246-1530
303-692-3500

Colorado Primary Drinking Water Regulations
Application Form
TNC Sodium Hypo Only Treatment

Application for Drinking Water Construction Approval
Application Information Form: Transient Non-Community, Sodium hypochlorite only treatment
Colorado Primary Drinking Water Regulations 1.11

A. Project and System Information	
System Name	
Project Title	
PWSID	
County	
Design Company Name	
Design Engineer/ Designer	CO License Number
Address	
Email	
Phone	Fax
Applicant / Entity	
Representative Name/Title	
Address	
Email	
Phone	Fax

B. Public Water System (PWS) Type		Community (CWS)	N/A	Non-Transient, Non-Community (NTNC)	N/A	Transient, Non-Community (TNC)	☐
C. Current Primary Source Classification		Surface Water/ GWUDI	N/A	Ground Water (GW)	☐	Consecutive / Purchased	N/A

D. Design Submittal Scope (Check all that apply)

Source		*Treatment Facility*		*Storage Tank*		*Other*	
New ground water (GW) source	☐	New Treatment Facility	☐	New Distribution System Tank	☐	State Revolving Fund (SRF) Project	N/A
New ground water under the direct influence of surface water (GWUDI) source	N/A	Expansion of existing treatment facility	☐	New Tank used for disinfection contact time	☐	Technical, Managerial, Financial Evaluation	N/A
New surface water (SW) source	N/A	Modification to existing treatment	☐	Modifications to existing tank	☐	Distribution System (SRF Projects Only)	N/A
Existing source modification	☐						
Other (Please describe)							

E. Estimated Project Schedule and Cost Estimate		F. Project Flows		G. Residual Plan (if applicable)	
Estimated Construction Start Date		Minimum Flow		CDPS Discharge Permit	N/A
Estimated Completion Date		Monthly Average		Impoundment	N/A
Estimated Project Cost		Peak Hour Flow		Class V injection well	N/A
H. Brief Project Summary					
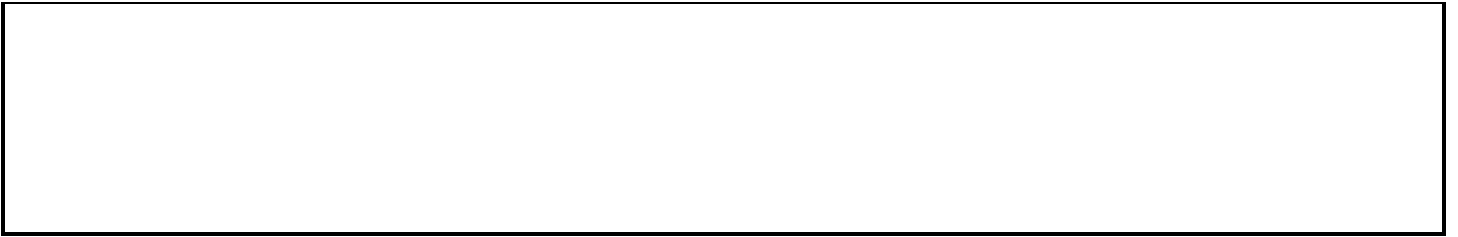
Colorado Department of Public Health and Environment
Water Quality Control Division
4300 Cherry Creek Drive South, B2
Denver, Colorado 80246-1530
303-692-3500

Colorado Primary Drinking Water Regulations
Application Form
TNC Sodium Hypo Only Treatment

Application for Drinking Water Construction Approval
Application Form: Transient Non-Community, Sodium hypochlorite only treatment
Project Information

Project and System Information	
Project Title	
System Name	
PWSID	
County	

Project Information and Vicinity Map	
G1	**Description and scope of proposed project. Please attach a potable water system schematic in Appendix D.** (e.g., The proposed project is improvements to an existing potable water system at a campground in La Plata County. The project will include: one new well (approx. 12 gpm), sodium hypochlorite treatment, three 100 gallon pressure tanks for disinfection contact time, and one 500 gallon buried distribution storage tanks. A schematic of the water system is available in the appendix.) *Response:*
G2	**Description of an existing water facility components utilized** (e.g., The existing Well 2, approved in 2007, will continue to be used as part of the potable water system. The existing treatment facility will be decommissioned and will no longer be used after proposed project is complete. The proposed raw water line connecting existing Well 2 to the proposed treatment facility can be seen on the vicinity map in the appendix.) *Response:*

Service Area, Potential Flows	
G3	**Service Area Description of the Public Water System** (e.g., The public water system currently serves a population of 40 transient customers. This project will serve a campground expansion which will increase the transient customers to 80. No further service area expansions are anticipated.) *Response:*

G4	**Service Area includes:**							
	Campground	☐	Restaurant, store	☐	School, daycare	☐	Day use site (e.g, Park)	☐
	Year round Housing Units (e.g., subdivision)	☐	Seasonal Housing Unit (e.g. rental cabin)	☐		☐	Other (describe below)	☐

	Response:
G5	**Future Service Area** Will the water system ever serve year round residents (e.g. a subdivision) or serve greater than 25 people for 6 months (e.g., daycare, school)?
	Response:
G6	*Potable Water Flowrates*
	Describe how the potable water system flowrates were projected and/or estimated (e.g., The flowrates were estimated using three methods and the system was designed based on an average flow rate of 5 gpm and a peak flow rate of 40 gpm. Method 1: The campground historic water flow data was projected for the incremental population increase. Method 2: International Plumbing Code fixture units estimation method. Method 3: Manual of campground design by the USFS. The calculations are included in Appendix G.)
	Response:
Project Disinfection Process	
G7	**Disinfection Process:** Please describe how the sources, lines, treatment facilities, and tanks will be disinfected prior to use including specific AWWA references (Required Design Criteria Section 3.14, Appendix I 1.0.17, Appendix I 2.5.6).
	Response:

Raw Water / Source Information: Reference Section 2 of the Design Criteria

Raw Water System Overview	
S1	**Source Description.** (e.g., Well #42 was drilled in June 2010 into the Cliff House Sandstone aquifer. The well is 200 feet deep with a first screen at 167 feet. The average well flowrate is 20 gallons per minutes (gpm) and the peak flowrate is 23 gpm. Water quality samples were taken in June 2010 and all raw water parameters tested were below the drinking water standards.).
	Response:
S2	**Other Sources.** Any other wells on site being used (e.g., existing wells) or that may be used?
	Response:

Well Summary: Division of Water Resources (aka the State Engineer's office) Well Permit and Well Drillers Log must be attached in Appendix C.	
S3	Well name	
	DWR Well Permit No.	
	Aquifer Name	
	Total Depth of well	
	Screened Interval Depth, top	
	Screened Interval Depth, bottom	
	Max pump rate	
	Nominal pump rate	
	Type of nearest surface water	
	Name of nearest surface water	
	How was distance to surface water measured?	

Raw Water Quality Summary: Laboratory Data on State Forms must be attached in the Appendix F.[1]	
S4	**Water Quality Parameter**	**Analysis Results**
	Nitrate	(mg/L)
	Nitrite	(mg/L)
	Bacteriological	
	Iron (Recommended - No State forms)	
	Manganese (Recommended - No State forms)	
	Hydrogen sulfide (Recommended - No State forms)	
	Inorganics (Recommended) – please note any results above the MCL	
	Organics (Recommended) – please note any results above the MCL	
	Corrosivity (Recommended) – please note any results above the MCL	
	Radionuclides (Recommended) – please note any results above the MCL	

Well Drawing (s) illustrating: Well Drawing must be attached in Appendix H.	
S5	Sanitary Well Seal including but not limited to: gaskets present, bolts, all penetrations sealed (required Design Criteria Section 2.1.5)	
	Well head elevation 12 inches above ground (required by *Rules and Regulations for Water Well Construction, Pump Installation, Cistern Installation and Monitoring and Observation Hole/Well Construction*)	
	Positive drainage slope away from well for at least 20 feet (Required Design Section 2.1.8)	
	4 foot by 4 foot sloping concrete pad to divert surface water away from well (Recommended for wells with static water less than 100 ft, Design Section	

---

[1] If only existing sources are used then new raw water chemical analyses are not required. However, source water quality information for existing sources should be summarized.

	2.1.8)	
	Vents screened with 24 Mesh screen (Required Design Criteria Section 2.1.7)	
S5 Cont	Grouting Detail including any changes from original well drillers log	
	Pitless Adapter Detail (include make or model)	
Well Location Information: 100 Year Floodplain Certification[2] must be attached in the Appendix E.		
S6	**Floodplain and Natural Hazards**	
	a) Is the facility located in a 100-year floodplain or other natural hazard area? If so, what precautions are being taken?	
S7	**Contamination Sources within 100 feet of well?**	
	a) Do any potential sources of contamination existing within 100 feet of the well (e.g., septic field, fueling stations)? If so, what precautions are being taken?	
S8	**Land Ownership**	
	a) Who owns the land upon which the well is constructed? Please attach copies of the document(s) creating authority for the applicant to construct the proposed facility at this site.	

---

[2] Floodplain certifications are required for all new sources and improvements to existing sources that might impact source footprint (e.g., an expanded well building).

Treatment System – Sodium Hypochlorite Treatment ONLY
Reference Section 3, 6, and 7 of the Design Criteria

	Treatment System Overview:
T1	**Treatment System Description. Please attach a treatment system process flow diagram in Appendix D.** (e.g., Raw water from the source enters the treatment facility. Diluted sodium hypochlorite (manufacturer Bob's chemical supply) will be added using a peristaltic pump (Manufacturer Bob's equipment, Model CF42). The chlorine dosing rate will be variable injection rate controlled by a flowmeter. After chlorination, the chlorinated water will flow through three pressure tanks (Manufacturer Bob's equipment, Model PT42) and then out to the distribution system. Sample taps will be installed for raw water and treated water samples (entry point). The well pump will provide pressure through the treatment facility and into the distribution system. The estimated system pressure is 75-85 psi. A schematic of the water system treatment is available in the appendix.)
	Raw water from source enters treatment facility. Diluted sodium hypochlorite will be added using a positive displacement pump with a fixed injection rate. The system flow rate will be monitored using a flow meter (preferably a rotameter). After chlorination, the chlorinated water will flow through four (4) 80 gallons pressure tanks and then on to the distribution system. Sample taps will be installed for raw water and treated water samples (entry point). The well pump will provide pressure through the treatment facility and into the distribution system. As shown in the schematic in the appendix, the series tank configuration requires a minimum inlet pressure of approximately 40-50 psi.
T2	**Treatment Alternatives:** Please describe any treatment alternatives (e.g., The campground considered several treatment alternatives: 1) expansion of the existing sodium hypochlorite feed system, 2) becoming a consecutive system to a nearby potable water system and 3) hauling water to the campground. Alternative 2, becoming a consecutive system, was preferred by management but an easement agreement with a property owner could not be reached. Alternative 3, hauling water, was not selected since a water hauler to serve the site could not be found. The system elected to expand the existing sodium hypochlorite system within the existing building. The system investigated three possible contact tank configurations (see calculations in Appendix G) and determined based on price and ability of the tanks to fit in the existing building to select the three pressure tanks alternative.)
T3	**Ground Water Rule (GWR) Compliance Strategy** (Article 13 of the *Colorado Primary Drinking Water Regulations*)

	☐	Triggered Source Water Monitoring (Default - Most GW systems: Sample sources if a positive distribution system bacteriological sample)
	☒	4 Log Certification (Please contact Compliance Assurance for the GWR 4 Log certification application to be submitted along with design review application)

	Proposed Chemical Feed System
T4	**Sodium Hypochlorite Feed Range** (e.g. 0.2-2 mg/L)
	Response:
T5	**Number of Chemical Feed Pumps** (reference Design Criteria Section 7.4**), if less than one please provide a justification for a variance** (e.g., The system will have a backup pump available on the shelf and spare parts readily available)
	Response:
T6	**Will the sodium hypochlorite be diluted?**
	Response:
T7	**Pump Type:**

	☒	Positive Displacement (PD) Pump
	☐	Peristaltic Pump
	☐	Other, Describe below
		Response:

	Chlorination Controls
T8	

	☒	Fixed injection rate (e.g., typically the source pump and chlorine pump are electrically connected)
	☐	Fixed injection rate – pressure switch
	☐	Fixed injection rate – reservoir water level sensors
	☐	Variable injection rate

		Other, Describe below
	☐	Response:

Proposed Disinfection Contact Tanks		
T9	**Disinfection Contact Tank Type**	
	☒	Pressure Tank(s), not bladder tanks
	☐	Pipeline Loop
	☐	Non-pressured storage tank (open to the atmosphere)
	☐	Other, Describe below
		Response:
T10	**Tank Volumes**	
	320	Total Tank Volume (gallon)
	320	Minimum Operating Level (gallon)
	320	Maximum Operating Level (gallon)
		Please describe how tank levels will be maintained
		Response: Pressurized tanks must be full for system operation
	Disinfection Contact Tank Baffle Factor	
	0.5	Proposed Baffle Factor for the Tanks, Describe below
		Response:

Treatment Facility Design Summary		
T11	*7*	Average flowrate (gpm)
	7	Peak Flowrate (gpm)
	320	Minimum Tank Operating Volume (gallon)
	0.5	Proposed Baffle Factor, BF (from item T10 above)
	7	Water pH
	10	Water temperature, degree Celsius, minimum
	1.0	Minimum Chlorine Residual, mg/L
	4	**Calculated Virus Inactivation – MUST be capable of four (4) log inactivation of viruses**

Treatment Facility Equipment Summary
Equipment Cut Sheets and ANSI/NSF Certification Documents must be attached in the Appendix I.

T12	**Equipment**	**Manufacturer, Model number**	**ANSI/NSF Certified or Chlorine Institute?** [3]
	Chemical Feed Pump(s)	*LMI A, B, C, and P series pumps* *Cole Parmer Peristaltic Pumps EW-74206 series pump* *Chem-Tech Series 100 & 150*	Yes ☒[3]
	Chemical Storage Tank(s)	*Pulsafeeder Top-Mount Tanks* *Chem-Tainer Polyethylene Tanks* *Snyder Flat Bottom Open Top Tanks*	Yes ☒[3]
	Secondary Containment Method		N/A
	Contact Storage Tank(s)	*Wellmate UT Quick Connect Series* *Flexcon Composite H2PRO Lite Series*	Yes ☒
	Other Equipment (e.g., Roughing Filter)	*6 or 12 element static mixer*	Yes ☐
	Other Equipment	*Schedule 80 PVC Piping and Valves*	Yes ☒
	Other Equipment	*Flexible tubing*	Yes ☒
Treatment Facility Appurtenances			

[3] For sodium hypochlorite storage tanks and chemical feed pumps submit either 1) evidence that the storage is constructed of appropriate material as listed in the Chlorine Institute Pamphlet 96 Sodium Hypochlorite Manual or 2) a manufacturer statement saying the material is compatible with sodium hypochlorite or the proposed chemical rather than of ANSI/NSF 61 certified

T13	If not included please include a justification below	
	☐	Raw Water Tap (required – Design Criteria Section 3.9)
	☐	Finished Water Tap (required – Design Criteria Section 3.9)
	☐	Flow meter (required – Design Criteria Section 3.12)
	☐	Chemical Containment (required – Design Criteria Section 7.13.8)
	☐	Chlorine analyzer (required Design Criteria 6.1.17-6.1.18)
	☐	Cross connection controls (required by Section 12 of the *Colorado Primary Drinking Water Regulations*)
	Other:	

Facility Location Information - 100 Year Floodplain Certification[4] must be attached in the Appendix E.

T15	**Floodplain and Natural Hazards**
	a) Is the facility located in a 100-year floodplain or other natural hazard area? If so, what precautions are being taken?
	No

T16	**Land Ownership**
	a) Who owns the land upon which the treatment facility will be constructed? Please attach copies of the document(s) creating authority for the applicant to construct the proposed facility at this site**.**

---

[4] Floodplain certifications are required for all new water treatment facilities and improvements/expansions that would impact building footprint.

Distribution System Tank
Reference Appendix I of the Design Criteria

Storage Tank Overview:	
DST1	**Distribution Tank Description. Please attach a drawing in Appendix.** (e.g., The distribution system storage tank, Coyote Tank is a 2,000 gallon buried steel tank located on campground circle B.)

Storage Tank Information		
DST2	**Storage Volumes**	
		Total Tank Volume (gallons)
		Minimum Tank Operating Volume (gallons)
		Maximum Tank Operating Volume (gallons)
DST3	**Tank Type**	
	☐	Buried Tank
	☐	Elevated Tank
	☐	Ground level
	☐	Other, Describe below
		Response:
DST4	**Tank Construction Material**	
	☐	Concrete
	☐	Plastic
	☐	Fiberglass
	☐	Steel
	☐	Other, Describe below
		Response:

Distribution System Tank Summary
Equipment Cut Sheets and ANSI/NSF Certification Documents must be attached in the Appendix I.

DST5	**Equipment**	**Manufacturer, Model number**	**ANSI/NSF Certified?**
	Storage Tank		Yes ☐
	Coatings (e.g., paint)		Yes ☐
	Other Equipment		Yes ☐
	Other Equipment		Yes ☐
	Other Equipment		Yes ☐

Tank Appurtenances		
DST6	If not included please include a justification below	
	☐	Drain (recommended – Design Criteria Appendix I Section 1.0.5) with 24 non corrosive mesh screen (required), and energy dissipation (required)
	☐	Overflow (recommended - Design Criteria Appendix I Section 1.0.6) with 24 non corrosive mesh screen (required), and energy dissipation (required)
	☐	Access hatch (recommended – Design Criteria Appendix I Section 1.0.7) with water tight overlapping cover elevated 24-36 inches above grade for ground level tanks or elevated 4-6 inches for above grade tanks
	☐	Vent (recommended - Design Criteria Appendix I Section 1.0.8) with 24 non corrosive mesh screen (required), exclusion of dust (required), and terminate in a "U" construction with the openings 12 inches above the average annual snow depth (recommended).
	☐	Roof and Sidewalls must be an impervious watertight material with no openings except vents, access ways, overflows, etc. (required - Design Criteria Appendix I Section 1.0.9).
Tank Location Information		
DST7	**Floodplain and Natural Hazards**	
	a) Is the facility located in a 100-year floodplain or other natural hazard area? If so, what precautions are being taken?	

DST8	**Land Ownership**	
	a) Who owns the land upon which the tank will be constructed? Please attach copies of the document(s) creating authority for the applicant to construct the proposed facility at this site.	
DST9	**Drain and Overflow discharge location**	
	a) Where does the drain line and overflow line discharge to? Does the drain have a direct connection to any sewer or storm drain? Does the discharge flow into State Waters?	

Application for Drinking Water Construction Approval
Application Form: Transient Non-Community, Sodium hypochlorite only treatment
Signature Sheet

A. Project and System Information	
System Name	
Project Title	
County	
PWSID	

Directions: Prior to submission to the Water Quality Control Division (Division), the construction application must be signed by the Owner and/or a System Legal Representative.

Signatures of System Representatives			
Role	**Date**	**Typed Name**	**Signature**
Owner			
The owner is an individual, corporation, partnership, association, state or political subdivision thereof, municipality, or other legal entity.			
Applicant / System Legal Representative			
The system legal representative is the legally responsible agent and decision-making authority for a public water system (e.g. mayor, president of a board, public works director). The Designer or Consulting Engineer is not the legal representative.			

2. Recommendation of local health authorities
The application for drinking water construction approval shall be forwarded to the local County Health authority or County Commissioner (if no County Health authority) in whose jurisdication(s) the drinking water facility is to be located.

Signatures of local health authorities					
Role	**Date**	**Typed Name / Agency**		**Signature**	
		Recommend Approval	☐	**Recommend Disapproval**	☐

County Health Comments:

Appendices

Appendix	Description	Required ?	Included
Appendix A:	Inventory Section of the Monitoring Plan	All Submittals	Yes ☐, No ☐
Appendix B:	Vicinity Map	All Submittals	Yes ☐, No ☐
Appendix C:	Water Rights and Well Information	Required for new sources	Yes ☐, No ☐
Appendix D:	Water System Schematic Process Flow Diagram (PFD)	All Submittals PDF Required for new treatment facilities or improvements modifications	Yes ☐, No ☐
Appendix E:	Floodplain Certification and supporting documents (e.g., FIRMette map)	Required for all projects that might be effected by flooding (e.g., new sources, facilities, tanks or building expansions)	Yes ☐, No ☐
Appendix F:	Raw Water Quality Results	Required for new sources	Yes ☐, No ☐
Appendix G:	Calculations	As applicable for project (e.g., treatment modifications require disinfection calculations)	Yes ☐, No ☐
Appendix H:	Project Drawings (e.g., well head improvements, treatment facility layouts)	As applicable for project construction and comprehension (e.g., treatment modifications require a treatment facility layout)	Yes ☐, No ☐
Appendix I:	Equipment Manufacturer Information & ANSI/NSF Potable Water Certification	Required for all proposed equipment	Yes ☐, No ☐

Information Sources

Latitude/Longitude Information (Inventory Section lat/long data)**:**
- http://www.findlatitudeandlongitude.com/
- http://www.mapquest.com/maps?form=maps&geocode=LATLNG

Vicinity Map

Water Rights and Well Information
- Colorado Department of Water Resources Homepage: http://water.state.co.us/Home/Pages/default.aspx
- Colorado Department of Water Resources Well Permit Search: http://www.dwr.state.co.us/WellPermitSearch/default.aspx

Floodplain Information
- FEMA Firmette Map Services Center: http://msc.fema.gov/webapp/wcs/stores/servlet/info?storeId=10001&catalogId=10001&langId=-1&content=firmetteHelp_A&title=FIRMettes

Raw Water Quality Results
- State of Colorado List of Certified Water Labs: http://www.cdphe.state.co.us/lr/certification/SDWlist.pdf

Calculations
- EPA Long Term 1 Homepage: http://water.epa.gov/lawsregs/rulesregs/sdwa/mdbp/lt1/lt1eswtr.cfm

Equipment Manufacturer Information & ANSI/NSF 60/61 Potable Water Certification
- Canadian Standards Association
  http://www.csa.ca/cm/ca/en/home
- NSF Water Treatment and Distribution Systems Program:
  http://www.nsf.org/business/water_distribution/index.asp?program=WaterDistributionSys
- NSF International Certified Products Search – Standard 60:
  http://www.nsf.org/Certified/PwsChemicals/
- NSF International Certified Products Search – Standard 60:
- http://www.nsf.org/Certified/PwsComponents/
- UL Certified Products Search:
  http://database.ul.com/cgi-bin/XYV/template/LISEXT/1FRAME/index.htm
- WQA Certified Products Search:
  http://www.wqa.org/

APPENDIX E

Masters Thesis - Qing Xu

Internal Hydraulics of Baffled Disinfection Contact Tanks Using Computational Fluid Dynamics

THESIS

INTERNAL HYDRAULICS OF BAFFLED DISINFECTION CONTACT TANKS

USING COMPUTATIONAL FLUID DYNAMICS

Submitted by

Qing Xu

Department of Civil and Environmental Engineering

In partial fulfillment of the requirements

For the Degree of Master of Science

Colorado State University

Fort Collins, Colorado

Summer 2010

APPENDIX F

International Symposium on Environmental Hydraulics Conference Proceeding

Hydraulic Efficiency of Baffled Disinfection Contact Tanks

Hydraulic Efficiency of Baffled Disinfection Contact Tanks

Q. Xu & S. K. Venayagamoorthy

Department of Civil and Environmental Engineering, Colorado State University, Fort Collins, CO, 80523-1372, USA

ABSTRACT: The present study focuses on understanding the internal hydraulic efficiency of baffled disinfection contact tanks using computational fluid dynamics (CFD). In particular, we seek to address the key question: for a given footprint of a contact tank, how does the hydraulic efficiency of the tank depend on the number and geometry of internal baffles? In an effort to address this question, we perform high resolution two-dimensional (planar) simulations to quantify the efficiency of a laboratory scale tank as a function of the number of baffles. Simulation results of the velocity field highlight dead (stagnant) zones in the tank that occur due to flow separation around the baffles. Simulated longitudinal velocity profiles show good agreement with previous experimental results. Our analysis of residence time distribution (RTD) curves obtained for different number of baffles for a given footprint of a tank indicate that there may be an optimum number of baffles for which near plug flow conditions is maximized. This study highlights the increasingly role and value of CFD in improving hydraulic design characteristics of water engineering structures.

1 INTRODUCTION

Chlorination is the most common method of disinfection in drinking water treatment systems in the United States. The United State Environmental Protection Agency (USEPA) Interim Enhanced Surface Water Treatment Rule (IESWTR) provides guidelines for the physical removal or inactivation of waterborne pathogens during disinfection in terms of CT which is the product of the outlet disinfectant residual concentration (C) and a characteristic contact time T (USEPA 1999). The effective contact time is usually taken to be T_{10} rather than the mean hydraulic residence time T_m. T_{10} is the time required for the first ten percent of a pulse of tracer to travel through the tank to the residual sampling point (usually the outlet) and T_m is the ratio of the storage volume V to the mean flow rate Q. Baffling is used in many contact tanks (basins) to increase the plug flow zone in the tank, and minimize short circuiting. USEPA provides guidelines developed from tracer studies for determining baffle factors based on baffling description. The baffle factor is taken as the ratio of T_{10} to the mean hydraulic residence time T_m as shown in Table 1 (USEPA 1999).

The disinfection criteria based on CT can be met by simply increasing the chlorine dosage but this is highly undesirable since a high dosage of chlorine can result in high concentration of disinfection by-products (DBP) (Hannoun *et al.* 1998). Therefore, the efficient way to optimize disinfection effectiveness is to increase the value of T_{10} which essentially implies optimizing the baffle factor in terms of the USEPA guidelines. Physically, this translates to obtaining near plug flow conditions in the disinfection tank. Baffles usually take the form of walls placed in the interior of contact tanks and provide for longer contact path and mixing within the tank, both of which may in theory extend the disinfection contact time. A key question that arises from this is whether there is an optimal number of baffles that will result in an internal flow field that is closest to plug

APPENDIX G

Masters Thesis - Jordan Wilson

Evaluation of Flow and Scalar Transport Characteristics of Small Public Drinking Water Disinfection Systems Using Computational Fluid Dynamics

THESIS

EVALUATION OF FLOW AND SCALAR TRANSPORT CHARACTERISTICS OF

SMALL PUBLIC DRINKING WATER DISINFECTION SYSTEMS USING

COMPUTATIONAL FLUID DYNAMICS

Submitted by

Jordan M. Wilson

Department of Civil and Environmental Engineering

In partial fulfillment of the requirements

For the Degree of Master of Science

Colorado State University

Fort Collins, Colorado

Spring 2011

Master's Committee:

    Advisor: S. Karan Venayagamoorthy

    Timothy K. Gates

    S. Ranil Wickramasinghe

APPENDIX H

Peer Reviewed Journal Article in Environmental Science and Technology

Evaluation of Hydraulic Efficiency of Disinfection Systems Based on Residence Time Distribution Curves

Evaluation of Hydraulic Efficiency of Disinfection Systems Based on Residence Time Distribution Curves

JORDAN M. WILSON AND
SUBHAS K. VENAYAGAMOORTHY*

*Department of Civil and Environmental Engineering,
Colorado State University, 1372 Campus Delivery, Fort
Collins, Colorado 80523-1372, United States*

Hydraulic efficiency is a vital component in evaluating the disinfection capability of a contact system. Current practice evaluates these systems based upon the theoretical detention time (*TDT*) and the rising limb of the residence time distribution (RTD) curve. This evaluation methodology is expected because most systems are built based on *TDT* under a "black-box" approach to disinfection system design. Within recent years, the proliferation of computational fluid dynamics (CFD) has allowed a more insightful approach to disinfection system design and analysis. Research presented in this study using CFD models and physical tracer studies shows that evaluation methods based upon *TDT* tend to overestimate, severely in some instances, the actual hydraulic efficiency as obtained from the system's flow and scalar transport dynamics and subsequent RTD curve. The main objective of this study was to analyze an alternative measure of hydraulic efficiency, the ratio t_{10}/t_{90}, where t_{10} and t_{90} are the time taken for 10 and 90% of the input concentration to be observed at the outlet of a system, respectively, for various disinfection systems, primarily a pipe loop system, pressurized tank system, and baffled tank system, from their respective RTD curves and compare the results to the current evaluation method.

Introduction

Hydraulic efficiency is an important component in the design and operation of disinfection systems, particularly chlorine contact tanks, considering the potential carcinogenic products formed in the chlorination process. Improving the hydraulic efficiency of a system allows for a smaller dose of disinfectant to be used thus reducing the formation of potential carcinogens (*1*, *2*). Until recently contact tanks used in water treatment have been largely regarded as "black boxes" and their design left up to the ideal assumption of plug flow, that is, the theoretical detention (or residence) time (*TDT*) of the system is simply the ratio of the system volume, *V*, to the average volumetric flow rate, *Q* (*3–5*). The reality is that very few contact tanks function in a strictly plug flow manner (further details can be found in ref *6*). Most contact tanks have an uneven flow path, inducing regions of recirculation or stagnation, commonly known as dead zones (*5*). These dead zones rely on the much slower process of diffusion to distribute the disinfectant, causing particles in the contact tank to reside longer than the *TDT*.

The problem with the *TDT* formulation is that this value is a prediction based on idealized plug flow conditions rather than the actual flow dynamics of the tank. The further the flow in the tank departs from plug flow (e.g., the more recirculation, turbulence, and stagnation fluid particles encounter), the further the actual detention time is from the *TDT* (*3*).

In order to evaluate the efficiency of contact tanks for disinfection purposes, the United States Environmental Protection Agency (USEPA) has established the practice of assigning tanks a baffle factor (*BF*) (*7*). The contact time of the disinfectant with the water in the tank is taken to be t_{10}, which is the time for 10% of the inlet concentration to be observed at the outlet. These quantities are typically obtained through tracer studies of an established system using conductivity measurements or tracer analysis using fluoride or lithium. *BF* is the ratio of t_{10} to *TDT* and ranges from a value of 0.1 representing an unbaffled tank with significant short-circuiting to an upper bound value of 1.0 representing ideal plug flow conditions as described by the Interim Enhanced Surface Water Treatment Rule (*7*). In addition, the Morrill Index (*MI*), used as a measure of hydraulic efficiency in Europe, evaluates the amount of diffusion in a system based on the ratio t_{90}/t_{10} (*6*, *8*). The USEPA's practice of assigning *BFs* assumes that a system can achieve plug flow through the use of *TDTs*. However, advances in numerical analysis and computational fluid dynamics (CFD) allow for a more comprehensive understanding into the flow dynamics of a system. The research presented in this paper shows that a better measure of hydraulic efficiency must include the complete flow dynamics of the system since it is the flow dynamics that governs the transport of a tracer from the inlet to outlet through time (*9*). This is usually depicted by a residence time distribution (RTD) or flow through curve (FTC), obtained by plotting the system's effluent concentration over time, as shown for example in Figure 1.

The shape of the RTD curve provides insight to the nature of the flow in the system (*10*). For example, a steeper gradient represents conditions closer to plug flow dominated by advective forces and a flatter gradient represents conditions further from plug flow dominated by diffusive forces. The RTD curve shows the complete interaction of the scalar (e.g., chlorine-containing species) and fluid flow field (*9*), thus, it should be used in its entirety to evaluate hydraulic efficiency. However, current practice only uses the rising limb, or rather the t_{10} value, from the RTD curve and compares it to a *TDT* value unrelated to the actual flow in the system. This
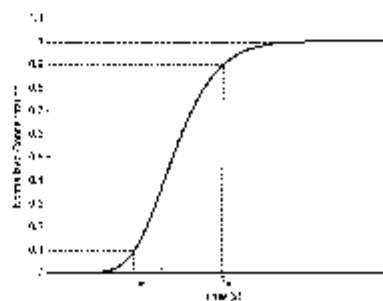

FIGURE 1. Residence time distribution (RTD) curve for an arbitrary disinfection system.

APPENDIX I

2011 World Environmental and Water Resources Congress Conference Proceedings

Hydraulics and Mixing Efficiency of Small Public Water Disinfection Systems

HYDRAULICS AND MIXING EFFICIENCY OF SMALL PUBLIC WATER DISINFECTION SYSTEMS

J. M. Wilson[1] and S. K. Venayagamoorthy[2]

[1]Graduate Research Assistant, Department of Civil and Environmental Engineering, Colorado State University, Campus Delivery 1372, Fort Collins, CO 80523-1372; Email: wilsonjm@engr.colostate.edu

[2]Assistant Professor, Department of Civil and Environmental Engineering, Colorado State University, Campus Delivery 1372, Fort Collins, CO 80523-1372; Phone: (970) 491-1915; Fax: (970) 491-7727; Email: vskaran@engr.colostate.edu

ABSTRACT

The research presented in this study focuses on the evaluation of flow and scalar transport characteristics of small disinfection systems, primarily through computational fluid dynamics (CFD) and physical conservative tracer studies overcoming the traditional "black-box" approach of disinfection tank design based on theoretical detention time (TDT). Original research was performed on a series of pressurized tanks systems and on two differing open surface tank systems. CFD allowed for evaluation of the systems' respective flow characteristics which govern the transport of any quantity. Residence time distribution (RTD), or flow-through, curves measuring the effluent concentration of a passive scalar or conservative tracer provide a physical measure of the hydraulic mixing efficiency. The series of pressurized tank systems exhibited significant regions of turbulent mixing and recirculation corresponding to a relatively low hydraulic efficiency. Both open surface tank systems showed highly uneven flow paths and corresponding low hydraulic efficiencies. The research presented in this study provides an extensive evaluation for the flow and scalar characteristics of the described small public drinking water disinfection systems.

1